

Active colloids in the context of chemical kinetics

G. Oshanin¹, M. N. Popescu^{2,3} & S. Dietrich^{2,3}

¹ Laboratoire de Physique Théorique de la Matière Condensée, UPMC, CNRS UMR 7600, Sorbonne Universités, 4 Place Jussieu, 75252 Paris Cedex 05, France

² Max-Planck-Institut für Intelligente Systeme, Heisenbergstr. 3, D-70569, Stuttgart, Germany

³ IV. Institut für Theoretische Physik, Universität Stuttgart, Pfaffenwaldring 57, D-70569 Stuttgart, Germany

E-mail: oshanin@lptmc.jussieu.fr, popescu@is.mpg.de, dietrich@is.mpg.de

Abstract. We study a mesoscopic model of a chemically active colloidal particle which on certain parts of its surface promotes chemical reactions in the surrounding solution. For reasons of simplicity and conceptual clarity, we focus on the case in which only electrically neutral species are present in the solution and on chemical reactions which are described by first order kinetics. Within a self-consistent approach we explicitly determine the steady state product and reactant number density fields around the colloid as functionals of the interaction potentials of the various molecular species in solution with the colloid. By using Teubner's reciprocal theorem, this allows us to compute and to interpret – in a transparent way in terms of the classical Smoluchowski theory of chemical kinetics – the external force needed to keep such a catalytically active colloid at rest (*stall* force) or, equivalently, the corresponding velocity of the colloid *if* it is free to move. We use the particular case of triangular-well interaction potentials as a benchmark example for applying the general theoretical framework developed here. For this latter case, we derive explicit expressions for the dependences of the quantities of interest on the diffusion coefficients of the chemical species, the reaction rate constant, the coverage by catalyst, the size of the colloid, as well as on the parameters of the interaction potentials. These expressions provide a detailed picture of the phenomenology associated with catalytically-active colloids and self-diffusiophoresis.

PACS numbers: 82.70.Dd, 05.70.Ln, 47.57.s, 47.70.n

Keywords: diffusiophoretic self-propulsion, catalytically-decorated colloids, chemical reactions, hydrodynamics

1. Introduction

The reduction in length scales brought about by lab-on-a-chip applications has raised a number of challenging issues. One of them is how to enable small objects to perform autonomous, directional motion (so-called self-propulsion) in a liquid environment [1–8]. For particles of micrometer size or smaller viscous and surface forces dominate the effects of inertia. Therefore, in order to achieve motion for them, new strategies have to be developed, which differ from those applicable for macroscopic objects [4, 5, 8, 9].

1.1. Active particles

Currently two main routes are followed towards this goal. The first one is based on mimicking the ingenious mechanical locomotion strategies of natural micro-organisms such as *E. Coli* or *Spiroplasma* [5]. These objects move by undergoing deformations of their bodies in a cyclic, non-reciprocal manner and by exploiting the anisotropy of the hydrodynamic drag. A thorough, extensive discussion of the developments in this area can be found in the recent reviews by Lauga and Powers [5], Elgeti, Winkler, and Gompper [10], Zöttl and Stark [11].

A promising alternative is that of employing catalytically activated chemical reactions to extract “chemical” free energy from the surrounding liquid environment and to transform it into mechanical energy (i.e., motion of microparticles), resembling the way in which biological molecular motors function. One class of mechanisms to achieve this builds on ideas borrowed from classic phoresis, i.e., colloid motion in externally maintained gradients of certain thermodynamic fields [12]. The basic idea to achieve *self*-phoresis is to use particles which are partially covered by a catalyst in a well controlled way, designed such that symmetry breaking occurs and the particle is endowed with a “polar” axis. The catalyst activates a chemical reaction in the surrounding solution [1, 8, 9, 13], generating gradients of reaction products across the surface of the colloidal particle. Owing to the solvent mediated, effective interactions between the reaction product molecules and the surface of the particle, within a thin interfacial layer a gradient in the osmotic pressure along the surface of the particle emerges. This leads to hydrodynamic flow of the solution around the particle and sets it into motion†. Furthermore, in addition to the mechanical swimmers and chemically powered active colloids discussed here, self-thermophoresis [24] and photophoresis in combination with radiation-pressure [25] have recently been proposed as alternative self-propulsion mechanisms. (In the scenario above the requirement, that only a portion

† We note that there are also other mechanisms to convert chemical free energy into mechanical motion, such as electrochemical pumping employed by bi-metallic rods used in early experiments dealing with active colloids [2, 4, 14], thermally induced demixing of a binary liquid mixture near its critical temperature [15], or the “micro-jet-engines” which rely on a bubble-pumping mechanism [6, 16–21]. At low Reynolds numbers, the latter has similarities with the mechanisms discussed theoretically in Ref. [22]. Yet another example is that of propulsion through pressure waves generated via catalyst activated chemical reactions in the surrounding fluid [23].

of the surface is catalytically active, is necessary for particles having axial- and fore-aft symmetry. For a shape missing the latter, self-phoresis may occur even if the whole surface of the particle is covered by catalyst. For example, for a uniform reaction rate (i.e., a constant flux of product molecules) across the surface of the particle, geometrical shape asymmetry is sufficient to induce an inhomogeneous number density of reaction products along the surface and therefore propulsion [26, 27].)

Several proof-of-concept proposals of such chemically self-propelled objects, employing either self-phoresis [13, 14, 28–35] or bubble-pumping [6, 16, 17, 19–21] mechanisms, have already been successfully tested experimentally. Because of the intrinsic non-equilibrium character and due to the subtle combination of physics and chemistry behind this type of self-induced motility, many of the experimental [4, 6, 8, 14, 16, 20, 21, 31, 36] and theoretical [9, 36–42] studies have so far been focusing on systems which can be approximated as being *unbounded*.[‡] Recent experimental work has addressed new issues, such as improving the directionality of the motion against Brownian diffusion either by using external magnetic fields and paramagnetic core particles [16, 19, 21, 28, 32], or by exploiting the emergence of surface-bounded steady states of motion as they can occur in the vicinity of hard walls [71, 72], or by using a collection of chemically active particles as an artificial, non-biological system in order to study chemotaxis [30].

One interesting theoretical approach consists of describing an active particle in terms of an effective Langevin equation [76–81]. This has been, however, critically examined experimentally by Bocquet et al who have pointed out that in these out-of-equilibrium systems the notion of an “effective temperature” and the mapping onto systems described by equilibrium statistical mechanics are problematic [82, 83]. The intriguing question concerning the extent to which similarities in collective behavior between active colloids and interacting Brownian particles can be captured by mappings with effective thermodynamic parameters has been recently scrutinized in Ref. [84]. This latter study established criteria under which certain models of “run-and-tumble” particles are equivalent with the models of active particles developed in Refs. [76, 77]. However, it is important to note that in general, such systems cannot be described in terms of an equation of state [85, 86].

The hydrodynamic interactions between active swimmers have been shown to give rise to a rich behavior, such as synchronization of the swimmers [87, 88]. Accordingly, studies of simple models for the collective dynamics of active particles are enjoying considerable attention [79, 80, 83, 89–91].

Returning to the framework of “single-colloid” systems and the emergence of self-phoresis, we note that a microscopic modeling of the processes in the interfacial region, explicitly taking into account the molecular structure of that region around a self-propeller, has been performed in Refs. [39, 40], and more recently in Ref. [92], by using molecular dynamics simulations. This approach allows one to keep track

[‡] See, however, the recent Refs. [43–75] which address the issue of confinement effects on self-propulsion.

of the molecular details for all species at the expense, however, that only relatively small systems and short time scales can be accessed. A different strategy, pursued in Refs. [9, 37, 38, 41, 43, 93], is based on a continuum description of these active particles, transferred from the classical theory of diffusiophoresis [12]. Although this approach involves numerous assumptions, which are discussed in detail in Refs. [38, 41, 43, 93, 94], a qualitative agreement between the theoretical predictions and available experimental results has been reported [31, 32]. On the other hand, a strong sensitivity of the self-propulsion velocity even on tiny traces of salt in the solution [95] seems to indicate a more complex picture of the motion mechanism. Furthermore, for a “dimer” model of an active particle (an active spherical colloid and an inert one of a different radius, connected via an infinitely thin rigid rod) quantitative agreement has been reported between this continuum description and the results of particle based numerical simulations [96]. Recently, a theoretical formulation of self-diffusiophoresis within the framework of classical non-equilibrium thermodynamics has been proposed [38, 94]. The influence of the details of the chemical reaction and of the transport of the reactants and products on the emerging self-phoretic motion has also been studied recently [94, 97–100].

In the context of chemically active particles, the question of the detailed structure of the non-equilibrium steady-state density distributions around active particles, which is central to the present study, has been investigated in Refs. [39, 40], as well as recently in Refs. [94, 99, 101, 102]. Focusing on spherical colloids with catalytically active spherical caps, in Refs. [94, 101, 102] the number density fields have been calculated for various types of interactions (hard core, exponentially decaying, power law resembling van der Waals interactions). These calculations have been carried out as perturbation series in the Peclet number, which for these active colloids is typically small (see, c.f., Sec. 2), and in the range of the interactions between the reactive species and the colloid at which these are significant with respect to the thermal energy (e.g., more than a percent of the latter). These ranges are assumed to be short compared to the size of the colloid. (If this assumption does not hold, carrying out numerical simulations seems to be the only option available [94, 102].) In principle, this systematic expansion allows one to estimate the accuracy of the approximation caused by truncating the expansion at a certain order, but it has the drawback of a dramatic increase in the difficulty of obtaining closed form expressions beyond the first or second term in the expansion. For the dimer-sphere model with one catalytic sphere rigidly connected to an inert one, in Refs. [39, 40, 99] a Boltzmann-like *ansatz* was employed for the non-equilibrium distribution of reactants and products. The prefactor of these distribution was chosen to be the corresponding solution of the steady-state diffusion equation in the absence of interactions (other than the impenetrability of the *active* sphere) and with the surface of the catalytic sphere acting as a sink for the reactants and a source for the products. Under the assumption that the influence of the inert sphere on the diffusion is negligible, the reactant and product distribution profiles have been calculated. Obviously, in this case the accuracy of these approximations cannot be assessed intrinsically but only *a posteriori* via comparison with results from experiments or numerical simulations. For

example, in Ref. [99] it has been shown that such *approximate analytic* results are in good agreement with data obtained from direct MD simulations. We note here, however, that as discussed in Ref. [42] it is important to account for the distortion of the density distributions due to the impenetrability of the inert sphere – in particular if the active sphere is only partially covered by catalyst and the two spheres do not touch – in order to fully understand how the inert sphere facilitates or hinders the emerging motion of the dimer.

1.2. Outline of the paper

Here we study in detail a mesoscopic model of an active colloid with a catalytic patch on its surface (see Fig. 1), so that the reactants, diffusing in a (*chemically passive*) solvent, react at this part of the surface by converting themselves into (diffusive) reaction products. The initial distribution of the reactants is taken to be homogeneous, but in the course of time and near the colloid a depletion zone for the reactants can emerge. We first focus on a simple reaction process in which a reactant A converts itself into a single product molecule B , but further on we consider also the more general dissociation reaction $A \rightarrow B + C$, in which two product molecules B and C emerge upon contact of an A molecule with the catalytic patch. We note that this latter process directly connects with, e.g., the dissociation of hydrogen peroxide into water and oxygen which has often been used in experimental realizations of chemically automotiv particles (see, e.g., Refs. [4, 31, 34].)

We focus on understanding the steady-state structure of the number density fields of the product(s) and reactants near the active colloid by taking into account that reactants and products may have different diffusion coefficients and different interaction potentials with the colloid. Distinct from the related previous approaches in Refs. [39, 40, 94, 99, 101, 102] discussed above, in order to calculate these non-equilibrium steady-state distributions we adopt an idea proposed previously and studied in the context of calculating chemical reaction rate constants [103]. By replacing therein the position dependent sink (for the reactant) and source (for products) boundary conditions on the surface of the active particle with certain effective ones, a *completely analytical* calculation of these steady-state density profiles can be carried out for quite general types of interactions between the diffusing species and the colloidal particle. These results allow us to compute that *part* of the force experienced by the colloidal particle which is solely due to the self-generated non-equilibrium spatial distributions of the reactive species. (We note that, on the other hand, the same interactions generate a force of the colloid acting on the reactive species which via their interaction with the solvent, encoded *inter alia* in the viscosity of the solution, transmit body forces acting on the solvent, inducing hydrodynamic flow and thus in turn a hydrodynamic force on the colloid (see, c.f., Sec. 4). At steady-state, and in the absence of external forces or torques acting on the colloid or on the fluid, this second *part* of the force experienced by the colloidal particle exactly cancels the first one, and therefore the net force on the

colloid vanishes.) This part of the force can be used to calculate either the hydrodynamic flow of the solution (i.e., the pumping strength) induced by the active colloid (if the colloid is spatially fixed, e.g., by optical tweezers) or the velocity of the colloid, if the colloid is free to move. Our analysis is reliable as long as in the steady state the diffusion of the reactants and product molecules – here and in the following referred to also as “solutes” – and the hydrodynamics in the system are such that the Peclet number (i.e., the ratio of the displacement of the solutes due to convection to that due to diffusion) and the Reynolds number (i.e., the ratio of the inertial to the viscous contribution to the hydrodynamic flow of the solution) are small (see Sec. 2). This implies that we disregard any change of the density distributions due to the flow of the solution. In this case, the diffusive and the convective (i.e., hydrodynamic) transport are effectively decoupled^{††}. The dependence of these quantities (i.e., the velocity of the colloid, if it is free to move, or the hydrodynamical pumping of the solution generated by an immobilized colloid) on the size of the colloid emerges naturally from the interplay between the reaction and diffusion constants, generalizing the results reported in Refs. [98, 106]. Therefore these results for the non-equilibrium spatial distributions of the reactive species – besides being of interest in their own right – can be immediately adopted in order to calculate the steady-state velocity of the self-propelled particle.

As a by-product of our analysis, in the case of triangular-well interaction potentials between the reactants and the colloidal particle we obtain several new results for effective reaction constants which, within the framework of the classical Smoluchowski theory of chemical kinetics [107], describe the reaction rates occurring at particles with inhomogeneous catalytic activity at their surface.

In the context of active particles, the detailed calculations and analyses noted above are motivated, *inter alia* by the following points:

- Most of the experimental studies of active particles have employed microscopy in order to trace the particle motion and to extract the corresponding velocity. However, carrying out such studies for a three-dimensional, bulk motion of active particles and determining their velocity V_{free} is very challenging. In Sec. 4.3 we show that measurements of the stall force, e.g., by employing an optical trapping of the particle, provide the same information as the knowledge of the velocity V_{free} in the bulk. In Sec. 4 the results of such measurements are related to detailed properties of the system, such as the coverage by catalyst, the interaction potentials between the particle and the molecular species, the rate of reaction, and the diffusion constants.
- In a stall configuration (“pumping”, i.e., although the particle is motionless, the fluid is in motion because of the reactions at the surface of the particle and of the interactions between molecular species and the particle), the stall force is balanced by a contribution solely due to the interactions between molecular species and

^{††}An analysis of the motion of a self-propelled colloid accounting for a non-zero Peclet number can be found in Refs. [104, 105].

the particle and a hydrodynamic contribution due to the flow. The latter can be inferred eventually by mapping the flow around the particle using particle image velocimetry. If it is possible to independently map the distribution of chemical species around the immobilized colloid (see, e.g., Ref [108]), the expressions for F_{chem} in Secs. 4.3 and 5 in connection with specific models for the interaction potentials allow one to estimate the parameters characterizing the potentials.

- If the interaction potentials between the various molecular species and the particle are known, measurements of the stall force for particles of different radii R provide the means, via the predicted dependence of the stall force on the radius (Sec. 4), for a critical test of the model assumptions for the mechanism of reaction and motion. Furthermore, by repeating such experiment at various temperatures of the system, and thus eventually exploring the crossover regime between the kinetically-controlled and the diffusion-controlled ones, the confidence limits of the model can be tightened.

The outline of the paper is as follows. In Sec. 2 we define our model for a translationally and rotationally immobile, chemically active colloid immersed in an unbounded system with randomly dispersed diffusive reactants. Section 3 is devoted to calculate the stationary density profiles of mutually non-interacting A (reactant) and B (product) molecules around the immobile colloid with a reactive patch covering partly its surface. There we also describe the self-consistent approximation used to determine the coefficients in the expansions of the density profiles in terms of eigenfunctions. Extending our approach towards the general case of a dissociation reaction (such as, e.g., $A \rightarrow B + C$) is straightforward (see Appendix B). In Sec. 4 we first calculate F_{chem} - that part of the force exerted on the immobile colloid which is due to its molecular interactions with the solvent and the solute molecules (i.e., species A , B , etc.), as well as that due to the hydrodynamic flow of the solution induced by the spatially non-uniform density profiles of the reactant and the products. Furthermore, by employing the reciprocal theorem in the presence of distributed body forces on the fluid [109,110], we obtain an explicit expression for the self-propulsion velocity \mathbf{V} of the colloid if it is free to move. Moreover we also derive an explicit expression for the stall force necessary to immobilize the active colloid which otherwise would move freely. In Sec. 5 these results are discussed further for the particular case of triangular-well interaction potentials. There, we present explicit expressions for the chemical force, the stall force, and the self-propulsion velocity as functions of the parameters of the triangular-well interaction potentials, the diffusion coefficients, the radius of the colloid, the size of the catalytic patch, and the chemical rate constants. The dependences on these parameters are discussed in detail and we highlight several counter-intuitive effects, such as that (i) for certain parameters F_{chem} and \mathbf{V} may have different signs; (ii) \mathbf{V} is a non-monotonic function of the value of the interaction potential at the surface of the colloid, and (iii) the maximal self-propulsion velocity, as function of the size of the catalytic patch, is in general attained at coverages by catalyst being smaller than one half. We summarize the

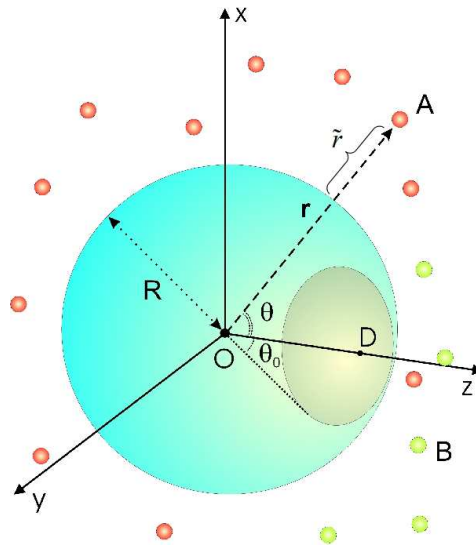


Figure 1. An immobile spherical colloid of radius R is centered and fixed at the origin O . A spherical cap with opening angle θ_0 and centered around the point D acts as a catalytic “patch” on the surface of the colloid. The z -axis runs through D . A and B are the reactant and product molecules, respectively. In view of their low number densities, they are considered to be pointlike. The position vector \mathbf{r} with $|\mathbf{r}| = r$ of a molecule A forms an angle θ with the symmetry axis. The molecule A has a distance \tilde{r} from the surface of the colloid so that $\tilde{r} = r - R$. The solvent molecules are not shown; they form a homogeneous background acting as a heat bath. The solvent is passive with respect to the chemical reaction.

results in Sec. 6 along with our conclusions. Certain important derivations are collected in the Appendices A - D. In Appendix E we provide a summary of our notations which is meant to ease following the text.

2. Model

We consider a macroscopically large reaction bath of volume \mathcal{V} in which a spherical colloidal particle of radius R is immersed. We choose the origin of the coordinate system to be at the center of the colloid (see Fig. 1). We consider two situations: either an immobile colloid (e.g., held by an optical tweezer or a very thin tethered spring), or an unconstrained colloid which at steady state moves with velocity \mathbf{V} through the solution. (In the absence of thermal fluctuations, due to the axial symmetry of the system the axis of the colloid does not rotate.) In the latter case, the coordinate system is attached to (and thus co-moving with) the colloid. The reaction bath consists of solvent molecules S , reactant molecules A , diffusing with diffusion coefficient D_A , and (after some time) product molecules B , diffusing with diffusion coefficient D_B . The reactant molecules A (molecular mass m_A), the product molecules B (molecular mass m_B), and the solvent molecules (molecular mass m_S) are much smaller than the colloid, so that the solution can be approximated as a continuum, apart from density oscillations in the molecular

vicinity of the colloid surface. The number densities (number of molecules per volume) of A and B molecules are taken to be very small compared with the number density of the solvent; therefore we assume that there are no AA , BB , and AB interactions. The interactions between the A (B) molecules and the solvent are encoded, together with those among the solvent molecules, *inter alia* in the viscosity μ of the solution treated as a continuous medium; they enter as well, e.g., via the Stokes-Einstein relation, into the corresponding diffusion coefficient D_A (D_B). The solution is assumed to behave as an incompressible, Newtonian fluid.

A spherical cap of the surface of the colloid particle, lying within the angular region $0 \leq \theta \leq \theta_0$ centered around D (see Fig. 1), has the following “catalytic” properties: As soon as an A molecule approaches the surface of the colloid at any point belonging to the catalytic patch (CP), within a minimal distance a (where $a \ll R$ is of the order of the size of the A molecule), it undergoes with probability p an irreversible reaction (conversion) into a product molecule B :



The probability p characterizes the elementary reaction act: $p = 0$ means that no reaction occurs, while for $p \rightarrow 1$ one has a “perfect” reaction, i.e., A turns into B upon any encounter with the surface. We assume that the catalyst is neither consumed by the reaction in Eq. (1), nor temporarily “passivated” by an intermediate product, and thus at any time it can participate actively in an unlimited number of chemical transformations. The solvent, acting as a heat bath, serves as a source or a sink of heat if the catalytic reaction is endothermic or exothermic, respectively. For reasons of conceptual clarity, we consider only the case that all species in the solution (S , A , B , etc.) are electrically neutral. The extension to the case of ionic species, which requires to consider charge conservation and its coupling to mass transport, eventually can be treated similarly to the cases discussed in, e.g., Refs. [93–95, 101].

In what follows we shall also consider a more general reaction scheme, corresponding to a catalytically induced dissociation reaction of the form



in which the reactant A , upon contact with the catalytic patch, breaks up into a pair of products B and C (with the latter two, in the general case, being different from the solvent molecules) created at a certain distance apart of each other. The diffusion coefficient of the C molecules will be denoted as D_C . Such a reaction is inspired by Pt-catalyzed dissociation of hydrogen peroxide into water and oxygen molecules, which has been used in many experimental realizations of self-propelling particles [97]. In the case of peroxide decomposition, if the solvent S is water the product molecules C are also water molecules so that the reaction produces excess solvent. The excess amount of solvent, which emerges in the course of this reaction is small because it is controlled by the concentration of A molecules (hydrogen peroxide) which is small. In this particular case the reaction scheme in Eq. (2) reduces to the simpler one in Eq. (1).

The initial state of the system, i.e., before the immersion of the chemically active colloid (or before switching on its catalytic activity), is that of a well stirred reaction bath: the A molecules are uniformly distributed within the reaction bath with mean number density $n_0^{(A)} = n_0$. (But in the course of time, upon turning on the reaction, a non-uniform concentration profile can emerge.) Initially the B molecules are absent in the system. The bath is in contact with a reservoir of A molecules which maintains this density $n_0^{(A)} = n_0$ at distances far away from the colloid at all times. We furthermore assume that the reaction bath is also in contact with a perfect sink of B molecules so that $n_0^{(B)} = 0$ far away from the colloid at all times; together with the reservoir for A molecules, this ensures that a steady state can be maintained in the bath if the reaction is active. As mentioned before, the mean number densities of the A and B molecules are assumed to be, at all times, much smaller than the mean number density $n_0^{(S)}$ of the solvent molecules; therefore the latter is assumed to be at all times approximately equal to its initial value $n_0^{(S)}$ before the reaction is turned on. The colloid is impermeable to any of the molecules (A , B , or S) in the mixture.

The solvent molecules interact among themselves and with the A and B molecules. As noted above, these interactions are, *inter alia*, accounted for by the viscosity μ of the mixture and by the diffusion constants D_A and D_B . They also interact with the colloid via a radially symmetric interaction potential $\tilde{\Phi}_S(\tilde{r})$ (per molecule of solvent), in addition to the hard core repulsion accounting for the impermeability of the colloid. Due to the spherical symmetry, for a molecule located at \mathbf{r} this distance from the colloid is given by $\tilde{r} = r - R$ (see Fig. 1) and thus for convenience we introduce the radially symmetric potential $\Phi_S(r) := \tilde{\Phi}_S(r - R)$. We account for the hard-core repulsion via $\Phi_S(r \leq R) = \infty$. (Note that in the latter condition the molecules are implicitly treated as pointlike particles because of their size being much smaller than R .) As already noted in the Introduction, we assume that the solvent is passive with respect to the reaction and that it acts as a macroscopic heat bath, which keeps the temperature constant even in the presence of the reactions.

Similarly, the A and B molecules interact with the colloid via an interaction potential $\tilde{\Phi}_{A,B}(\tilde{r})$ (per molecule), respectively, in addition to the hard core repulsion which makes the colloid impermeable for the molecules in the mixture. We introduce the radially symmetric potentials $\Phi_{A,B}(r) := \tilde{\Phi}_{A,B}(r - R)$ and account for the impenetrability of the colloid via $\Phi_{A,B}(r \leq R) = \infty$. Thus we disregard the possibility that the catalytic patch introduces an angular dependence on θ of any of the interaction potentials $\Phi_{A,B,S}(r)$ between the molecules and the colloid, as well as the influence of the eventual size disparity between the three types of molecules on the location of the "hard wall" surface of the colloid (see also the succinct discussion below). For reasons of having simple notations later on (see, c.f., Sec. 3), we also introduce here the interaction potentials of the A and B molecules with the colloid relative to the corresponding potential for the solvent molecules weighted by the ratio of the mass of

the A (B) molecules to the mass of the solvent molecules (see Appendix A):

$$W_{A,B} := \Phi_{A,B}(r) - \frac{m_{A,B}}{m_S} \Phi_S(r), \quad r > R. \quad (3)$$

For the case of the reaction in Eq. (1), mass conservation obviously requires $m_A = m_B$. However, in order to keep the formulation consistent with the more general reaction processes, involving more than one species of product molecules, which are considered later on, we maintain the labels A and B even for this simple case.

Before proceeding with the analysis of the dynamics of the system, it is important to clarify the choice of the position of the hard wall. In general this is a complicated issue for interfaces involving more than two molecular species. Additionally, the divergences of the interaction potentials (and of their derivatives) caused by molecular hard cores in the limit $\tilde{r} \rightarrow 0$ significantly complicate the mathematical arguments given below (see, c.f., Sec. 3). This leads us to use the following approach. Within a point-particle description of all molecular species, the radius R of the colloid, and thus the position of the hard wall, is fixed by the most outward layer of molecules composing the colloid. We assume that each of the molecular pair interactions between a molecule from the colloid and a molecule of species j ($j = A, B, S$) is described well by a Lennard-Jones 6-12 potential. This involves the parameters σ_j (corresponding to the molecular diameter) and ϵ_j (corresponding to the characteristic energy, in units of the thermal energy $k_B T$, where k_B denotes the Boltzmann constant and T the absolute temperature), and leads to the "exact" interaction potentials $W(r)$ which (all of them) diverge as $r \rightarrow R$. Subsequently, the radius R , and therefore the position of the hard wall, is redefined as $R \rightarrow R + \epsilon$, with $0 < \epsilon \ll R$ of the order of a molecular size. These truncated potentials are bounded at $r = R$ (with R interpreted as the shifted radius), at the expense that $W_j(R)$ now turn into phenomenological, effective parameters, and that the results depend on the choice of ϵ . The arbitrariness can be reduced by further modifying the shape of the potentials $W_j(r)$, e.g., by adjusting the point at which their tails are truncated while requiring that the excess adsorption of each component, which is an experimentally measurable quantity, is the same for the shifted and modified potentials and for the exact ones. On one hand this does not eliminate the dependence on the choice of ϵ , on the other hand it provides a prescription based on which, in principle, this dependence can be explored systematically. While this approach cannot be justified rigorously, we note that such a procedure has been employed recently with satisfying results for describing equilibrium properties, such as phase coexistence and interfacial properties, by using triangular-well potentials, "mimicking" (in the above sense) Lennard-Jones interactions [111–113].

Focusing on the reaction scheme given in Eq. (1), the goal is to determine the spatial distributions of the A and B molecules once a steady state has been attained and to study the resulting chemical force $\mathbf{F}_{chem} = \mathbf{F}_{chem}(\theta_0, D_A, D_B, R, p; [W_A, W_B], \mu)$ exerted on the immobile colloid by the inhomogeneously distributed A and B molecules, the velocity \mathbf{V} (as a function of the same parameters) if the colloid is free to move, and the stall force \mathbf{F}_{ext} necessary to immobilize a freely moving colloid. (It is straightforward

to consider the more general dissociation reaction in Eq. (2); therefore we shall merely present the corresponding results without providing their derivation.)

3. Steady state distribution of reactant and product molecules

Within the framework of the classical theory of linear non-equilibrium thermodynamics [94,102,114,115], and under the assumptions of small number densities, negligible cross-diffusion, and small Péclet numbers of the A and B molecules, the dynamics of the number density distributions are governed by the diffusion equations (see Appendix A)

$$\frac{\partial n_j}{\partial t} = D_j \nabla \cdot [e^{-\beta W_j(r)} \nabla (e^{\beta W_j(r)} n_j)] , \quad j = A, B . \quad (4)$$

At steady state, the time derivatives in Eq. (4) are zero, and the resulting partial differential equations are to be solved subject to appropriate boundary conditions.

The coordinate system (see Fig. 1) is chosen such that the z -axis passes through the center of the patch (point D). The system exhibits azimuthal symmetry around the z -axis and therefore the densities $n_{A,B}(\mathbf{r}, t)$ of the A and B molecules, respectively, are independent of the corresponding azimuth angle ϕ around the z -axis.

3.1. Steady state distribution of the reactant

In terms of spherical polar coordinates and by dropping the dependence on the azimuthal angle ϕ , one finds that at steady state the number density n_A of the reactant A molecules fulfills (see Eq. (4))

$$\begin{aligned} 0 = & \frac{D_A}{r^2} \frac{\partial}{\partial r} \left(r^2 \frac{\partial n_A}{\partial r} \right) + \frac{\beta D_A}{r^2} \frac{\partial}{\partial r} \left(r^2 n_A \frac{dW_A}{dr} \right) + \\ & + \frac{D_A}{r^2 \sin \theta} \frac{\partial}{\partial \theta} \left((\sin \theta) \frac{\partial n_A}{\partial \theta} \right) , \end{aligned} \quad (5)$$

where θ is the polar angle measured with respect to the z -axis (see Fig. 1). For Eq. (5) to be well defined for all $r > R$ we restrict our analysis, as discussed in Sec. 2, to interaction potentials $W_A(r)$ which are finite for all $r > R$, have a finite first derivative for all $r > R$, and vanish sufficiently fast as $r \rightarrow \infty$ (see also below and, c.f., Sec. 4).

Equation (5) is to be solved subject to the boundary condition

$$n_A|_{r \rightarrow \infty} = n_0 , \quad (6)$$

which stipulates that the solute number density n_A approaches the reservoir number density n_0 for $r \rightarrow \infty$, and subject to an effectively reflective boundary condition valid at the non-catalytic part of the surface of the colloidal particle ($r = R$, $\theta_0 < \theta \leq \pi$):

$$j_A := -D_A (n'_A + \beta n_A W'_A)|_{r=R} = 0 , \quad \theta_0 < \theta \leq \pi , \quad (7)$$

where $j_A := \mathbf{e}_r \cdot \mathbf{j}_A$ denotes the radial component of the current of A molecules at the point θ on the surface $r = R$ of the particle, $W'_A = dW_A/dr$, and $n'_A = \partial n_A(r, \theta, t)/\partial r$ (see Eq. (4)), with the convention that all the evaluations at $r = R$ are interpreted as evaluating at $r = R + \epsilon \rightarrow R$.

Next we turn to the boundary condition at the catalytic part of the colloid surface which accounts for the conversion of A molecules into B molecules. Under general conditions such a conversion can be taken into account by requiring that at any point within the area of the catalytic patch ($r = R$, $0 \leq \theta \leq \theta_0$) the current of A molecules normal to the surface equals the rate of their annihilation due to the chemical reaction, i.e., by imposing the so-called radiation [123] (or imperfectly absorbing) boundary condition

$$j_A := -D_A (n'_A + \beta n_A W'_A)|_{r=R} = -\kappa n_A|_{r=R}, \quad 0 \leq \theta \leq \theta_0, \quad (8)$$

where $\kappa > 0$, such that the right hand side has the proper meaning of an "annihilation" term. (Eq. (8) can be alternatively interpreted as a current "into the particle" on the left-hand side (lhs), thus reducing the number density of A species in solution, which is given by κn_A on the right-hand side (rhs).) Note that in Eq.(8) j_A varies as function of θ . Before proceeding it is useful to comment on the proportionality factor κ (with the units of length/time). This factor can be expressed [124] as the ratio of the elementary reaction act constant K (volume times number of acts per unit of time within this volume) and the surface area of the catalytic patch:

$$\kappa = \frac{K}{4\pi R^2 f_g}, \quad (9)$$

where $f_g = f_g(\theta_0) = \sin^2(\theta_0/2)$ is the so-called geometric steric factor characterizing the fraction of the surface of the particle covered by the catalytic patch. In turn, the elementary reaction act constant is given by $K \equiv W_0 V_a$ [124], where W_0 is the rate describing the number of reaction acts per unit of time within the volume V_a of the reaction zone. In the present system the reaction occurs within a segment of a spherical shell given by $R \leq r \leq R + a$ and $0 \leq \theta \leq \theta_0$ with a the minimal distance (Fig. 1). This volume is $V_a = 4\pi R^2 a f_g$, $a \ll R$. Thus the proportionality factor is given by

$$\kappa = W_0 a \quad (10)$$

and is independent of θ_0 . Via W_0 this factor depends, however, on the probability p of the $A \rightarrow B$ conversion because $W_0 \propto p/[(1-p)\tau]$, where τ is a typical time spent by an A molecule within the reaction zone [125]. (A full equation for W_0 is not available.) This implies that for $p = 0$ (i.e., no reaction) one has $\kappa = 0$ and the rhs of Eq. (8) vanishes, i.e., in this limit the reflecting boundary condition for the normal current is recovered. For $p \rightarrow 1$ (i.e., the reaction is perfect and A turns into B upon any encounter with the surface) one has $\kappa \rightarrow \infty$. Since we have assumed that the gradient of the interaction potential is bounded for $r \rightarrow R$, the lhs of Eq. (8) is bounded. This can be reconciled with $\kappa \rightarrow \infty$ on the rhs only if in this limit $n_A|_{r=R} \rightarrow 0$ such that $0 < \kappa n_A|_{r=R} < \infty$. Thus in this limit one finds the perfect sink boundary condition. For $\kappa < \infty$ (i.e., $p < 1$), the boundary condition in Eq. (8) is therefore equivalent to the physical assumption that not all encounters of the A molecules with the catalytic part of the surface of the colloid lead to a reaction event.

For systems which are catalytically active as a whole (i.e., $\theta_0 = \pi$) and in the absence of the interaction potential (apart from the hard-core repulsion) between the colloid

and the A molecules, such a boundary condition has first been proposed by Collins and Kimball [123] (see also Ref. [126]) as a generalization of the conventional Smoluchowski theory [107] which stipulates a perfect sink boundary condition. Furthermore, for $\theta_0 = \pi$ an exact calculation of the steady-state diffusion problem defined by Eqs. (4), (7), and (8) is possible for quite general forms of the interaction potential $W_A(r)$ as well as for a spatially varying diffusion constant $D_A(r)$ [127, 128].

In the absence of interactions (apart from the hard-core repulsion) between the colloid and the A and B molecules, the solution of the diffusion equation (Eqs. (5) - (8)) subject to such *mixed* boundary conditions (i.e., different boundary conditions are used on different parts of the boundary of the domain of the equation) has been studied by several groups in the past. This started with the seminal work by Solc and Stockmayer [129, 130], who developed an approximate method to treat this mathematical problem. (For this case of $W_{A,B} = 0$, also several other approximations have been proposed (see, e.g., Refs. [124, 130, 131]).) Moreover, an exact solution based on the so-called dual series relations is available [132, 133]. However, this procedure is not only cumbersome, but it also does not render a transparent, analytical form of the solution and thus masks the physical content of the results.

In what follows we resort to an approximate approach as the one proposed in Ref. [103]. This choice is motivated by the fact that the approach developed in Ref. [103] is rather straightforward and is known to yield – in the absence of interactions – results which are in a good agreement with numerical solutions of the original problem [132]. Here, we generalize this approach by taking into account the interactions between the molecules and the colloid, which are absent in the original work [103]. As a byproduct of our analysis, this allows us to obtain several new results concerning the effective reaction constants and density profiles for systems with heterogeneous reactivity in the presence of interaction potentials.

In accordance with Ref. [103], the boundary condition in Eq. (8) is replaced by

$$-D_A (n'_A + \beta n_A W'_A)|_{r=R} = -Q, \quad 0 \leq \theta \leq \theta_0, \quad (11)$$

where $Q > 0$ is a "trial" constant, independent of θ , which is determined self-consistently by requiring that the *former* condition given by Eq. (8) holds *only* on average over the region $0 \leq \theta \leq \theta_0$ of the catalytic patch, i.e.,

$$D_A \int_0^{\theta_0} d\theta \sin \theta (n'_A + \beta n_A W'_A) \Big|_{r=R} = \kappa \int_0^{\theta_0} d\theta \sin \theta n_A(r = R, \theta). \quad (12)$$

Equations (12) and (11) imply (see also Eq. (8))

$$Q(1 - \cos \theta_0) = \kappa \int_0^{\theta_0} d\theta \sin \theta n_A(R, \theta). \quad (13)$$

Since via Eq. (11) $n_A(r, \theta)$ depends on Q , Eq. (13) represents an implicit equation for $Q(\kappa)$ (see below).

We seek the solution of Eq. (5), which is the steady-state solution of Eq. (4), via the *ansatz*

$$n_A(r, \theta) = n_0 e^{-\beta W_A(r)} \left[1 + \sum_{n=0}^{\infty} a_n g_n(r) P_n(\cos \theta) \right], \quad (14)$$

where a_n are dimensionless coefficients to be determined from the boundary conditions and $P_n(\cos \theta)$ is the Legendre polynomial of order n . We note that the first term on the rhs of Eq. (14) is the *equilibrium* Boltzmann distribution of A molecules around the colloid (see Eq. (6)), e.g., in the absence of the chemical reaction or for an infinitely fast diffusion of A molecules (i. e., $D_A = \infty$) in which case all coefficients a_n vanish (see below). Therefore the second term represents the whole out-of-equilibrium contribution to the concentration distribution due to the chemical reaction and due to a finite value of the diffusion constant D_A of the A molecules.

Upon inserting Eq. (14) into Eq. (5), one finds that the former is the solution of the latter if the functions $g_n(r)$ solve

$$g_n''(r) + \left(\frac{2}{r} - \beta W_A'(r) \right) g_n'(r) - \frac{n(n+1)}{r^2} g_n(r) = 0. \quad (15)$$

Moreover, in order that $n_A(r, \theta)$ given by Eq. (14) satisfies the boundary condition in Eq. (6), the solutions $g_n(r)$ of Eq. (15) are subject to the boundary condition that they vanish for $r \rightarrow \infty$. For each n the solutions $g_n(r)$ of Eq. (15) are defined up to multiplicative constants. Without loss of generality, as explained below, we fix these constants by choosing the normalization $g_n(r = R) = 1$. This renders the coefficients a_n to be unique.

For $n = 0$, from Eq. (15) one finds

$$g_0(r) = R_D \int_r^{\infty} du \frac{e^{\beta W_A(u)}}{u^2} \quad (16)$$

with $g_0(r \rightarrow \infty) = R_D/r$, where R_D is related to the so-called Debye radius (see Ref. [134]):

$$R_D = \left(\int_R^{\infty} du \frac{e^{\beta W_A(u)}}{u^2} \right)^{-1}; \quad (17)$$

note that $R_D = R$ for $W_A = 0$. For $n \geq 1$, Eq. (15) cannot be solved analytically for a generic interaction potential $W(r)$. However, for $r \rightarrow \infty$ the interaction potentials of interest for our system decay $\sim 1/r$ or faster so that $\beta W_A'(r) \ll 1/r$ for $r \gg R$. Accordingly, at large distances $r \gg R$ Eq. (15) reduces to the differential equation satisfied by the radial functions of the Laplace equation. This ensures that for any $n \geq 1$ Eq. (15) admits a solution $g_n(r)$ with the asymptotic behavior $g_n(r \gg R) \sim r^{-(n+1)}$ and thus obeying the boundary condition to vanish for $r \rightarrow \infty$.

Combining the boundary conditions in Eqs. (7) and (11) and inserting therein the expansion given by Eq. (14) leads to

$$\sum_{n=0}^{\infty} a_n g_n'(R) P_n(\cos \theta) = \frac{Q e^{\beta W_A(R)}}{D_A n_0} \Theta(\theta_0 - \theta), \quad (18)$$

where $\Theta(x)$ is the Heaviside step function ($\Theta(x) = 1$ for $x \geq 0$ and zero otherwise). Multiplying both sides of Eq. (18) by $(\sin \theta) P_n(\cos \theta)$, integrating them over θ from 0 to π , and using the orthogonality of the Legendre polynomials one obtains

$$a_n = \frac{Q e^{\beta W_A(R)} \phi_n(\theta_0)}{2 D_A n_0 g'_n(R)}, \quad n \geq 0, \quad (19)$$

where

$$\phi_n(\theta_0) = P_{n-1}(\cos \theta_0) - P_{n+1}(\cos \theta_0), \quad n \geq 0, \quad (20)$$

with the standard convention $P_{-1}(\cos \theta_0) = 1$. We note that because $a_n \sim 1/g'_n(R)$, one has $a_n g_n \sim g_n/g'_n$. Thus in the final result in Eq. (14) the normalization amplitude of g_n drops out and $n_A(r, \theta)$ is independent of the choice for this normalization, as it should.

After substituting a_n from Eq. (19) into Eq. (14), inserting the resulting expression into Eq. (13), and taking advantage of the relation

$$\phi_n(\theta_0) = (2n + 1) \int_0^{\theta_0} d\theta \sin \theta P_n(\cos \theta), \quad (21)$$

one finds the following explicit expression for Q :

$$Q = \frac{4\kappa n_0 D_A e^{-\beta W_A(R)} \phi_0(\theta_0)}{\left(4D_A \phi_0(\theta_0) - \kappa \sum_{n=0}^{\infty} \frac{\phi_n^2(\theta_0) g_n(R)}{(n+1/2) g'_n(R)}\right)}, \quad (22)$$

where $\phi_0(\theta_0) = 1 - \cos \theta_0 = 2 \sin^2(\theta_0/2)$. In the following, due to the normalization choice for the functions $g_n(r)$ the ratio $g_n(R)/g'_n(R)$ inside the sum will be replaced by $1/g'_n(R)$. This concludes the calculation of the distribution $n_A(r, \theta)$ of reactant molecules (Eqs. (14), (15), and (19) - (22)).

Upon closing this subsection we emphasize that within the expansion in Eq. (14) the radial and angular forms of the functions are exact. Only the coefficients a_n are determined approximately, using a generalized self-consistent approach [103]. In the following, we shall evaluate the contributions to the force F_{chem} exerted on the immobile colloid (and, if it is free to move, to its velocity V) stemming from the interactions of the colloid with the A molecules, the spatial distribution of which is given by Eq. (14) with the coefficients a_n defined by Eqs. (19) and (22) (and similarly due to the interactions with the B and C molecules, the distributions of which will be determined in Subsec. 3.3 and Appendix B). To this end, one has to integrate the distribution in Eq. (14) multiplied by the gradient of the interaction potential in order to determine F_{chem} , and multiplied by the gradient of the interaction potential and by the axially symmetric part of the velocity field in order to calculate V , which will be carried out in Sec. 4. We proceed by showing that the contributions to F_{chem} and V due to the interactions of the colloid with the A molecules are given by $F_{chem} = (4\pi n_0/3) a_1 I_A$ and $V = (2n_0/9\mu R) a_1 \mathcal{J}_A$, where I_A and \mathcal{J}_A are *exact* functional expressions of the interaction potentials and only the coefficient a_1 , which due to the symmetry of the system is the only relevant one, is determined approximately.

The accuracy of the approximation for the coefficient a_1 can be estimated from the following simple argument. Suppose that one is able to solve the mixed boundary problem defined by Eqs. (5), (6), (7) and (8) exactly, and hence, to obtain the exact expressions for the expansion coefficients a_n in Eq. (14). Then, inserting this expansion into Eq. (8), multiplying both sides by $\sin(\theta)\cos(\theta)$ and integrating over θ from 0 to π (recall that $j_A := 0$ for $\theta_0 < \theta \leq \pi$), one obtains the following relation between the exact coefficient a_1 and the exact current j_A (which in general is a function of θ):

$$a_1 = -\frac{3}{4} \frac{e^{\beta W_A(R)}}{n_0 D_A g_1'(R)} \int_0^{\theta_0} j_A \sin(2\theta) d\theta. \quad (23)$$

On the other hand, the relations in Eqs. (19) and (21) provide the following approximate expression for a_1 :

$$a_1 = \frac{3}{4} \frac{e^{\beta W_A(R)}}{n_0 D_A g_1'(R)} Q \int_0^{\theta_0} \sin(2\theta) d\theta. \quad (24)$$

Therefore the accuracy of estimating the coefficient a_1 via using the self-consistent approach [103] turns out to be the same as the one associated with approximating the integral on the rhs of Eq. (23) as

$$-\int_0^{\theta_0} j_A \sin(2\theta) d\theta \approx Q \int_0^{\theta_0} \sin(2\theta) d\theta. \quad (25)$$

On physical grounds, one may expect that j_A depends very weakly on θ within the interior part of the catalytic patch away of its periphery. Hence, for the major part of the integration interval the current j_A will factor out from the integral rendering Eq. (25) to be an equality (compare with Eqs. (8) and (11)). An appreciable dependence of the current on θ may appear only in the vicinity of $\theta = 0$ and $\theta = \theta_0$, where j_A drops to zero. Therefore one can expect that the self-consistent approximation in Ref. [103] will provide an accurate estimate for a_1 provided that θ_0 is not too small. Remarkably, even in the limit $\theta_0 \rightarrow 0$, in which one may expect the most significant deviations, the self-consistent approximation is surprisingly reliable, as evidenced by the numerical analyses in Ref. [132] and more recently in Ref. [135], which studied the so-called narrow escape problem in the presence of long-ranged interactions with the confining boundary using essentially the same approximate approach as the present one. It was shown in Ref. [135] that the self-consistent approximation captures adequately even the dependences of those terms, which dominate in the limit $\theta_0 \rightarrow 0$, on all pertinent parameters and it only slightly underestimates the numerical factors.

Finally, in Sec. 5 we shall show that for the particular case $\theta_0 = \pi/2$ (i.e., for the so-called Janus colloids) and for short-ranged triangular-well interaction potentials, our general results reproduce the known limiting forms of the self-propulsion velocity as obtained in Ref. [98] within an approach based on the concepts of the effective Derjaguin length and the phoretic slip.

3.2. Chemical kinetics interpretation: effective reaction constants

In order to translate our results into the usual nomenclature of chemical kinetics, we follow Refs. [103, 127] and introduce an “effective” reaction constant K_{eff} , which accounts for the combined effect of the nonzero reaction probability at the catalytic patch and the diffusive transport of the reactants to the patch. K_{eff} is defined as the number of A molecules, which are distributed according to $n_A(r, \theta)$ and which would flow, per time, through the surface $r = R$ if the colloid was permeable, divided by n_0 . Using Eqs. (7), (8), and (12) this takes the form

$$\begin{aligned} K_{eff} &= \frac{2\pi R^2 D_A}{n_0} \int_0^\pi d\theta \sin \theta (n'_A + \beta n_A W'_A)|_{r=R} \\ &= \frac{2\pi R^2 \phi_0(\theta_0)}{n_0} Q. \end{aligned} \quad (26)$$

We note that the coefficients a_n in Eq. (19) can be expressed in terms of this effective reaction constant as

$$a_n = \frac{K_{eff}}{K_S} \frac{e^{\beta W_A(R)}}{R g'_n(R)} \frac{\phi_n(\theta_0)}{\phi_0(\theta_0)}, \quad n \geq 0, \quad (27)$$

where $K_S = 4\pi D_A R$ is the Smoluchowski constant [107]. K_{eff} and K_S have the units of volume per time, as K does.

By replacing Q with the expression in Eq. (22), and by noting that Eq. (16) implies $R_D = -R^2 g'_0(R) e^{-\beta W_A(R)}$, Eq. (26) can be cast into the physically intuitive form

$$\frac{1}{K_{eff}} = \frac{1}{K^*} + \frac{1}{K_{SD} f_{dc}(\theta_0)}, \quad (28)$$

where dc stands for diffusion controlled. The Smoluchowski-Debye constant K_{SD} [134] (compare Eq. (17))

$$K_{SD} = 4\pi D_A R_D \quad (29)$$

equals the flux (divided by n_0) of diffusive molecules, the density of which at $r \rightarrow \infty$ is kept fixed and equal to n_0 , through the hypothetical surface of an immobile, perfectly absorbing sphere interacting with the molecules via a radially symmetric potential $W_A(r)$. The quantity

$$\begin{aligned} K^* &= 2\pi R^2 \phi_0(\theta_0) \kappa e^{-\beta W_A(R)} = \\ &= 4\pi R^2 f_g \kappa e^{-\beta W_A(R)} = K e^{-\beta W_A(R)} \end{aligned} \quad (30)$$

is an *effective* constant for an elementary reaction act factored into a term K (see Eq. (9)), which depends only on the reaction kinetics κ and the geometry (via θ_0) of the catalytic patch, and a term which depends only on the interaction potential. In the *diffusion-controlled* limit $K^* \rightarrow \infty$ (in the sense that $K^* \gg K_{SD} f_{dc}(\theta_0)$, but not necessarily infinitely large, see below), the quantity

$$f_{dc}(\theta_0) = 2\phi_0^2(\theta_0) / \left(g'_0(R) \sum_{n=0}^{\infty} \frac{\phi_n^2(\theta_0)}{(n + 1/2) g'_n(R)} \right) \quad (31)$$

plays the role of an *effective* steric factor: it shows how the reaction rate in Eq. (29) is reduced effectively due to the fact that the catalytic patch occupies only some part of the colloid surface. As will be seen below, it shows a different angular behavior as compared with the purely geometric steric factor $f_g = \sin^2(\theta_0/2)$. We emphasize that the full functional form of $W_A(r)$ enters both into K_{SD} (see Eqs. (29) and (17)) and into f_{dc} (via $g_n(r)$; see Eqs. (31) and (15)) whereas K^* depends only on $W_A(r = R)$ (Eq. (30)). (Here we recall that the argument $r = R$ must be interpreted as $r = R + \epsilon \rightarrow R$ and that we assume the potential and its derivatives to be bounded at $r = R + \epsilon$.)

Equation (28), which resembles the law of addition of inverse resistances, bears out the combined effect of two rate-limiting steps: the random, diffusive search of the A molecules for the catalytic patch and the subsequent elementary reaction act. Such a form allows one to distinguish easily between the so-called *diffusion-controlled* limit, in which the time needed by the A molecule to diffuse to the catalytic patch is the rate-limiting step (with the elementary reaction contribution $1/K^*$ itself being negligible in comparison), and *kinetically-controlled* reactions for which the opposite holds, i.e., $K^* \ll K_{SD}f_{dc}(\theta_0)$. In the following, we shall denote this limit symbolically as " $D_A \rightarrow \infty$ ", which does not imply, however, that D_A is infinitely large, but it only means that the latter inequality holds.

One can readily check that in the absence of interaction potentials, i.e., for $W_A(r) \equiv 0$, the result in Eq. (28) reduces to (see Eq. (30))

$$\frac{1}{K_{eff}^{(0)}} = \frac{1}{K} + \frac{1}{K_S f_{dc}^{(sl_s)}(\theta_0)}, \quad (32)$$

with $K_{eff}^{(0)} \equiv K_{eff}[W_A(r) \equiv 0]$. This is the result presented in Ref. [103] and earlier, within the framework of a different approximate approach, in Ref. [130]. In this case the steric factor in Eq. (31) attains the form

$$f_{dc}^{(sl_s)}(\theta_0) = 2\phi_0^2(\theta_0) / \sum_{n=0}^{\infty} \frac{\phi_n^2(\theta_0)}{(n+1/2)(n+1)}, \quad W_A(r) \equiv 0, \quad (33)$$

where the superscript "sls" is a tribute to Shoup, Lipari, and Szabo, who reported this result in Ref. [103]. The steric factor $f_{dc}^{(sl_s)}(\theta_0)$ is a monotonically increasing function of θ_0 , interpolating between $f_{dc}^{(sl_s)}(\theta_0 = 0) = 0$ and $f_{dc}^{(sl_s)}(\theta_0 = \pi) = 1$ (see, e.g., Fig. 3 in Ref. [132]). These limits can be understood as follows. Since for $n \geq 0$ the Legendre polynomials have defined parity, $P_n(x) = (-1)^n P_n(-x)$, and satisfy $P_n(1) = 1$, it follows that for $\theta_0 \rightarrow \pi$ one has $\phi_n(\pi) = 2\delta_{0,n}$ for $n \geq 0$ (Eq. (20)). Thus for $\theta_0 \rightarrow \pi$ in the sum in the denominator only the term $n = 0$ survives and therefore $f_{dc}^{(sl_s)}(\theta_0 = \pi) = 1$. The limit $\theta_0 \rightarrow 0$ is more involved because $P_n(1) = 1$ and thus $\phi_n(\theta_0 = 0) = 0$ for all $n \geq 0$. However, noting that to first order in $(1 - \cos \theta_0)$ one has $\phi_n(\theta_0 \rightarrow 0) = (2n+1)(1 - \cos \theta_0)$ (Eq. (21)), the steric factor $f_{dc}^{(sl_s)}$ behaves as $f_{dc}^{(sl_s)}(\theta_0 \rightarrow 0) \propto 1 / \sum_{n=0}^{\infty} \frac{(2n+1)^2}{(n+1/2)(n+1)}$ and thus vanishes in the limit $\theta_0 \rightarrow 0$ due to the divergence of the series in the denominator. The exact asymptotic behavior in this latter limit was analyzed thoroughly in Refs. [103] and [132], and more recently, in Ref. [135] with the result that in the limit $\theta_0 \rightarrow 0$ the effective steric factor behaves as $f_{dc}^{(sl_s)}(\theta_0 \rightarrow 0) = (3\pi/32)\theta_0$. The geometric steric factor

$f_g = \sin^2(\theta_0/2)$ behaves as $f_g(\theta_0 \rightarrow 0) = (\theta_0)^2/4$ and hence is much smaller than $f_{dc}^{(sls)}$. This implies that in the limit $\theta_0 \rightarrow 0$ the first term on the right-hand side of Eq. (28) becomes the dominant one ($K^* \sim (\theta_0)^2$ while $K_{SD} f_{dc}(\theta_0) \sim \theta_0$ for $\theta_0 \rightarrow 0$), so that the reaction becomes kinetically controlled. Interestingly, in the case in which precisely one half of the particle is covered by catalyst, i.e., for a so-called Janus particle, the value $f_{dc}^{(sls)}(\theta_0 = \pi/2) \approx 0.706$ substantially exceeds 1/2, which is the value of the geometric steric factor for the same coverage.

In the case $W_A \neq 0$, without the explicit dependence of g_n on $W_A(r)$ being available in closed form for arbitrary θ_0 , one cannot state much concerning the behavior of the steric factor in Eq. (31), except that (based on the same argument as above) for arbitrary potentials $W_A(r)$ it equals 1 for $\theta_0 = \pi$, i.e., $f_{dc}(\theta_0 = \pi) = 1$ if the whole surface of the particle is catalytic. In the opposite limit of having no catalytic properties, i.e., $\theta_0 \rightarrow 0$, some general statements concerning the form of the coefficients belonging to the leading terms were made recently [135].

As discussed above, in the case that the catalytic patch covers the entire surface of the colloid, i.e., if $\theta_0 = \pi$, one has $f_{dc}(\theta_0 = \pi) = 1$ for arbitrary $W_A(r)$. In this case one therefore recovers the classic result [127] (see also Refs. [136,137])

$$\frac{1}{K_{eff}} = \frac{1}{K^*} + \frac{1}{K_{SD}}, \quad \theta_0 = \pi, \quad W_A(r) \neq 0. \quad (34)$$

If in addition there is no interaction potential $W_A(r)$ one has $K^* = K$ and $R_D = R$. In this case Eq. (34) reduces to the celebrated relation

$$\frac{1}{K_{eff}^{(0)}} = \frac{1}{K} + \frac{1}{K_S}, \quad \theta_0 = \pi, \quad W_A(r) \equiv 0, \quad (35)$$

due to Collins and Kimball [123]. The relation in Eq. (35) can be derived also from microscopic stochastic dynamics which allows one to identify the elementary reaction act constant K through the reaction probability p [138].

In the diffusion-controlled limit corresponding to $K^* \rightarrow \infty$ (and with D_A fixed, such that the molecular diffusion is the rate-limiting step), the effective reaction constant K_{eff} is given by (see Eq. (28))

$$K_{eff}(K^* \rightarrow \infty) = K_{SD} f_{dc}(\theta_0). \quad (36)$$

Combining Eqs. (26) and (36), in the diffusion-controlled limit the factor Q can be written as

$$Q(K^* \rightarrow \infty) = \frac{n_0 K_{SD} f_{dc}(\theta_0)}{2\pi R^2 \phi_0(\theta_0)}. \quad (37)$$

In this case, the coefficients a_n in Eq. (27), which enter into the series representation of the number density profile of the reactant (Eq. (14)), can be written as

$$a_n(K^* \rightarrow \infty) = \frac{R_D}{R} \frac{e^{\beta W_A(R)}}{R g'_n(R)} \frac{\phi_n(\theta_0)}{\phi_0(\theta_0)} f_{dc}(\theta_0), \quad n \geq 0. \quad (38)$$

Finally, for completeness we note that according to Eq. (27) in the kinetically-controlled limit, in which K^* is fixed while $D_A \rightarrow \infty$, such that $K_{eff} \rightarrow K^*$, the coefficients a_n reduce to

$$a_n(D_A \rightarrow \infty) = \frac{K}{K_S} \frac{1}{R g'_n(R)} \frac{\phi_n(\theta_0)}{\phi_0(\theta_0)}, \quad n \geq 0. \quad (39)$$

Since $K_S = 4\pi D_A R$, in this limit the coefficients a_n decay with D_A as $a_n \sim 1/D_A$ so that n_A converges to the equilibrium distribution $n_A(r) = n_0 e^{-\beta W_A(r)}$ (see Eq. (14)) if $D_A \rightarrow \infty$. In this extreme limit n_A does not depend on the angle θ , and thus Eq. (11) turns to an exact expression. If the diffusion constant of the A molecules is finite, (recall that the kinetically-controlled limit should be interpreted as $K^* \ll K_{SD} f_{dc}(\theta_0)$, and thus the coefficients $a_n \neq 0$ are nonzero, albeit small in magnitude), the chemical reaction enforces an angular dependent, out-of-equilibrium steady state for the distribution of the reactant molecules.

3.3. Steady state distributions of the reaction products

For $r > R$ the local number density of the reaction products B obeys the differential equation

$$\begin{aligned} 0 = & \frac{D_B}{r^2} \frac{\partial}{\partial r} \left(r^2 \frac{\partial n_B}{\partial r} \right) + \frac{\beta D_B}{r^2} \frac{\partial}{\partial r} \left(r^2 n_B \frac{dW_B}{dr} \right) + \\ & + \frac{D_B}{r^2 (\sin \theta)} \frac{\partial}{\partial \theta} \left((\sin \theta) \frac{\partial n_B}{\partial \theta} \right), \end{aligned} \quad (40)$$

which has the same form as Eq. (5). Equation (40) is to be solved subject to a sink boundary condition at macroscopic distances from the colloid:

$$n_B|_{r \rightarrow \infty} = 0, \quad (41)$$

which has to be complemented by the reaction boundary condition across the catalytic patch and the zero current boundary condition across the non-catalytic part of the surface, similar to those for the A molecules. Within the mean-field approximation as used above, these latter two conditions can be combined into the equation

$$D_B (n'_B + \beta n_B W'_B)|_{r=R} = -Q \Theta(\theta_0 - \theta), \quad (42)$$

where we have used the fact that the creation of a B molecule is tied to the annihilation of an A molecule so that here the current is opposite to the one on the right hand side of Eq. (11). (With $Q > 0$, the signs in Eq. (42) correspond, as they should, to molecules of species B being “released” into the solution.) We seek the stationary solution of Eq. (40) via the ansatz

$$n_B(r, \theta) = n_0 e^{-\beta W_B(r)} \sum_{n=0}^{\infty} b_n j_n(r) P_n(\cos \theta), \quad (43)$$

where b_n are dimensionless coefficients to be determined from the boundary condition in Eq. (42). This ansatz solves the stationary Eq. (40) provided the functions $j_n(r)$ are those solutions of

$$j_n''(r) + \left(\frac{2}{r} - \beta W_B'(r) \right) j_n'(r) - \frac{n(n+1)}{r^2} j_n(r) = 0 \quad (44)$$

which vanish for $r \rightarrow \infty$. As for the functions $g_n(r)$ in Eq. (15) we choose the normalization $j_n(r = R) = 1$. For the interaction potential $W_B(r)$ we require similar properties as for W_A , i.e., being continuous and bounded, with continuous and bounded first derivative, and vanishing for $r \rightarrow \infty$ (see the previous subsection). The potential $W_B(r)$ does not comprise the hard-core repulsion, which is taken into account by the boundary condition in Eq. (42). Following the same steps as for the case of the reactants and recalling the relation between Q and K_{eff} in Eq. (26), we obtain the coefficients b_n in the series representation of $n_B(r)$:

$$\begin{aligned} b_n &= - \frac{Q e^{\beta W_B(R)} \phi_n(\theta_0)}{2 D_B n_0 j_n'(R)} \\ &= - \frac{K_{eff}}{4 \pi D_B R} \frac{e^{\beta W_B(R)} \phi_n(\theta_0)}{R j_n'(R) \phi_0(\theta_0)}, \quad n \geq 0. \end{aligned} \quad (45)$$

In the diffusion-controlled limit corresponding to $K^* \rightarrow \infty$ the latter equation reduces to

$$b_n(K^* \rightarrow \infty) = - \frac{D_A}{D_B} \frac{R_D}{R} \frac{e^{\beta W_B(R)} \phi_n(\theta_0)}{R j_n'(R) \phi_0(\theta_0)} f_{dc}(\theta_0), \quad n \geq 0. \quad (46)$$

We note that, via Q (see Eq. (22)) in the boundary condition in Eq. (42), $n_B(r, \theta)$ depends on the characteristics of the A particles such as n_0 , D_A , and $W_A(r)$. On the other hand, $n_A(r, \theta)$ is independent of the characteristics of the B particles; this is due to the absence of interactions between A and B molecules. In Eq. (46) R_D and $f_{dc}(\theta_0)$ are the expressions given by Eqs. (17) and (31), respectively. Thus they are determined by $W_A(r)$ only and are independent of $W_B(r)$.

In the kinetically-controlled limit, corresponding to $D_A \rightarrow \infty$ with K^* fixed such that $K_{eff} \rightarrow K^*$, we have

$$b_n(D_A \rightarrow \infty) = - \frac{K^*}{4 \pi D_B R} \frac{e^{\beta W_B(R)} \phi_n(\theta_0)}{R j_n'(R) \phi_0(\theta_0)}, \quad n \geq 0. \quad (47)$$

In this limit the coefficients b_n are independent of D_A and nonzero.

Finally, we note that the distribution of the product molecules C , in the case of the reaction described in Eq. (2), can be calculated in a similar way. We relegate these straightforward calculations to Appendix B.

4. The force exerted on an immobile colloid and the velocity of a force-free colloid

In this section we consider the two contributions to the force exerted on the colloid due to the chemical reaction. They stem (i) from the hydrodynamic flow of the mixture,

driven by the inhomogeneous distribution of the components and their interactions with the colloid, and (ii) from the interactions with the reactants, products, and solvent molecules. For brevity, we focus on the $A + \text{CP} \rightarrow B + \text{CP}$ reaction (Eq. (1)); the generalization to the case of the catalytically induced dissociation (Eq. (2)) is straightforward and we will merely list the corresponding results.

4.1. Hydrodynamics of the solution

The conservation of momentum for the mixture requires that the barycentric velocity \mathbf{u} satisfies the Navier-Stokes equations [139]. At steady state and under the assumption that the Reynolds number $Re = R\rho U_0/\mu$ is very small (which typically is the case for the flows generated by catalytically active colloids [9, 43, 94, 102]), for an incompressible Newtonian fluid of spatially and temporally constant viscosity μ and mass density ρ , subject to the force density $\tilde{\mathbf{f}}(\mathbf{r})$, the Navier-Stokes equations are replaced by the Stokes equations [139]:

$$\begin{aligned}\nabla \cdot \hat{\mathbf{\Pi}} &= -\tilde{\mathbf{f}} \Rightarrow \mu \nabla^2 \mathbf{u} = \nabla P - \tilde{\mathbf{f}}, \\ \nabla \cdot \mathbf{u} &= 0.\end{aligned}\tag{48}$$

In these equations $\tilde{\mathbf{f}}$ denotes the *external* force density acting on the mixture as a body force (such as, e.g., gravity or the forces due to the interaction of the molecules in the mixture with the colloid) while $\hat{\mathbf{\Pi}}$ is the Newtonian stress tensor

$$\hat{\Pi}_{i,j} = -P \delta_{i,j} + \mu \left(\frac{\partial u_i}{\partial x_j} + \frac{\partial u_j}{\partial x_i} \right).\tag{49}$$

The scalar pressure field $P(\mathbf{r})$, which is equal to 1/3 of the trace of the stress tensor, plays the role of an auxiliary field[¶] ensuring that the velocity field \mathbf{u} obeys the incompressibility condition $\nabla \cdot \mathbf{u} = 0$.

Under the assumption that the mass density ρ of the solution is spatially uniform, gravity plays no role here. Thus for the present system the force density $\tilde{\mathbf{f}}$ acting on the solution is solely due to the interactions of the colloid with the molecules in the mixture:

$$\begin{aligned}\tilde{\mathbf{f}} &= -(n_A \nabla \Phi_A + n_B \nabla \Phi_B + n_S \nabla \Phi_S) \\ &= -\frac{\rho}{m_S} \nabla \Phi_S - (n_A \nabla W_A + n_B \nabla W_B) \\ &=: -\frac{\rho}{m_S} \nabla \Phi_S + \mathbf{f}.\end{aligned}\tag{50}$$

Here we have used the definition (Eq. (3)) of the interaction potentials $W_{A,B}$ and the fact that, by definition, $n_S = (\rho - n_A m_A - n_B m_B)/m_S$ (Eq. (A.1)). Since ρ and m_S are constants, and noting that Φ_S depends only on r , the term $(\rho/m_S)\Phi_S$ can be included

[¶] $P(\mathbf{r})$ is obtained as the solution of the Poisson equation $\nabla^2 P = \nabla \cdot \tilde{\mathbf{f}}$, which follows by taking the divergence of the first equation in Eq. (48), subject to the boundary condition that $P(r \rightarrow \infty) = P_0$, where P_0 is the (spatially constant) bulk value of the pressure. Since no other boundary condition is imposed on P , the remaining integration constants are determined, after solving for \mathbf{u} , by requiring that $\nabla \cdot \mathbf{u} = 0$ is satisfied.

in the definition of the pressure P (i.e., the isotropic part of the stress tensor). Thus the force exerted by the colloid on the small volume element $\delta\mathcal{V}$ of the solution is given by $\mathbf{f} \delta\mathcal{V}$, with $\mathbf{f} = -(n_A \nabla W_A + n_B \nabla W_B)$, and \mathbf{f} replaces $\tilde{\mathbf{f}}$ in Eq. (48).

The solution $\mathbf{u}(\mathbf{r})$ of Eq. (48) is subject to appropriate boundary conditions. At the surface of the colloid we assume the usual no-slip boundary condition to hold. Here, it is convenient to consider the general case that the colloid is in motion with velocity $\mathbf{V} = V \mathbf{e}_z$; the case of an immobile colloid is obtained by setting $\mathbf{V} = 0$. In the laboratory (fixed) system of reference, the no-slip boundary condition on the surface of the colloid then takes the form

$$\mathbf{u}|_{r=R} = \mathbf{V}. \quad (51)$$

Far away from the colloid the mixture is taken to be at rest, i.e.,

$$|\mathbf{u}(r \rightarrow \infty)| = 0. \quad (52)$$

From Eqs. (48), (50), (51), and (52), with the densities n_A and n_B computed according to the steps described in Sec. 3, in principle the hydrodynamic flow $\mathbf{u}(\mathbf{r})$ is obtained (in practice may be in a very involved way) as a function of the yet unknown constant velocity \mathbf{V} of the colloid. The additional equation needed in order to complete the calculation follows from the condition that the colloid is in steady-state motion, which implies a vanishing net force acting on the colloid. Therefore one has

$$\int_{r=R} dS \hat{\mathbf{\Pi}} \cdot \mathbf{e}_r + \int_{\mathcal{V}} d^3\mathbf{r} (-\mathbf{f}) + \mathbf{F}_{\text{ext}} = \mathbf{0}, \quad (53)$$

where the first term is the hydrodynamic force \mathbf{F}_{hyd} acting on the colloid due to the flow of the surrounding solution, and the second term accounts for the force \mathbf{F}_{chem} on the colloid due to the interaction with the molecules in solution. Since the colloid exerts a force $\mathbf{f} d\mathcal{V}$ on the volume element $d\mathcal{V}$ of the solution, due to Newton's third law an opposite force of equal magnitude is exerted by $d\mathcal{V}$ on the colloid. The last term \mathbf{F}_{ext} is the sum of all external forces (e.g., an optical trapping) acting on the colloid. The typical set-up is that the external forces are given and the quantity of interest is the velocity of the colloid \mathbf{V} , which is determined from Eq. (53). We are interested in:

(i) the particular case of force free motion, i.e., finding the velocity \mathbf{V} if $\mathbf{F}_{ext} = 0$; and

(ii) the external force \mathbf{F}_{ext} needed to immobilize the colloid, so that $\mathbf{V} = 0$.

These two quantities are calculated in, c.f., Subsec. 4.3 by using the reciprocal theorem [109, 110] which allows one to by-pass the issue of solving the complex hydrodynamics problem laid out above.

Before proceeding with these analyses, a succinct discussion of each of the terms in Eq. (53) in terms of their experimental accessibility is in order. Obviously, \mathbf{F}_{ext} is that contribution which is simplest to access as it accounts for external, prescribed forces acting on the colloid. The first and second terms account for contributions which seem to be difficult, if not impossible, to separate from each other, and thus *de facto* cannot be accessed directly. The first term, \mathbf{F}_{hyd} , requires knowledge of the hydrodynamic flow

in order to be able to compute the stress tensor $\hat{\mathbf{\Pi}}$. (Here it is important to note that for the system under study the pressure part – including the term $\sim \Phi_S$ – of the stress tensor $\hat{\mathbf{\Pi}}$ is isotropic and therefore does not contribute to \mathbf{F}_{hyd} .) In principle this can be achieved, although being technically very challenging, by using methods such as particle image velocimetry, as shown in Ref. [140] for swimming microorganisms. The second term, which we consider to be the “chemical” contribution \mathbf{F}_{chem} , can be calculated if the distributions of the molecular species can be measured (assuming the potentials $W_{A,B,\dots}$ to be known). While one can think of methods such as fluorescence spectroscopy to determine the spatial distribution of chemical species, if they are fluorescent, it is likely that in general it will be very difficult, if not impossible, to determine experimentally the dependence of these distributions on r and θ . However, as we show in the following subsection, the problem can be reduced to that of knowing only their first moment rather than the whole distribution, which may turn out to be a significant step towards rendering \mathbf{F}_{chem} experimentally accessible.

4.2. Force contribution \mathbf{F}_{chem} due to the anisotropic distributions of reactants, products, and solvent

Once the steady state spatial distributions of reactants (A) and products (B) are known, the force \mathbf{F}_{chem} they exert on the immobile colloid due to the interaction potentials W_A and W_B can be computed. Since the potential Φ_S is radially symmetric and the mass density ρ is uniform due to incompressibility, for a spherical colloid the first term in Eq. (50) does not contribute to the force $\mathbf{F}_{chem} = -\int_{\mathcal{V}} d^3\mathbf{r} \mathbf{f}$, where \mathcal{V} denotes the (macroscopic) volume of the reaction bath. Furthermore, because of the axial symmetry of the system, only the z -component of this force is non-zero so that $\mathbf{F}_{chem} = F_{chem} \mathbf{e}_z$. According to Eqs. (50), (14), and (43) this component is given by

$$\begin{aligned} F_{chem} &= -\mathbf{e}_z \cdot \int_{\mathcal{V}} d^3\mathbf{r} \mathbf{f} = -\left[\int_{\mathcal{V}} d^3\mathbf{r} (-n_A \nabla W_A - n_B \nabla W_B) \right] \cdot \mathbf{e}_z \\ &= 2\pi \int_R^\infty dr r^2 \int_0^\pi d\theta \sin\theta (n_A W'_A + n_B W'_B) \cos\theta \\ &= \frac{4\pi n_0}{3} (a_1 I_A + b_1 I_B) \end{aligned} \quad (54)$$

where

$$\begin{aligned} I_A &= \int_R^\infty dr r^2 g_1(r) W'_A(r) e^{-\beta W_A(r)}, \\ I_B &= \int_R^\infty dr r^2 j_1(r) W'_B(r) e^{-\beta W_B(r)}, \end{aligned} \quad (55)$$

and a_1 and b_1 are given, for arbitrary K^* , by Eq. (27) and Eq. (45), respectively. We note that the above expressions for I_A and I_B are exactly valid, while the expression in Eq. (54) is approximate, because the factors a_1 and b_1 are determined by using an approximate, self-consistent approach (see the discussion at the end of Subsec. 3.1).

Since W_A and W_B vanish for $r \rightarrow \infty$, in this limit the terms $\beta W'_A$ and $\beta W'_B$ multiplying g'_n in Eqs. (15) and (44) decay more rapidly than the term $2/r$ therein

and thus represent subdominant contributions. A straightforward perturbation theory analysis then shows (see also Appendix D) that for $r \rightarrow \infty$ the leading asymptotic decay of both g_1 and j_1 is $\sim 1/r^2$. Consequently, the integrals in Eqs. (55) are finite. In the limiting case that on the surface of the particle no reaction takes place ($K^* \rightarrow 0$), Eq. (28) implies that $K_{eff} = 0$ and therefore $a_1 = b_1 = 0$ [see Eqs. (27) and (45)]. Thus, as expected, at the steady state and in the absence of a chemical reaction one has $F_{chem} = 0$. Obviously this result holds even if the bulk number density of B molecules is non-zero (i.e., maintained at $n_0^{(B)}$ by a reservoir, as for species A). Moreover, for $K > 0$, $W_A(r) = W_B(r)$, and $D_A = D_B$, i.e., if the reaction amounts to just a re-labeling of the molecules, one has $a_1 = -b_1$ (see Eqs. (27) and (45)) while $I_A = I_B$. Therefore, as expected, Eq. (54) predicts that also in this case one has $F_{chem} = 0$.

In the case of diffusion-controlled reactions, i.e., for $K^* \rightarrow \infty$ (see Eqs. (38) and (46)) Eq. (54) reduces to the simpler form

$$F_{chem} = \frac{4\pi n_0 R_D}{3R^2} \Omega^{(AB)} \Psi(\theta_0), \quad K^* \rightarrow \infty, \quad (56)$$

where

$$\Omega^{(AB)} = \frac{e^{\beta W_A(R)}}{g_1'(R)} I_A - \frac{D_A}{D_B} \frac{e^{\beta W_B(R)}}{j_1'(R)} I_B \quad (57)$$

depends on both interaction potentials and on the ratio of the diffusion coefficients D_A/D_B , but it is independent of the patch size (characterized by θ_0). On the other hand, the function $\Psi(\theta_0)$ absorbs the whole dependence of the force on θ_0 :

$$\Psi(\theta_0) = \frac{f_{dc}(\theta_0) \phi_1(\theta_0)}{\phi_0(\theta_0)} \geq 0, \quad (58)$$

where $f_{dc}(\theta_0)$ is given by Eq. (31) (and thus it is determined by W_A), while $\phi_0(\theta_0) = 2 \sin^2(\theta_0/2) \geq 0$ and $\phi_1(\theta_0) = (3/2) \sin^2(\theta_0) \geq 0$ (Eq. (20)) are functions of θ_0 only.

Several general conclusions can be drawn from Eq. (56), i.e., in the diffusion-controlled limit, upon setting formally $K^* = \infty$:

- If the A and the B particles have the same interaction potentials with the colloid, i.e., $W_A(r) \equiv W_B(r)$, so that $I_A = I_B$ and $j_1(r) = g_1(r)$ (since g_1 and j_1 fulfill the same differential equation with the same boundary condition to vanish for $r \rightarrow \infty$), but have different diffusion coefficients, $D_A \neq D_B$, one has (Eqs. (27), (45), and (54)) $F_{chem} \sim (1/D_A)(1 - D_A/D_B)$. Therefore its sign depends on the ratio of the diffusion coefficients. This holds beyond the diffusion-controlled limit $K^* = \infty$ (Eq. (54)).
- For a completely catalytic colloid ($\theta_0 = \pi$) or a chemically inert one ($\theta_0 = 0$) one has $\Psi(\theta_0 = 0, \pi) = 0$. For $\theta_0 = \pi$, $\phi_0(\pi) = 2$ is nonzero, while $\phi_1(\pi) = 0$ and the effective steric factor attains the value $f_{dc}(\pi) = 1$ (see the discussion following Eq. (33)). For $\theta_0 = 0$ this is the case because the ratio $\phi_1(0)/\phi_0(0) = 3$ is finite, while $f_{dc}(0)$ is expected to vanish (see the discussion following Eq. (33)). Therefore, as expected, in these cases there is no force F_{chem} acting on the particle because the system exhibits full radial symmetry. We remark, however, that our model is

a mean-field one, so that one can not rule out the possibility that there will be a non-zero force due to fluctuations in spatial distributions of the reactants and products (see, e.g., the situations discussed in Refs. [104, 141]).

- Since $\Psi(\theta_0)$ is continuous and $\Psi(0) = \Psi(\pi) = 0$, there exists a catalyst coverage characterized by $0 < \tilde{\theta}_0 < \pi$ for which $|F_{chem}|$ is maximal; $\tilde{\theta}_0$ is a functional of $W_A(r)$ and $W_B(r)$.
- F_{chem} can be positive or negative, or equal to zero, depending on the relations between $W_A(r)$ and $W_B(r)$ and those between the diffusion coefficients. But the expression in Eq. (57) is too complex to allow one to obtain analytically exact criteria for certain properties of F_{chem} .

In the opposite limit, i.e., in the kinetically-controlled regime ($D_A \rightarrow \infty$, $K_{eff} \rightarrow K^*$ fixed), one has (Eqs. (39), (47), (54), (57), (9), and (30))

$$\begin{aligned} F_{chem} &= \frac{n_0 K^* \cos^2(\theta_0/2)}{R^2} \left(\frac{I_A e^{\beta W_A(R)}}{D_A g'_1(R)} - \frac{I_B e^{\beta W_B(R)}}{D_B j'_1(R)} \right) \\ &= \pi n_0 \frac{a W_0}{D_A} e^{-\beta W_A(R)} \Omega^{(AB)} (\sin \theta_0)^2, \end{aligned} \quad (59)$$

which shows that the force F_{chem} vanishes in perfectly stirred systems, in which both D_A and D_B tend to infinity. For $D_{A,B}$ very large but finite, it is obvious that all the above bullet points apply to this case, too. Moreover, in this case the strength of the force attains its maximum at $\theta_0 = \pi/2$, i.e., for a symmetric Janus colloid.

Lastly, we note that the result in Eq. (54) can be straightforwardly generalized in order to cover the dissociation reaction described in Eq. (2). For this case we find that the force F_{chem} exerted on the colloid by the ‘‘frozen’’ spatial distributions of the A , B , C , and S molecules due to the interaction potentials Φ_A , Φ_B , Φ_C , and Φ_S (compare Eq. (50)), respectively, is given by (compare Eq. (54))

$$\begin{aligned} F_{chem} &= - \left[\int_{\mathcal{V}} d^3 \mathbf{r} (-n_A \nabla W_A - n_B \nabla W_B - n_C \nabla W_C) \right] \cdot \mathbf{e}_z \\ &= \frac{4\pi n_0}{3} (a_1 I_A + b_1 I_B + \gamma_1 I_C), \end{aligned} \quad (60)$$

where, for arbitrary K^* , a_1 , b_1 , and γ_1 are given by the corresponding Eqs. (27), (45), and (B.4), respectively, the expressions I_A and I_B are defined in Eq. (55), and

$$I_C = \int_R^\infty dr r^2 h_1(r) W'_C(r) e^{-\beta W_C(r)}. \quad (61)$$

(Similarly as the expressions for I_A and I_B , the expression I_C for the force integral is exact, too.)

Accordingly, using Eqs. (38), (46), and (B.5) one finds for the diffusion-controlled regime (compare Eq. (56))

$$F_{chem}(K^* \rightarrow \infty) = \frac{4\pi n_0 R_D}{3R^2} \Omega^{(ABC)} \Psi(\theta_0). \quad (62)$$

$\Omega^{(ABC)}$ depends on the relative interaction potentials W_A , W_B , and W_C , as well as on the ratios D_A/D_B and D_A/D_C of the diffusion coefficients:

$$\Omega^{(ABC)} = \frac{e^{\beta W_A(R)}}{g'_1(R)} I_A - \frac{D_A}{D_B} \frac{e^{\beta W_B(R)}}{j'_1(R)} I_B - \frac{D_A}{D_C} \frac{e^{\beta W_C(R)}}{h'_1(R)} I_C. \quad (63)$$

But $\Omega^{(ABC)}$ is independent of the catalytic patch size characterized by θ_0 . As before, the whole dependence on θ_0 is captured by the factor $\Psi(\theta_0)$ defined in Eq. (58).

For the kinetically-controlled regime one has (compare Eq. (59))

$$F_{chem} = \pi n_0 \frac{a W_0}{D_A} e^{-\beta W_A(R)} \Omega^{(ABC)} (\sin \theta_0)^2. \quad (64)$$

The force F_{chem} vanishes in perfectly stirred systems, in which D_A , D_B , and D_C tend to infinity.

4.3. The velocity of a force-free catalytically-active colloid and the force needed to immobilize it

At steady state and upon neglecting the thermal fluctuations giving rise to rotational diffusion of the symmetry axis in z direction, the results obtained so far can be straightforwardly employed to determine the velocity $\mathbf{V} = V \mathbf{e}_z$ of an active colloid in “force free” (i.e., $\mathbf{F}_{ext} = 0$) motion, or the external force $\mathbf{F}_{ext} = F_{ext} \mathbf{e}_z$ needed to immobilize the active colloid (i.e., $\mathbf{V} = 0$).

The calculation is based on employing the generalized reciprocal theorem due to Teubner (see Appendix C) [94, 101, 109, 110]. This states that for two incompressible Newtonian flows characterized by $\{\mu, \mathbf{u}, \hat{\Pi}\}$ and $\{\mu', \mathbf{u}', \hat{\Pi}'\}$, respectively, and solving the Stokes equations (Eq. (48)) for force densities \mathbf{f} and \mathbf{f}' , respectively, within the domain \mathcal{D} exterior to a closed surface $\partial\mathcal{D}$, whereby $\hat{\Pi}$, \mathbf{u} , and \mathbf{f} , as well as the primed ones, vanish sufficiently fast with increasing distance from $\partial\mathcal{D}$, the following relation holds [110]:

$$\mu' \left[\int_{\partial\mathcal{D}} \mathbf{u}' \cdot \hat{\Pi} \cdot d\mathbf{s} - \int_{\mathcal{D}} \mathbf{u}' \cdot \mathbf{f} d^3\mathbf{r} \right] = \mu \left[\int_{\partial\mathcal{D}} \mathbf{u} \cdot \hat{\Pi}' \cdot d\mathbf{s} - \int_{\mathcal{D}} \mathbf{u} \cdot \mathbf{f}' d^3\mathbf{r} \right]. \quad (65)$$

Here the orientation of the surface element $d\mathbf{s} := dS \mathbf{e}_r$ is the one given by the *inner* normal (i.e., pointing *into* the fluid domain \mathcal{D}).

For the unprimed system we choose the fluid motion as the one corresponding to the self-propelled colloid moving with velocity $\mathbf{V} = V \mathbf{e}_z$ (in this case $\partial\mathcal{D}$ is the surface $r = R$ of the sphere and the fluid domain \mathcal{D} is the volume \mathcal{V} of the solution):

$$\begin{aligned} \nabla \cdot \hat{\Pi} &= -\mathbf{f} := -f \mathbf{e}_r, \quad \nabla \cdot \mathbf{u} = 0, \\ \mathbf{u}(r = R) &= V \mathbf{e}_z, \quad \mathbf{u}(r \rightarrow \infty) = 0, \end{aligned} \quad (66)$$

where in the first equation we have used the fact that \mathbf{f} has only a radial component $f := \mathbf{f} \cdot \mathbf{e}_r$ (due to $W_{A,B}$ being radially symmetric, see Eq. (50)).

For the primed system we choose the one corresponding to the motion of the fluid (of the same viscosity, i.e., $\mu' = \mu$) due to a sphere of radius R translating along the z -direction with uniform velocity $\mathbf{U}_0 = U_0 \mathbf{e}_z$:

$$\begin{aligned} \nabla \cdot \hat{\boldsymbol{\Pi}}' &= 0, \quad \nabla \cdot \mathbf{u}' = 0, \\ \mathbf{u}'(r = R) &= U_0 \mathbf{e}_z, \quad \mathbf{u}'(r \rightarrow \infty) = 0. \end{aligned} \quad (67)$$

For the latter system the solution is known and the axially symmetric velocity field \mathbf{u}' is given in spherical coordinates by (see, e.g., Ch. 4 in Ref. [139])

$$\begin{aligned} u'_r &= \frac{U_0}{2} \left[3 \left(\frac{R}{r} \right) - \left(\frac{R}{r} \right)^3 \right] \cos \theta := U_0 \xi(r) \cos \theta, \\ u'_\theta &= -\frac{U_0}{4} \left[3 \left(\frac{R}{r} \right) + \left(\frac{R}{r} \right)^3 \right] \sin \theta. \end{aligned} \quad (68)$$

By using Eqs. (66) and (67), and noting that in the latter case $\mathbf{f}' \equiv 0$ while \mathbf{U}_0 and \mathbf{V} are constants with respect to the integration over the spherical surfaces, Eq. (65) leads to

$$\mathbf{U}_0 \cdot \int_{r=R} \hat{\boldsymbol{\Pi}} \cdot \mathbf{e}_r dS - \int_{\mathcal{V}} \mathbf{u}' \cdot \mathbf{f} d^3\mathbf{r} = \mathbf{V} \cdot \int_{r=R} \hat{\boldsymbol{\Pi}}' \cdot d\mathbf{s}. \quad (69)$$

The last integral is the drag force acting on the translating sphere and it is given by the well known Stokes formula (see, e.g., Ch. 4 in Ref. [139]), $\int_{r=R} \hat{\boldsymbol{\Pi}}' \cdot d\mathbf{s} = -6\pi\mu R \mathbf{U}_0$. By noting that the surface integral on the left hand side of Eq. (69) is the contribution \mathbf{F}_{hyd} of the force acting on the colloid, and by using Eq. (53) to eliminate it in favor of the other two force contributions, we arrive at

$$\mathbf{U}_0 \cdot [-\mathbf{F}_{ext} + 6\pi\mu R \mathbf{V}] = \int_{\mathcal{V}} d^3\mathbf{r} (\mathbf{u}' - \mathbf{U}_0) \cdot \mathbf{f}. \quad (70)$$

The two cases of interest are immediately obtained from the general result in Eq. (70) as follows.

(i) *Velocity of the force free colloid.*

With $\mathbf{F}_{ext} = 0$, and by noting that $\cos \theta = \mathbf{e}_z \cdot \mathbf{e}_r$, Eq. (70) renders

$$\begin{aligned} V &= \frac{1}{6\pi\mu R} \int_{\mathcal{V}} d^3\mathbf{r} [\xi(r) - 1] f \cos \theta \\ &= \frac{1}{6\pi\mu R} \int_{\mathcal{V}} d^3\mathbf{r} \left[\frac{3}{2} \left(\frac{R}{r} \right) - \frac{1}{2} \left(\frac{R}{r} \right)^3 - 1 \right] f \cos \theta. \end{aligned} \quad (71)$$

(We recall that $f = \mathbf{f} \cdot \mathbf{e}_r$ with \mathbf{f} given by Eq. (50).)

As the next step, using the equality in the first line in Eq. (54), we express the self-propulsion velocity V in terms of the coefficients with index $n = 1$ in the

expansions of the densities of the reactants and products. For the simplest type of reaction $A + CP \rightarrow B + CP$, one has

$$V = \frac{2n_0}{9\mu R} (a_1 J_A + b_1 J_B) , \quad (72)$$

where

$$J_A = \int_R^\infty dr r^2 g_1(r) W'_A(r) \left(1 + \frac{1}{2} \left(\frac{R}{r} \right)^3 - \frac{3R}{2r} \right) e^{-\beta W_A(r)} \quad (73)$$

and

$$J_B = \int_R^\infty dr r^2 j_1(r) W'_B(r) \left(1 + \frac{1}{2} \left(\frac{R}{r} \right)^3 - \frac{3R}{2r} \right) e^{-\beta W_B(r)} . \quad (74)$$

Similarly as the expressions I_A and I_B for the force integrals, the expressions J_A and J_B for the velocity integrals are exact, too.

In turn, for a more general catalytically-induced dissociation in Eq.(2) we obtain

$$V = \frac{2n_0}{9\mu R} (a_1 J_A + b_1 J_B + \gamma_1 J_C) , \quad (75)$$

where γ_1 is defined in Eq. (B.4) and

$$J_C = \int_R^\infty dr r^2 h_1(r) W'_C(r) \left(1 + \frac{1}{2} \left(\frac{R}{r} \right)^3 - \frac{3R}{2r} \right) e^{-\beta W_C(r)} . \quad (76)$$

(ii) Stall force F_{ext} needed to immobilize a colloid.

With $\mathbf{V} = 0$ and $\cos \theta = \mathbf{e}_z \cdot \mathbf{e}_r$, Eq. (70) yields

$$F_{ext} = - \int_{\mathcal{V}} d^3 \mathbf{r} [\xi(r) - 1] f \cos \theta . \quad (77)$$

The stall force is proportional to the velocity V_{free} (Eq. (71)) of a force-free colloid,

$$F_{ext} = -6\pi\mu R V_{free} , \quad (78)$$

and has the same form as the Stokes formula. This result follows directly from Eq. (70). Therefore it is very general, in the sense that this result does not depend on the details of the chemical activity but only on the assumptions of a spherical shape, steady state motion, and (negligibly) small Re and Pe numbers.

Therefore, by using Eqs. (72) and (75) F_{ext} can be expressed explicitly as

$$F_{ext} = -\frac{4\pi n_0}{3} (a_1 J_A + b_1 J_B) , \quad A + CP \rightarrow B + CP \quad (79)$$

and as

$$F_{ext} = -\frac{4\pi n_0}{3} (a_1 J_A + b_1 J_B + \gamma_1 J_C) , \quad A + CP \rightarrow B + C + CP , \quad (80)$$

respectively.

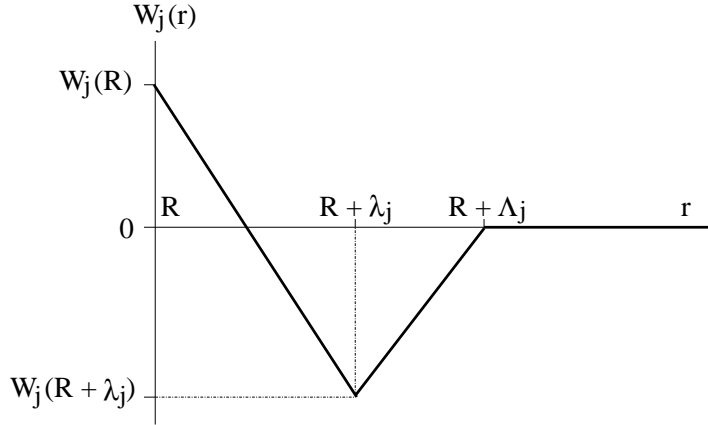


Figure 2. Illustration of the triangular-well potential $W_j(r)$ defined by Eqs. (81) and (84).

5. Triangular-well potentials as a case study

We illustrate the general results derived in the previous section by choosing a particular form of the interaction potential between the colloid and the various molecular species involved in the reaction. This allows us to obtain sufficiently simple explicit expressions for the force contribution \mathbf{F}_{chem} (Eq. (60)), the stall force \mathbf{F}_{ext} (Eq. (78)), or, equivalently, the velocity \mathbf{V} (Eq. (71)) of a force-free colloid, such that their dependences on the strength of the interactions, catalytic coverage, chemical rates, diffusion coefficients of the reactants and products, and radius of the colloid can be determined and discussed. This choice is provided by the so-called triangular-well potentials (depicted in Fig. 2) which, despite their simplicity, capture well the thermodynamic properties of fluids with Lennard-Jones pair interactions, provided the defining parameters of the triangular-well potentials are tuned suitably (see, e.g., Refs. [111–113] for a detailed discussion of this issue). For this choice of the potential one can derive *explicit* formulae for the chemical and the stall force, which allows one to highlight several counter-intuitive effects concerning diffusiophoretic self-propulsion.

We stipulate that the potential $W_j(r)$ for the interactions of the colloid with the j -th species ($j = A, B, C$) is a piece-wise continuous function defined as follows (see Fig. 2):

$$W_j(R \leq r \leq R + \lambda_j) \equiv W_j^<(r) = -\xi_1^j r + (W_j(R) + \xi_1^j R), \quad (81)$$

where

$$\xi_1^j = \frac{W_j(R) - W_j(R + \lambda_j)}{\lambda_j} = \frac{\Delta\varepsilon_j}{\beta\lambda_j} \quad (82)$$

with

$$\Delta\varepsilon_j \equiv \varepsilon_w^j - \varepsilon_m^j = \beta W_j(R) - \beta W_j(R + \lambda_j) \quad (83)$$

in the inner region $r \in (R, R + \lambda_j)$;

$$W_j(R + \lambda_j \leq r \leq R + \Lambda_j) \equiv W_j^I(r) = \xi_2^j r - \xi_2^j(R + \Lambda_j), \quad (84)$$

where

$$\xi_2^j = -\frac{\varepsilon_m^j}{\beta(\Lambda_j - \lambda_j)}, \quad (85)$$

in the intermediate region $r \in (R + \lambda_j, R + \Lambda_j)$. In the outer region $r \in (R + \Lambda_j, \infty)$ the potential vanishes:

$$W_j(r \geq R + \Lambda_j) \equiv W_j^>(r) \equiv 0. \quad (86)$$

The parameters (the value at the wall, the depth, and the location of the well) defining the interactions of the colloid with the j -th species are, in general, different. In the following we shall focus the discussion of the results on the situation depicted in Fig. 2, i.e., $\Delta\varepsilon_j \geq 0$ and $\varepsilon_m^j \leq 0$. (Nonetheless, the derivation of the results is carried out for both signs of these parameters.)

Furthermore, we introduce the dimensionless parameters $q_j = \lambda_j/R$, $Q_j = \Lambda_j/R$, and $z_j = Q_j/q_j \geq 1$. The derivation of the radial functions $g_n(r)$ (Eq. (15)) for arbitrary values of the parameters q_A and Q_A , ε_m^A and ε_w^A is detailed in Appendix D. (The corresponding results for the other species follow, as in Sec. 3, by simply switching label A with B or C .) Based on these functions, in Appendix D we also derive the general expressions for the integrals I_j (Eq. (55)) and J_j (Eqs. (73), (74), and (76)) for $j = A, B, C$. Here we restrict the discussion to the physically meaningful limit $\lambda_j/R \ll 1$ (at fixed $z_j \geq 1$) and retain only the leading order term. For colloids of radii $R \gtrsim 1 \mu\text{m}$ and typical surface interactions, the parameter λ_j/R is expected to be of the order of 10^{-2} or smaller. Thus the corrections $O(\lambda_j/R)$ to the leading order term (which are included in Appendix D) are expected to be negligibly small.

5.1. The contribution \mathbf{F}_{chem} due to the direct interactions of the colloid with the molecular species

In leading order in λ_j/R , the force integrals (Eq. (55)) are given by

$$I_j = -\frac{(1 - e^{-\varepsilon_w^j})}{\beta} R^2. \quad (87)$$

This shows that, somewhat surprisingly, the leading order value of I_j is controlled only by the value of the potential at the wall and is independent of the depth ε_m^j of the well. The leading order value of I_j is negative for $\varepsilon_w^j > 0$ (repulsion from the wall) and positive for $\varepsilon_w^j < 0$ (attraction to the wall). The corrections depend on ε_m^j and may be positive or negative hinging on the relation between ε_m^j and ε_w^j (see Eq. (D.22) in Appendix D).

In this limit the Debye radius (Eq. (17)) is simply given by $R_D = R$ (the correction terms are given by Eq. (D.2) in Appendix D), the steric factor $f_{dc}(\theta_0)$ (Eq. (31)) turns

into $f_{dc}(\theta_0) = f_{dc}^{(sls)}(\theta_0)$ (Eq. (33)), and the derivative of the first radial function at the wall is

$$g_1'(R) = -\frac{2e^{\varepsilon_w^A}}{R}. \quad (88)$$

Consequently, we find (Eqs. (28), (29), and (30)) that in this limit the coefficient a_1 (Eq. (27)) is

$$a_1 = -\frac{3}{8} \frac{\kappa e^{-\varepsilon_w^A} R}{\left(\kappa e^{-\varepsilon_w^A} R \sin^2(\theta_0/2) + D_A f_{dc}^{(sls)}(\theta_0)\right)} \sin^2(\theta_0) f_{dc}^{(sls)}(\theta_0); \quad (89)$$

therefore, the contribution of the A molecules to the force F_{chem} (Eq. (54)) is given by

$$F_{chem}^A = \frac{\pi n_0}{2\beta} \frac{\kappa e^{-\varepsilon_w^A} (1 - e^{-\varepsilon_w^A}) R^3}{\left(\kappa e^{-\varepsilon_w^A} R \sin^2(\theta_0/2) + D_A f_{dc}^{(sls)}(\theta_0)\right)} \sin^2(\theta_0) f_{dc}^{(sls)}(\theta_0). \quad (90)$$

In this limit, the sign of F_{chem}^A is determined fully by the sign of ε_w^A : for $\varepsilon_w^A > 0$, i.e., if the A molecules are repelled from the surface of the colloid, F_{chem}^A is positive. This is a simple consequence of the fact that, due to the reaction, the A molecules are depleted in the region $z > 0$, as compared to the region at the other side of the catalytic patch, which effectively pushes the colloid into the positive z -direction. We further remark that F_{chem}^A is a non-monotonic function of ε_w^A and vanishes if either $\varepsilon_w^A \rightarrow 0$ or $\varepsilon_w^A \rightarrow \infty$. The latter can be understood by noting that an infinitely strong repulsion prevents the A molecules from approaching the catalytic patch and hence completely suppresses the reaction, which renders a radially symmetric distribution.

We proceed with the calculation of the coefficients b_1 and γ_1 defined in Eqs. (45) and (B.4). Since the derivatives of the radial functions $j_1(r)$ and $h_1(r)$, defined by Eqs. (44) and (B.3), have the same form as $g_1'(R)$ but with ε_w^A replaced by ε_w^B or ε_w^C , in leading order in λ_j/R the coefficients b_1 and γ_1 are given by

$$b_1 = \frac{3D_A}{8D_B} \frac{\kappa e^{-\varepsilon_w^A} R}{\left(\kappa e^{-\varepsilon_w^A} R \sin^2(\theta_0/2) + D_A f_{dc}^{(sls)}(\theta_0)\right)} \sin^2(\theta_0) f_{dc}^{(sls)}(\theta_0), \quad (91)$$

and

$$\gamma_1 = \frac{3D_A}{8D_C} \frac{\kappa e^{-\varepsilon_w^A} R}{\left(\kappa e^{-\varepsilon_w^A} R \sin^2(\theta_0/2) + D_A f_{dc}^{(sls)}(\theta_0)\right)} \sin^2(\theta_0) f_{dc}^{(sls)}(\theta_0). \quad (92)$$

Consequently, we arrive at the following explicit expressions for the force F_{chem} :

- the case $A + CP \rightarrow B + CP$:

$$F_{chem} = \frac{\pi n_0 R^3 D_A}{2\beta} \frac{\kappa e^{-\varepsilon_w^A}}{\left(\kappa e^{-\varepsilon_w^A} R \sin^2(\theta_0/2) + D_A f_{dc}^{(sls)}(\theta_0)\right)} \times \left(\frac{(1 - e^{-\varepsilon_w^A})}{D_A} - \frac{(1 - e^{-\varepsilon_w^B})}{D_B} \right) \sin^2(\theta_0) f_{dc}^{(sls)}(\theta_0); \quad (93)$$

- the case $A + CP \rightarrow B + C + CP$ (dissociation reaction):

$$F_{chem} = \frac{\pi n_0 R^3 D_A}{2\beta} \frac{\kappa e^{-\varepsilon_w^A}}{\left(\kappa e^{-\varepsilon_w^A} R \sin^2(\theta_0/2) + D_A f_{dc}^{(sls)}(\theta_0) \right)} \times \left(\frac{(1 - e^{-\varepsilon_w^A})}{D_A} - \frac{(1 - e^{-\varepsilon_w^B})}{D_B} - \frac{(1 - e^{-\varepsilon_w^C})}{D_C} \right) \sin^2(\theta_0) f_{dc}^{(sls)}(\theta_0). \quad (94)$$

If the values ε_w^j are equal to each other, i.e., $\varepsilon_w^A = \varepsilon_w^B = \varepsilon_w^C$, Eqs. (93) and (94) take the simple forms ($A + CP \rightarrow B + CP$)

$$F_{chem} = \frac{\pi n_0 R^3 D_A}{2\beta} \frac{\kappa e^{-\varepsilon_w^A} (1 - e^{-\varepsilon_w^A})}{\left(\kappa e^{-\varepsilon_w^A} R \sin^2(\theta_0/2) + D_A f_{dc}^{(sls)}(\theta_0) \right)} \times \left(\frac{1}{D_A} - \frac{1}{D_B} \right) \sin^2(\theta_0) f_{dc}^{(sls)}(\theta_0) \quad (95)$$

and ($A + CP \rightarrow B + C + CP$)

$$F_{chem} = \frac{\pi n_0 R^3 D_A}{2\beta} \frac{\kappa e^{-\varepsilon_w^A} (1 - e^{-\varepsilon_w^A})}{\left(\kappa e^{-\varepsilon_w^A} R \sin^2(\theta_0/2) + D_A f_{dc}^{(sls)}(\theta_0) \right)} \times \left(\frac{1}{D_A} - \frac{1}{D_B} - \frac{1}{D_C} \right) \sin^2(\theta_0) f_{dc}^{(sls)}(\theta_0), \quad (96)$$

respectively. Thus, in this case the sign of F_{chem} is determined by the relation between the diffusion coefficients of the reactive species.

Focusing here on the case of the reaction $A + CP \rightarrow B + CP$, we discuss the limiting behavior of the force F_{chem} in Eq. (93), rendering explicit results for several general conclusions presented above in Subsec. 4.2. To this end, we first consider the so-called diffusion-limited case and assume that the parameters of the model obey the following inequality:

$$\kappa e^{-\varepsilon_w^A} R \sin^2(\theta_0/2) \gg D_A f_{dc}^{(sls)}(\theta_0). \quad (97)$$

(We remark that, in contrast to the case discussed by Collins and Kimball, (Eq. (35)), here the lhs of the inequality depends also on ε_w^A and both sides depend on θ_0 . Therefore, this limit has to be taken with appropriate caution, if one intends to study the dependence of F_{chem} on θ_0 in the limit $\theta_0 \rightarrow 0$.) Since $\sin^2(\theta_0/2) \sim \theta_0^2$, while $f_{dc}^{(sls)}(\theta_0) \sim \theta_0$, for fixed κ , R , D_A , and ε_w^A , which obey the inequality in Eq. (97) for moderate θ_0 , the sign of the inequality changes for sufficiently small values of θ_0 . In other words, as we have already noted in the text after Eq. (33), for $\theta_0 \rightarrow 0$ there is always the kinetically-controlled regime, but not the diffusion-controlled one. Similarly, the dependence of F_{chem} on ε_w^A (as well as the one of F_{ext} or, equivalently, V , which will be discussed below) obtained for this regime cannot be extrapolated to arbitrarily large values of ε_w^A . The reason for this is that the effective reduction of the reactivity due to an increase of the repulsion at the wall (and hence, on the catalytic patch) ultimately causes a reversal of the inequality in Eq. (97).

In the diffusion-controlled limit Eq. (93) attains the form

$$F_{chem} = \frac{2\pi n_0 R^2}{\beta} \left(1 - e^{-\varepsilon_w^A} - \frac{D_A}{D_B} \left(1 - e^{-\varepsilon_w^B} \right) \right) \times \cos^2(\theta_0/2) f_{dc}^{(sls)}(\theta_0). \quad (98)$$

In this regime, the force is proportional to R^2 (i.e., the *area* of the colloid) and attains its maximal value for θ_0 close to $\pi/2$ (but not exactly equal to it, see the discussion in Subsec. 4.2). The sign of the force depends on the diffusion coefficients of both species and on the amplitudes of their interaction potentials with the wall. For

$$\frac{\left(1 - e^{-\varepsilon_w^A} \right)}{D_A} > \frac{\left(1 - e^{-\varepsilon_w^B} \right)}{D_B} \quad (99)$$

the force F_{chem} is positive, while it is negative if the inequality is reversed.

In the limit of the kinetic control, if D_A is sufficiently large so that the inequality in Eq. (97) is reversed, one has

$$F_{chem} = -\frac{\pi n_0 R^3}{2\beta D_B} \kappa e^{-\varepsilon_w^A} \left(1 - e^{-\varepsilon_w^B} \right) \sin^2(\theta_0). \quad (100)$$

In this regime the force is proportional to the R^3 (i.e., *volume* of the colloid), attains the maximal value for $\theta_0 \equiv \pi/2$, (i.e., in the case of Janus particles with the catalytic patch occupying exactly one half of the surface), and its sign is determined by the sign of ε_w^B . For positive values of ε_w^B , i.e., if the products B are repelled from the surface of the colloid, the force F_{chem} is negative, and is positive in the case of negative values of ε_w^B . In the limit $D_B \rightarrow \infty$ the force vanishes $\sim 1/D_B$.

5.2. Stall force F_{ext} and self-propulsion velocity V of a force-free colloid

Next we turn to the analysis of the stall force F_{ext} (Eqs. (79) and (80)) and, equivalently (see Eq. (78)), of the self-propulsion velocity V of a force-free colloid. For the triangular well potentials, the exact expressions for the integrals J_j (Eqs. (73), (74), and (76)) entering the definition of F_{ext} and V are presented in Appendix D. Analogous to the previous section, here we focus on the leading order term in λ_j/R , which is given by

$$J_j = \mathcal{J}_j \frac{\lambda_j^2}{\beta}, \quad (101)$$

with

$$\begin{aligned} \mathcal{J}_j = & -\frac{3e^{-\varepsilon_w^j}}{2\Delta\varepsilon_j^2} \left(e^{\Delta\varepsilon_j} (1 + (\Delta\varepsilon_j - 1)^2) - 2 \right) + \\ & + \frac{3}{2(\varepsilon_m^j)^2} \left((z_j - 1)^2 \left(e^{-\varepsilon_m^j} - 1 \right) + \right. \\ & \left. + (\varepsilon_m^j - z_j + 1)^2 e^{-\varepsilon_m^j} - (1 + z_j \varepsilon_m^j - z_j)^2 \right). \end{aligned} \quad (102)$$

We note that, in contrast to I_j , J_j depends on the depth ε_m^j of the potential well even in leading order. Mathematically, this is a consequence of the additional factor

$(1 + (R/r)^3/2 - 3R/(2r))$ in the integrands in Eqs. (73), (74), and (76). Consequently, the dependence of \mathcal{J}_j on the parameters characterizing the interaction potentials (Eqs. (101) and (102)) is more complex.

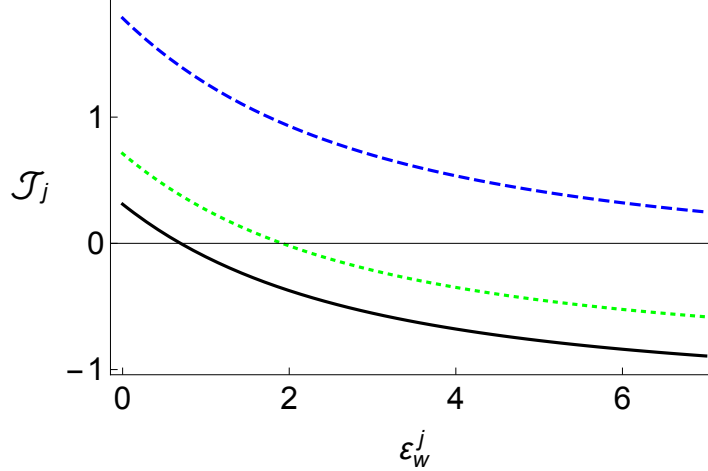


Figure 3. Dimensionless factor \mathcal{J}_j (Eq. (102)) in the integral J_j (Eq. (101)) as a function of ε_w^j for $z_j = \Lambda_j/\lambda_j = 2$ (see Fig. 2) and $\varepsilon_m^j = -0.1$ (solid line), $\varepsilon_m^j = -0.22$ (dotted line), and $\varepsilon_m^j = -0.5$ (dashed line).

In Fig. 3 we show \mathcal{J}_j (Eq. (102)) as a function of ε_w^j for several values of the depth of the well. We observe that even for the smallest value of ε_m^j (here, $\varepsilon_m^j = -0.1$), a significant repulsion at the wall ($\varepsilon_w^j \approx 0.6$) is needed in order to have \mathcal{J}_j becoming negative. This is in contrast to the behavior exhibited by I_j , which is negative as soon as ε_w^j is negative. For a slightly deeper well ($\varepsilon_m^j = -0.22$) a much stronger repulsion at the wall ($\varepsilon_w^j \approx 2$) is required for turning \mathcal{J}_j negative. Furthermore, for $\varepsilon_m^j = -0.5$, \mathcal{J}_j remains positive for ε_w^j as large as $\varepsilon_w^j \approx 7$. This leads to the conclusion that, while the sign of I_j is dominated by the value of the interaction potential at the wall, the sign of J_j depends strongly on the depth of the well. Thus, for sufficiently small values of ε_w^j , one can observe an intriguing behavior in that the contributions \mathbf{F}_{chem}^j and \mathbf{F}_{ext}^j , respectively, of the molecular species j to the chemical and stall force, respectively, have the same direction. Due to Eq. (78) this implies that the self-propulsion velocity V_j and F_{chem}^j have opposite signs. For small values of ε_w^j and $|\varepsilon_m^j|$, the Taylor series in powers of ε_w^j and ε_m^j of the right-hand-side of Eq. (102) can be truncated at first order. In this case, one obtains

$$\mathcal{J}_j \approx -\frac{z_j(z_j + 1)}{2}\varepsilon_m^j - \frac{1}{2}\varepsilon_w^j, \quad (103)$$

which, in the case of sufficiently small interaction parameters ε_w^j and $|\varepsilon_m^j|$, provides a simple criterion for the sign of \mathcal{J}_j , and hence of F_{ext}^j and V_j .

Furthermore, Eqs. (54), (60), (72), (75), (79), and (80) imply that the contribution to F_{ext}^j (or, equivalently, to V_j) due to the interactions with the molecular species j is

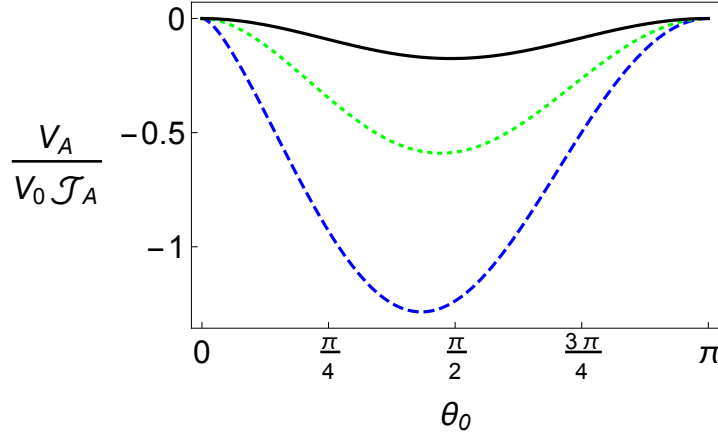


Figure 4. Reduced velocity $V_A/(V_0\mathcal{J}_A)$ (Eq. (106)) as a function of the catalytic coverage θ_0 for several values of the parameter D_A ($\exp(\varepsilon_w)/(\kappa R)$): 0.1 (dashed line), 1 (dotted line), and 5 (solid line).

related to F_{chem}^j as

$$F_{ext}^j = \left(\frac{\lambda_j}{R}\right)^2 \frac{\mathcal{J}_j}{(1 - e^{-\varepsilon_w^j})} F_{chem}^j \quad (104)$$

and equivalently,

$$V_j = -\frac{1}{6\pi\mu R} \left(\frac{\lambda_j}{R}\right)^2 \frac{\mathcal{J}_j}{(1 - e^{-\varepsilon_w^j})} F_{chem}^j. \quad (105)$$

Equations (104) and (105) lead to various conclusions. First, they show that F_{ext}^j and V_j are, by a factor $(\lambda_j/R)^2$, much smaller than the force contribution F_{chem}^j . Second, the dependence of F_{ext}^j (and thus also that of V_j) on θ_0 , κ , and D_j comes about only via F_{chem}^j . The factor $\mathcal{J}_j/(1 - \exp(-\varepsilon_w^j))$ implies that only for ε_w^j sufficiently large (ensuring that $\mathcal{J}_j > 0$) the stall force contribution F_{ext}^j and the velocity contribution V_j have signs which are opposite and equal, respectively, to F_{chem}^j , which one might expect *a priori* on intuitive grounds. These properties are, as explained above, due to the fact that for not too large ε_w^j the integrals J_j , which determine F_{ext}^j and V_j , are dominated by the depth of the well, while the integrals I_j , which determine F_{chem}^j , are always dominated by ε_w^j .

The overall dependence of V_j (or, equivalently, of the contribution F_{ext}^j to the stall force) on ε_w^A and ε_m^A requires further analysis because, as explained earlier, upon a gradual increase of ε_w^A the system, which is in the diffusion-limited regime for small values of this parameter, eventually crosses over into the kinetic control regime. We illustrate this behavior for $j = A$. The general dependence on κ and D_A is given by

$$V_A = -V_0 \left(\frac{\sin^2(\theta_0/2)}{f_{dc}^{(sls)}(\theta_0)} + \frac{D_A}{\kappa R} e^{\varepsilon_w^A} \right)^{-1} \mathcal{J}_A \sin^2(\theta_0), \quad V_0 = \frac{n_0 \lambda_A^2}{12\beta\mu R}. \quad (106)$$

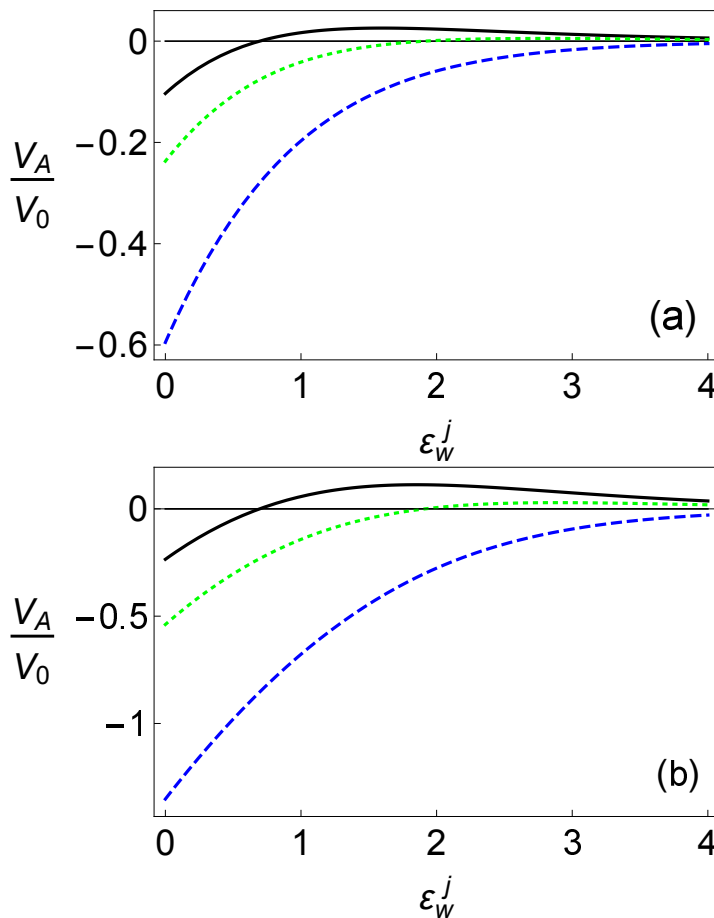


Figure 5. Reduced velocity V_A/V_0 (Eq. (106)) of a Janus colloid ($\theta_0 = \pi/2$) as a function of ε_w^A for $z_A = \Lambda_A/\lambda_A = 2$ (see Fig. 2) and $\varepsilon_m^A = -0.1$ (solid line), $\varepsilon_m^A = -0.22$ (dotted line), and $\varepsilon_m^A = -0.5$ (dashed line). The scaled velocity depends on the ratio $D_A/(\kappa R)$, which is 2 in (a) and 0.32 in (b).

V_0 is independent of ε_w^A and ε_m^A , while the ratio $D_A/(\kappa R)$ can be estimated from available experimental data. In particular, for the experimental situation studied in Ref. [31] one has the ratio $D_A/(\kappa R) \approx 2$.

In Fig. 4 we plot the rescaled velocity $V_A/(V_0\mathcal{J}_A)$ with V_A and \mathcal{J}_A defined in Eqs. (106) and (102), respectively, as a function of the catalytic coverage θ_0 . Interestingly one finds that the maximum of the absolute value of the self-propulsion velocity is attained at coverages close to $\theta_0 = \pi/2$ (i.e., for Janus colloids), only if the parameter $D_A(\exp(\varepsilon_w))/(\kappa R)$ is sufficiently large, which corresponds to the regime of kinetic control. For small values of $D_A(\exp(\varepsilon_w))/(\kappa R)$, one finds that the maximum is shifted to values of θ_0 lower than $\pi/2$, which matches with the observations we made above in Subsec. 4.2.

Further on, we focus on the special case of Janus colloids (i.e., $\theta_0 = \pi/2$ and $f_{dc}^{(sls)}(\pi/2) \approx 0.706$) and analyze the behavior of V_A in Eq. (106) as a function of the parameters of the triangular-well interaction potential. In Fig. 5 we show V_A/V_0

as a function of ε_w^A for three different values of ε_m^A and for two values of the ratio $D_A/(\kappa R)$ (i.e., two values of R with D_A and κ kept at fixed values). We observe that for sufficiently small values of ε_m^A , here $\varepsilon_m^A = -0.1$, the contribution V_A to the self-propulsion velocity V , generated by the interactions with the A molecules, exhibits a non-monotonic behavior. For small ε_w^A , V_A/V_0 is negative (hence V and F_{chem} have opposite signs). Upon increasing ε_w^A it crosses 0, attains a peak value at $\varepsilon_w^A \approx 1.4$ (Fig. 5(a)) and $\varepsilon_w^A \approx 1.8$ (Fig. 5(b)), respectively, and decreases to zero for large ε_w^A . According to Eq. (106), this decrease is exponential in ε_w^A , which is due to the crossover to the regime of kinetic control. For larger value of ε_m^A , (e.g., $\varepsilon_m^A = -0.5$ in Fig. 5), the velocity remains negative over the whole interval $\varepsilon_w^A \in (0, 4)$. In principle, for such values of ε_m^A , the reduced velocity will also attain positive values and will exhibit a non-monotonic behavior, but this behavior is shifted to very large values of ε_w^A , which can be unphysical. Moreover, the peak values of V_A are small. We also observe that the maximal absolute values of V_A/V_0 are achieved for $\varepsilon_w^A = 0$, which signals that the most effective self-propulsion (due to interactions with the A molecules) takes place for potentials which have a deep minimum and no repulsion at the wall, beyond the hard-wall interaction. This conclusion remains valid if the multi-species interactions are the same for all species, i.e., $\mathcal{J}_A = \mathcal{J}_B = \mathcal{J}_C = \mathcal{J}$, in which case the integral \mathcal{J} will factor out (see Eqs. (107) and (108) below). Of course, in the general case this may not hold because the contributions to V stemming from different species (which appear with different signs) may compensate each other. We note, as well, that even for $\mathcal{J}_A = \mathcal{J}_B = \mathcal{J}_C = \mathcal{J}$, the sign of V is not determined by the sign of \mathcal{J} but depends also on the relation between the diffusion coefficients D_A , D_B , and D_C .

Next we discuss the dependence of the velocity V and of F_{ext} (Eqs. (72), (75), and (78)) on the size R of the colloid. From our results in Eqs. (72) and (75), we find that in leading order the self-propulsion velocity of the colloid for a reaction $A + CP \rightarrow B + CP$ is given by

$$V = -\frac{n_0 D_A}{12\beta\mu} \frac{\kappa e^{-\varepsilon_w^A}}{\left(\kappa e^{-\varepsilon_w^A} R \sin^2(\theta_0/2) + D_A f_{dc}^{(sls)}(\theta_0)\right)} \times \left(\frac{\lambda_A^2 \mathcal{J}_A}{D_A} - \frac{\lambda_B^2 \mathcal{J}_B}{D_B}\right) \sin^2(\theta_0) f_{dc}^{(sls)}(\theta_0), \quad (107)$$

while for a dissociation reaction $A + CP \rightarrow B + C + CP$ it is given by

$$V = -\frac{n_0 D_A}{12\beta\mu} \frac{\kappa e^{-\varepsilon_w^A}}{\left(\kappa e^{-\varepsilon_w^A} R \sin^2(\theta_0/2) + D_A f_{dc}^{(sls)}(\theta_0)\right)} \times \left(\frac{\lambda_A^2 \mathcal{J}_A}{D_A} - \frac{\lambda_B^2 \mathcal{J}_B}{D_B} - \frac{\lambda_C^2 \mathcal{J}_C}{D_C}\right) \sin^2(\theta_0) f_{dc}^{(sls)}(\theta_0). \quad (108)$$

In the diffusion controlled limit (Eq. (97)), Eqs. (107) and (108) reduce to

$$V = -\frac{n_0}{3\beta\mu R} \left(\lambda_A^2 \mathcal{J}_A - \frac{D_A \lambda_B^2 \mathcal{J}_B}{D_B}\right) \cos^2(\theta_0/2) f_{dc}^{(sls)}(\theta_0) \quad (109)$$

and

$$V = -\frac{n_0}{3\beta\mu R} \left(\lambda_A^2 \mathcal{J}_A - \frac{D_A \lambda_B^2 \mathcal{J}_B}{D_B} - \frac{D_A \lambda_C^2 \mathcal{J}_C}{D_C} \right) \cos^2(\theta_0/2) f_{dc}^{(sls)}(\theta_0), \quad (110)$$

respectively. In this limit one has $V \sim 1/R$. Hence, in accordance with Eq. (78) and in leading order, the stall force F_{ext} is independent of R . In the kinetic control limit, Eqs. (107) and (108) yield

$$V = -\frac{n_0}{12\beta\mu} \kappa e^{-\varepsilon_w^A} \left(\frac{\lambda_A^2 \mathcal{J}_A}{D_A} - \frac{\lambda_B^2 \mathcal{J}_B}{D_B} \right) \sin^2(\theta_0) \quad (111)$$

and

$$V = -\frac{n_0}{12\beta\mu} \kappa e^{-\varepsilon_w^A} \left(\frac{\lambda_A^2 \mathcal{J}_A}{D_A} - \frac{\lambda_B^2 \mathcal{J}_B}{D_B} - \frac{\lambda_C^2 \mathcal{J}_C}{D_C} \right) \sin^2(\theta_0), \quad (112)$$

respectively. Therefore, in the limit of kinetic control V is *independent* of R , and hence $F_{ext} \sim R$.

The dependence on R predicted by our analysis is consistent with previous theoretical [98] arguments and experimental observations [31, 98] which tell that for R larger than a certain threshold value the velocity V decreases $\sim 1/R$ upon increasing R [98], while for R smaller than this threshold value the velocity saturates at a value independent of R [31]. As follows, this size dependence can be understood from the inequality in Eq. (97), which distinguishes between the diffusion-controlled and the kinetically-controlled regimes. For fixed physical parameters κ , ε_w^A , θ_0 , and D_A , there is a threshold value of R at which Eq. (97) turns into an equality. For R below this threshold value, the system is in the kinetic control regime, in which V is independent of R (which is consistent with the observations in Ref. [31]). Conversely, if R exceeds the threshold value upon increasing R further, the system gradually crosses over into the diffusion control regime and, accordingly, $V \sim 1/R$ (which agrees with the experimental results and the theoretical arguments reported in Ref. [98]).

Finally, we compare the dependences on *all* physical parameters of our predicted self-propulsion velocity with the results obtained in Ref. [98] for the particular case of Janus colloids, and for a diffusion-reaction model of the hydrogen peroxide dissociation in water, using the concept of the effective Derjaguin length and phoretic slip. This provides the means for *a posteriori* checks of the accuracy of the self-consistent approximation used for solving the diffusion equations (Sec. 3). Before we proceed, we remark that the reaction scheme considered in Ref. [98] is slightly more complicated than the one used in our analysis: there, a two-step process has been assumed in which the hydrogen peroxide first forms a complex with the platinum (at a rate K_1) and then, at a rate K_2 , it dissociates into a water and an oxygen molecule. Our setting becomes identical to the one Ref. [98], if we consider the reaction in Eq. (1) (rather than the one in Eq. (2), because one of the reaction products is the same as the solvent) and if we set $K_2 = \infty$ in the results of Ref. [98]. With this, our general prediction for the self-propulsion velocity is given by Eq. (107).

First we consider the limit $R \gg D_A/K_1$. Calculating the Derjaguin length for the triangular-well potentials, we find that in the present notation the self-propulsion velocity defined by Eq. (8) in Ref. [98] is given by

$$V = -0.1 \frac{n_0}{\beta\mu R} \left(\lambda_A^2 \mathcal{J}_A - \frac{D_A \lambda_B^2 \mathcal{J}_B}{D_B} \right), \quad (113)$$

where \mathcal{J}_A and \mathcal{J}_B are the velocity integrals defined in Eq. (102) above. In view of Eq. (97) with $\theta_0 = \pi/2$, this limit corresponds to the regime of diffusion control, and hence, to our result in Eq. (109) with $\theta_0 = \pi/2$. It turns out that the expression in Eq. (113), obtained from Ref. [98], and our prediction in Eq. (109) exhibit the same dependences on the diffusion coefficients of A and B molecules, the radius R of the colloid, the viscosity, and, most importantly, the same rather non-trivial dependences on the parameters of the interaction potentials. The two expressions differ only slightly with respect to the numerical prefactor: 0.1 in Eq. (113) and 0.117 in Eq. (109).

Further on, within the opposite limit $R \ll D_A/K_1$, which in our analysis corresponds to the limit of reaction control, in the present notation Eq. (8) in Ref. [98] is given by

$$V = -\frac{n_0}{12\beta\mu D_A} K_1 \left(\lambda_A^2 \mathcal{J}_A - \frac{D_A}{D_B} \lambda_B^2 \mathcal{J}_B \right). \quad (114)$$

Taking into account $\sin^2(\pi/2) = 1$ and identifying K_1 with $\kappa \exp(-\varepsilon_w^A)$, we find perfect agreement (even concerning the numerical prefactors) between our prediction in Eq. (111) for $\theta_0 = \pi/2$ and the prediction of Ref. [98] given by Eq. (114).

6. Summary and Conclusions

We have studied theoretically the dynamics of a chemically active colloid, i.e., a particle which has parts of its surface decorated by a catalyst promoting a chemical reaction in the surrounding solution. We have focused on the steady state stall force needed to immobilize it or, equivalently, its self-phoretic velocity if it is free to move. As a model system we have analyzed a spherical particle with a catalytic patch (CP) forming a spherical cap with opening angle θ_0 . The particle is immersed in an unbounded Newtonian liquid solution, initially containing solvent (S) and reactant (A) molecules. We have considered two types of catalytically-activated reactions in which the A molecules enter upon approaching the CP: either the simple conversion into product molecules B , i.e., $A + \text{CP} \rightarrow B + \text{CP}$, or a dissociation reaction $A + \text{CP} \rightarrow B + C + \text{CP}$. An example of the latter is the platinum catalyzed dissociation of hydrogen peroxide into oxygen and water, which is often employed in experimental studies of chemically-induced self-propulsion. All molecular species (S , A , B , C) exhibit interactions with the surface of the colloid (in addition to entering into the chemical reactions), which in general differ from species to species. Furthermore the reactant molecules and the product molecules of various species diffuse in the solution with, in general distinct, diffusion coefficients D_A , D_B , and D_C .

In order to derive the equations governing the steady-state dynamics, we have employed the framework of classical linear non-equilibrium thermodynamics [114]. The number densities of the reactant and product molecules are taken to be sufficiently small so that they can be considered as an ideal-gas and that the Reynolds number and the corresponding Péclet number are very small (which is valid for typical experimental setups). On this basis we have arrived (Sec. 3) at a Smoluchowski reaction-diffusion problem with external interaction potentials (relative to the solvent one) W_k , $k = A, B, C$ for each species, and a Stokes flow problem with body forces determined by the distributions of molecular species and the potentials W_k . By generalizing a self-consistent approximation, developed originally in Ref. [103] in order to reduce the boundary conditions to the simple form of a “constant flux” (Sec. 3.B), we have solved the reaction-diffusion equations via separation of variables in spherical coordinates. The steady-state density distributions $n_k(r, \theta)$ of the various molecular species around the colloid are thus obtained in the typical form of series involving products between certain radial functions and Legendre polynomials. Interpreting the results within the chemical kinetics framework allowed us to calculate an effective reaction rate K_{eff} (Eq. (37)) and an effective steric factor $f_{dc}(\theta_0)$ (Eq. (42)) for particles exhibiting non-spherical chemical reactivity. This effective reaction rate K_{eff} satisfies a generalized form (Eq. (39)) of the well known “Collins and Kimball relation”.

The knowledge of the steady-state density distributions $n_k(r, \theta)$ has allowed for a straightforward calculation of the general expression for the force \mathbf{F}_{chem} (Eq. (54)) experienced by the colloid due the interactions with the molecules in solution (i.e., species A , B , and C). This general expression is valid for arbitrary interaction potentials and diffusion coefficients. These density distributions correspond to an out-of-equilibrium state which is maintained by the chemical reaction. Since \mathbf{F}_{chem} is only one of the contributions to the total force on the colloid (which includes also at least a hydrodynamic contribution), it is not directly measurable. But it can be accessed indirectly, e.g., by marking the molecular species and measuring their steady state distributions around the colloid with the chemical reaction switched on and off, respectively. This general expression allows one to infer various implications (Sec. 4.2) such as the following: (i) As a function of the size θ_0 of the catalyst patch, F_{chem} is non-monotonic and exhibits a maximum magnitude for an angle θ_0 which in general differs from $\pi/2$. (ii) The direction of \mathbf{F}_{chem} depends on the relative magnitude of the various diffusion coefficients.

The use of the reciprocal theorem [109, 110] facilitates to express the main quantities of interest, i.e., the stall force F_{ext} and the self-propulsion velocity V (which are both directly measurable), solely in terms of the contribution $n = 1$ of the series representations of the densities $n_k(r, \theta)$ (Eqs. (78) and (72)). The direct calculations of the hydrodynamic force exerted on the colloid (via determining the flow of the solution) turned out to be a rather challenging problem. Since this is not playing a crucial role in the present study, we leave this issue to future studies.

The general theoretical framework established here is illustrated by choosing

so-called triangular-well potentials as examples of the basic underlying interaction potentials $W_k(r)$. These potentials are characterized for each of the species by a fixed value $W_j(R)$ of the potential at the wall (i.e., the colloid surface), by the well depth $W_j(R + \lambda_j)$ at $r = R + \lambda_j$, and by being truncated at $r = R + \Lambda_j$, $j = A, B, C$. In the physically relevant limit $\lambda_j/R \ll 1$, with λ_j/Λ_j kept fixed, this choice of the interaction potentials allows one to obtain analytic expressions for F_{chem} , F_{ext} , and V in leading order in λ_j/R .

This analysis reveals that the behavior of F_{chem} is dominated by the values $W_j(R)$ of the potentials at the wall, while the behavior of the self-propulsion velocity V and of the stall force F_{ext} depends primarily on the depths $W_j(R + \lambda_j)$ of the potential wells. These expressions predict that within certain parameter ranges F_{chem} and V may have opposite signs; the same sign occurs for sufficiently strong repulsive interactions with the wall. In general, it appears that not only the calculation of the values of F_{chem} and V , but even determining their signs, is a rather complicated problem which involves all interaction parameters and all diffusion coefficients. Our analysis shows that, similarly to F_{chem} , F_{ext} and hence V attain, in general, as functions of θ_0 their maximal values for θ_0 close to but not exactly at $\pi/2$ (Janus particles); only in the limit of kinetic control the maximum of these properties is attained exactly at $\theta_0 = \pi/2$. Finally, we have found that for sufficiently small colloids the propulsion velocity is independent of their size. For large colloids, V decreases with their size as $1/R$. Our conclusions concerning the dependence of V on R are consistent with previous theoretical arguments and experimental observations [31,98]. Lastly, we have shown that, for short-ranged triangular-well potentials, in two limiting situations (the reaction control and the diffusion control regimes) our general results reproduce the results obtained in Ref. [98] by using the concepts of the effective Derjaguin length and phoretic slip.

There are several directions along which generalizations of the approach developed here are feasible and could provide significant physical insight. First, one can invoke more involved contributions of the catalyst to the reaction scheme, for example the formation of catalyst-bounded activated complexes with finite lifetimes, as considered in Ref. [98]. Second, it is plausible that the dissociation reaction at the catalyst is accompanied by recombination or annihilation of some (or all) of the products in the bulk solution or in a different region on the surface of the particles; such systems can be expected to exhibit a significantly richer behavior resulting from the interplay between the different time- and length-scales of the various reactions. Third, since most of the experimental studies of chemically active colloids involve particles suspended in (weak) electrolytes and reactions which are expected to produce ionic radicals, it is natural to consider extending the approach developed here by adding to the present description the corresponding equations which account for charge conservation. Last but not least, the influence of rotational diffusion of an active particle on the stall force or on the self-propulsion velocity can be straightforwardly included into the framework presented here.

Acknowledgments

GO and SD acknowledge partial financial support by and the hospitality of the Kavli Institute for Theoretical Physics, UCSB, where this study was pursued during the Focused Working Group on Self-Propelled Micro-Objects hosted by KITP.

References

- [1] Ismagilov R F, Schwartz A, Bowden N and Whitesides G M 2002 *Angew. Chem. Int. Ed.* **41** 652–654
- [2] Paxton W F, Kistler K C, Olmeda C C, Sen A, St Angelo S K, Cao Y Y, Mallouk T E, Lammert P E and Crespi V H 2004 *J. Am. Chem. Soc.* **126** 13424–13431
- [3] Ozin G A, Manners I, Fournier-Bidoz S and Arsenault A 2005 *Adv. Mater.* **17** 3011–3018
- [4] Paxton W F, Sundararajan S, Mallouk T E and Sen A 2006 *Angew. Chem. Int. Ed.* **45** 5420–5429
- [5] Lauga E and Powers T R 2009 *Rep. Prog. Phys.* **72** 096601:1–36
- [6] Solovev A A, Mei Y F, Urena E B, Huang G S and Schmidt O G 2009 *Small* **5** 1688–1692
- [7] Mirkovic T, Zacharia N S, Scholes G D and Ozin G A 2010 *Small* **6** 159–167
- [8] Ebbens S J and Howse J R 2010 *Soft Matter* **6** 726–738
- [9] Golestanian R, Liverpool T B and Ajdari A 2005 *Phys. Rev. Lett.* **94** 220801:1–4
- [10] Elgeti J, Winkler R G and Gompper G 2014 *Rep. Prog. Phys.* **78** 056601:1–50
- [11] Zöttl A and Stark H 2016 *J. Phys.: Condens. Matter* **28** 253001:1–28
- [12] Anderson J L 1989 *Ann. Rev. Fluid. Mech.* **21** 61–99
- [13] Catchmark J M, Subramanian S and Sen A 2005 *Small* **1** 202–206
- [14] Paxton W F, Baker P T, Kline T R, Wang Y, Mallouk T E and Sen A 2006 *J. Am. Chem. Soc.* **128** 14881–14888
- [15] Buttinoni I, Volpe G, Kümmel F, Volpe G and Bechinger C 2012 *J. Phys.: Condens. Matter* **24** 284129:1–6
- [16] Sanchez S, Solovev A A, Schulze S and Schmidt O G 2011 *Chem. Commun.* **47** 698–700
- [17] Sanchez S, Solovev A A, Harazim S M and Schmidt O G 2011 *J. Am. Chem. Soc.* **133** 701–703
- [18] Sanchez S, Ananth A N, Fomin V, Viehrig M and Schmidt O G 2011 *J. Am. Chem. Soc.* **133** 14860–14863
- [19] Solovev A A, Sanchez S, Pumera M, Mei Y F and Schmidt O G 2010 *Adv. Funct. Mater.* **20** 2340–2345
- [20] Gao W, Uygun A and Wang J 2012 *J. Am. Chem. Soc.* **134** 897–900
- [21] Balasubramanian S, Kagan D, Jack Hu C M, Campuzano S, Lobo-Castanon M J, Lim N, Kang D Y, Zimmerman M, Zhang L and Wang J 2011 *Angew. Chem. Int. Ed.* **50** 4161–4164
- [22] Spagnolie S E and Lauga E 2010 *Phys. Fluids* **22** 081902:1–18
- [23] Felderhof B 2010 *J. Chem. Phys.* **133** 064903:1–7
- [24] Jiang H R, Yoshinaga N and Sano M 2010 *Phys. Rev. Lett.* **105** 268302:1–4
- [25] Qian B, Montiel D, Bregulla A, Cichos F and Yang H 2013 *Chem. Sci.* **4** 1420–1429
- [26] Shklyaev S, Brady J F and Córdova-Figueroa U M 2014 *J. Fluid Mech.* **748** 488–520
- [27] Michelin S and Lauga E 2015 *Eur. Phys. J. E* **38** 1–16
- [28] Kline T R, Paxton W F, Mallouk T E and Sen A 2005 *Angew. Chem. Int. Ed.* **44** 744–746
- [29] Fournier-Bidoz S, Arsenault A C, Manners I and Ozin G A 2005 *Chem. Commun.* 441–443
- [30] Hong Y, Blackman N M K, Kopp N D, Sen A and Velegol D 2007 *Phys. Rev. Lett.* **99** 178103:1–4
- [31] Howse J R, Jones R A L, Ryan A J, Gough T, Vafabakhsh R and Golestanian R 2007 *Phys. Rev. Lett.* **99** 048102:1–4
- [32] Erbe A, Zientara M, Baraban L, Kreidler C and Leiderer P 2008 *J. Phys.: Condens. Matter* **20** 404215:1–5
- [33] Laocharoensuk R, Burdick J and Wang J 2008 *ACS Nano* **2** 1069–1075

- [34] Baraban L, Tasinkevych M, Popescu M N, Sanchez S, Dietrich S and Schmidt O 2012 *Soft Matter* **8** 48–52
- [35] Pavlick R, Sengupta S, McFadden T, Zhang H and Sen A 2011 *Angew. Chem. Int. Ed.* **50** 9374–9377
- [36] Ajdari A and Bocquet L 2006 *Phys. Rev. Lett.* **96** 186102:1–4
- [37] Golestanian R, Liverpool T B and Ajdari A 2007 *New J. Phys.* **9** 126:1–9
- [38] Jülicher F and Prost J 2009 *Eur. Phys. J. E* **29** 27–36
- [39] Ruckner G and Kapral R 2007 *Phys. Rev. Lett.* **98** 150603:1–4
- [40] Tao Y G and Kapral R 2008 *J. Chem. Phys.* **128** 164518:1–8
- [41] Popescu M N, Dietrich S, Tasinkevych M and Ralston J 2010 *Eur. Phys. J. E* **31** 351–367
- [42] Popescu M N, Tasinkevych M and Dietrich S 2011 *EPL* **95** 28004:1–6
- [43] Popescu M N, Dietrich S and Oshanin G 2009 *J. Chem. Phys.* **130** 194702:1–16
- [44] Crowdy D G 2013 *J. Fluid Mech.* **735** 473–498
- [45] Kaiser A, Wensink H H and Löwen H 2012 *Phys. Rev. Lett.* **108** 268307:1–5
- [46] Kaiser A, Popowa K, Wensink H H and Löwen H 2013 *Phys. Rev. E* **88** 022311:1–9
- [47] Lefauve A and Saintillan D 2014 *Phys. Rev. E* **89** 021002:1–5
- [48] Menzel A M 2013 *J. Phys.: Cond. Matter* **25** 505103:1–17
- [49] Berke A P, Turner L, Berg H C and Lauga E 2008 *Phys. Rev. Lett.* **101** 038102:1–4
- [50] Pototsky A and Stark H 2012 *EPL* **98** 50004:1–6
- [51] Pototsky A, Hahn A M and Stark H 2013 *Phys. Rev. E* **87** 042124:1–6
- [52] ten Hagen B, van Teeffelen S and Löwen H 2009 *Cond. Matt. Phys.* **12** 725–738
- [53] Lee C F 2013 *New J. Phys.* **15** 055007:1–11
- [54] Takagi D, Palacci J, Braunschweig A B, Shelley M J and Zhang J 2014 *Soft Matter* **10** 1784–1789
- [55] Marsden E J, Valeriani C, Sullivan I, Cates M E and Marenduzzo D 2014 *Soft Matter* **10** 157–165
- [56] Volpe G, Buttinoni I, Vogt D, Kümmerer H J and Bechinger C 2011 *Soft Matter* **7** 8810–8815
- [57] Elgeti J and Gompper G 2013 *EPL* **101** 48003:1–6
- [58] Hsu J P, Luu X C and Hsu W L 2010 *J. Phys. Chem. B* **114** 8043–8055
- [59] Mijalkov M and Volpe G 2013 *Soft Matter* **9** 6376–6381
- [60] van Teeffelen S, Zimmermann U and Löwen H 2009 *Soft Matter* **5** 4510–4519
- [61] Brotto T, Caussin J B, Lauga E and Bartolo D 2013 *Phys. Rev. Lett.* **110** 038101:1–5
- [62] Hsieh T H and Keh H J 2013 *J. Chem. Phys.* **138** 074105:1–8
- [63] Spagnolie S and Lauga E 2012 *J. Fluid Mech.* **700** 105–147
- [64] Ishimoto K and Gaffney E A 2013 *Phys. Rev. E* **88** 062702:1–12
- [65] Uspal W E, Popescu M N, Dietrich S and Tasinkevych M 2015 *Soft Matter* **11** 434 – 438
- [66] Uspal W E, Popescu M N, Dietrich S and Tasinkevych M 2015 *Soft Matter* **11** 6613 – 6632
- [67] Würger A 2014 *J. Fluid Mech.* **752** 589 – 601
- [68] Lauga A and Davis A 2012 *J. Fluid Mech.* **705** 120–133
- [69] Masoud H and Stone H A 2014 *J. Fluid Mech.* **741** R4:1–7
- [70] Domínguez A, Margaretti P, Popescu M N and Dietrich S 2016 *Phys. Rev. Lett.* **116** 078301:1–5
- [71] Das S, Garg A, Campbell A I, Howse J, Sen A, Velegol D, Golestanian R and Ebbens S J 2015 *Nat. Comm.* **6** 8999:1–10
- [72] Simmchen J, Katuri J, Uspal W E, Popescu M N, Tasinkevych M and Sánchez S 2016 *Nat. Comm.* **7** 10598:1–9
- [73] Margaretti P, Popescu M N and Dietrich S 2016 *Soft Matter* **12** 4007 – 4023
- [74] Mozaffari A, Sharifi-Mood N, Koplik J and Maldarelli C 2016 *Phys. Fluids* **28** 053107:1–35
- [75] Uspal W E, Popescu M N, Dietrich S and Tasinkevych M 2016 *Phys. Rev. Lett.* **117** 048002:1–5 (2016).
- [76] ten Hagen B, van Teeffelen S and Löwen H 2011 *J. Phys.: Condens. Matter* **23** 194119:1–16
- [77] ten Hagen B, Wittkowski R and Löwen H 2011 *Phys. Rev. E* **84** 031105:1–6
- [78] Taktikos J, Zaburdaev V and Stark H 2011 *Phys. Rev. E* **84** 041924:1–11
- [79] Enculescu M and Stark H 2012 *Phys. Rev. Lett.* **107** 058301:1–5

- [80] Taktikos J, Zaburdaev V and Stark H 2012 *Phys. Rev. E* **85** 051901:1–12
- [81] Zöttl A and Stark H 2012 *Phys. Rev. Lett.* **108** 218104:1–4
- [82] Palacci J, Cottin-Bizonne C, Ybert C and Bocquet L 2010 *Phys. Rev. Lett.* **105** 088304:1–4
- [83] Theurkoff I, Cottin-Bizonne C, Palacci J, Ybert C and Bocquet L 2012 *Phys. Rev. Lett.* **108** 268303:1–4
- [84] Cates M E and Tailleur J 2013 *EPL* **101** 20010:1–6
- [85] Solon A P, Fily Y, Baskaran A, Cates M E, Kafri Y, Kardar M and Tailleur J 2015 *Nat. Phys.* **11** 673–678
- [86] Solon A P, Stenhammar J, Wittkowski R, Kardar M, Kafri Y, Cates M E and Tailleur J 2014 *Phys. Rev. Lett.* **114** 198301:1–6
- [87] Pooley C M, Alexander G P and Yeomans J M 2007 *Phys. Rev. Lett.* **99** 228103:1–4
- [88] Golestanian R, Yeomans J M and Uchida N 2011 *Soft Matter* **7** 3074–3082
- [89] Bialké J, Speck T and Löwen H 2012 *Phys. Rev. Lett.* **108** 168301:1–5
- [90] Kaiser A, Wensink H H and Löwen H 2012 *Phys. Rev. Lett.* **108** 268307:1–5
- [91] Wensink H H, Dunkel J, Heidenreich S, Drescher K, Goldstein R E, Löwen H and Yeomans J M 2012 *Proc. Nat. Acad. Sci.* **109** 14308–14313
- [92] Sharifi-Mood N, Koplik J and Maldarelli C 2013 *Phys. Rev. Lett.* **111** 184501:1–5
- [93] de Graaf J, Rempfer G and Holm C 2015 *IEEE Trans Nanobioscience* **14** 272–288
- [94] Sabass B and Seifert U 2012 *J. Chem. Phys.* **136** 064508:1–15
- [95] Ebbens S, Gregory D A, Dunderdale G, Howse J R, Ibrahim Y, Liverpool T B and Golestanian R 2014 *EPL* **106** 58003:1–6
- [96] Reigh S and Kapral R 2015 *Soft Matter* **13** 3149–3158
- [97] Ebbens S, Buxton G, Alexeev A, Sadeghi A and Howse J 2012 *Soft Matter* **8** 3077–3082
- [98] Ebbens S, Tu M H, Howse J R and Golestanian R 2012 *Phys. Rev. E* **85** 020401(R):1–4
- [99] Thakur S and Kapral R 2011 *J. Chem. Phys.* **135** 024509:1–9
- [100] Thakur S, Chen J X and Kapral R 2011 *Angew. Chem. Int. Ed.* **50** 10165–10169
- [101] Sabass B and Seifert U 2012 *J. Chem. Phys.* **136** 214507:1–13
- [102] Sharifi-Mood N, Koplik J and Maldarelli C 2013 *Phys. Fluids* **25** 012001:1–34
- [103] Shoup D, Lipari G and Szabo A 1981 *Biophys. J.* **36** 697–714
- [104] Michelin S, Lauga E and Bartolo D 2013 *Phys. Fluids* **25** 061701:1–7
- [105] Michelin S and Lauga E 2014 *J. Fluid Mech.* **747** 572–604
- [106] Manjare M, Wu Y T, Yang B and Zhao Y P 2014 *Appl. Phys. Lett.* **104** 054102:1–5
- [107] Smoluchowski M 1917 *Z. Phys. Chem.* **92** 129–168
- [108] Farniya A A, Esplandiu M J, Reguera D and Bachtold A. 2013 *Phys. Rev. Lett.* **111** 168301:1 – 5
- [109] Kim S and Karrila S J 1991 *Microhydrodynamics: Principles and Selected Applications* (Butterworth–Heinemann, New York)
- [110] Teubner M 1982 *J. Chem. Phys.* **76** 5564–5573
- [111] Fowler R H, Graben H W, De Rocco A G and Feinberg M J 1965 *J. Chem. Phys.* **43** 1083
- [112] Bárcenas M, Reyes Y, Romero-Martínez A, Odriozola G and Orea P 2015 *J. Chem. Phys.* **142** 074706:1–5
- [113] Sengupta A and Adhikari J 2016 *Chem. Phys.* **469–470** 16 – 24
- [114] de Groot S R and Mazur P 1962 *Non-equilibrium Thermodynamics* (North-Holland, Amsterdam)
- [115] Landau L and Lifshitz E M 1973 *Fluid Mechanics (2nd Edition)* (Elsevier, Oxford)
- [116] Dunlop P J and Gosting L J 1959 *J. Phys. Chem.* **63** 86–93
- [117] Gupta P K and Cooper Jr A R 1971 *Physica* **54** 35–59
- [118] Mangiapia G, Paduano L, Ortona O, Sartorio R and D’Errico G 2013 *J. Phys. Chem. B* **117** 741–749
- [119] Liu X, Martín-Calvo A, McGarrity E, Schnell S K, Calero S, Simon J M, Bedeaux D, Kjelstrup S, Bardow A and Vlugt T J H 2012 *Ind. Eng. Chem. Res.* **51** 10247–10258
- [120] Miller D G, Vitagliano V and Sartorio R 1986 *J. Phys. Chem.* **90** 1509–1519

- [121] Rard J A, Albright J G, Miller D G and Zeidler M E 1996 *J. Chem. Soc., Faraday Trans.* **92** 4187–4197
- [122] Mialdun A, Sechenyh V, Legros J C, de Zárata J M O and Shevtsova V 2013 *J. Chem. Phys.* **139** 104903:1–16
- [123] Collins F and Kimball G 1949 *J. Colloid Sci.* **4** 425–437
- [124] Berdnikov V and Doktorov A 1982 *Chem. Phys.* **69** 205–212
- [125] Redner S 2001 *A Guide to First-Passage Processes* (Cambridge University Press, New York)
- [126] Weiss G H 1986 *J. Stat. Phys.* **42** 3–36
- [127] Shoup D and Szabo A 1982 *Biophys. J.* **40** 33–39
- [128] Shulten Z and Shulten K 1977 *J. Chem. Phys.* **66** 4616–4634
- [129] Solc K and Stockmayer W 1971 *J. Chem. Phys.* **54** 2981–2988
- [130] Solc K and Stockmayer W 1973 *Int. J. Chem. Kinet.* **5** 733–752
- [131] Samson R and Deutch J 1978 *J. Chem. Phys.* **68** 285–290
- [132] Traytak S D 1997 *Chem. Phys.* **192** 1–7
- [133] Traytak S and Price W 2007 *J. Chem. Phys.* **127** 184508:1–8
- [134] Debye P 1942 *Trans. Electrochem. Soc.* **82** 265–272
- [135] Grebenkov D S and Oshanin G 2017 *Phys. Chem. Chem. Phys.*, **19** 2723 – 2739
- [136] Oshanin G S, Ovchinnikov A A and Burlatsky S F 1989 *J. Phys. A: Math. Gen.* **22** L977–L982
- [137] Oshanin G S, Moreau M and Burlatsky S F 1994 *Adv. Coll. Interf. Sci.* **49** 1–46
- [138] Bénichou O, Moreau M and Oshanin G 2000 *Phys. Rev. E* **61** 3388–3406
- [139] Happel J and Brenner H 1973 *Low Reynolds number hydrodynamics* (Noordhoff International, Leyden)
- [140] Drescher K, Goldstein R, Michel N, Polin M and Tuval I 2010 *Phys. Rev. Lett.* **105** 168101:1–4
- [141] de Buyl P, Mikhailov A S and Kapral R 2013 *EPL* **103** 60009:1–6
- [142] Abramowitz M and Stegun I R 1972 Eds. *Handbook of mathematical functions* (Dover, New York)

Appendix A. Spatial distribution of the molecular components of the mixture

We aim at describing the distribution of the molecular components in the mixture within the standard theory of linear non-equilibrium thermodynamics [94, 102, 114, 115]. The solution as a whole is assumed to behave as an incompressible Newtonian fluid. The reaction will be accounted for via boundary conditions on the surface of the colloid. Therefore, the description of the dynamics of the mixture will involve (i) continuity equations (conservation of mass) for the mixture and for the A and B species; (ii) linear relations between the conjugate thermodynamic fluxes and forces determining the entropy production rate; (iii) the Navier-Stokes equations obeyed by the barycentric velocity $\mathbf{u}(\mathbf{r})$ of the mixture (i.e., conservation of momentum).

The liquids involved in typical experimental studies have a very low compressibility; therefore they can be assumed to have a constant mass density $\rho(\mathbf{r}, t) := \rho = \text{const.}$ (For a discussion of the more general case in which this assumption is softened one can consult, e.g., Ref. [93].) In terms of the number densities $n_{A,B,S}$ and the molecular masses, and accounting for the fixed number densities of A and S molecules far from the colloid, this can be expressed as

$$\begin{aligned} \rho(\mathbf{r}, t) &= \rho = n_A(\mathbf{r}, t) m_A + n_B(\mathbf{r}, t) m_B + n_S(\mathbf{r}, t) m_S \\ &= n_0^{(A)} m_A + n_0^{(S)} m_S \end{aligned} \tag{A.1}$$

where the rhs corresponds to $\rho(\mathbf{r}, t = 0)$. The local number density of the solvent can be determined once ρ and the number densities of the A and B species are known.

Considering total mass conservation in a small volume element δV located at \mathbf{r} (which, however, is sufficiently large to contain a large number of A , B , and S molecules such that their number densities in δV are well defined) leads to the continuity equation for the mixture:

$$\frac{\partial \rho}{\partial t} + \nabla(\rho \mathbf{u}) = 0 \stackrel{\rho = \text{const}}{\implies} \nabla \mathbf{u} = 0, \quad (\text{A.2})$$

where $\rho \mathbf{u}$ is the mass current density or the momentum density; \mathbf{u} is the barycentric velocity, i.e., the momentum density divided by the mass density.

Assuming local equilibrium, the free energy $F(T, V, N_A, N_B, N_S)$ of the isothermal fluid mixture in contact with the colloidal particle can be written in terms of a local free energy density (per volume) $f(T, n_A := \delta N_A / \delta V, n_B := \delta N_B / \delta V, n_S := \delta N_S / \delta V)$ as $F = \int_V dV f$, where

$$df = -s dT + \tilde{\mu}_A dn_A + \tilde{\mu}_B dn_B + \tilde{\mu}_S dn_S. \quad (\text{A.3})$$

In the expression above $s := \delta S / \delta V$ is the local entropy density, $\delta N_{A(B,S)}$ is the number of A (B , S) molecules, respectively, in the volume δV and the interactions with the colloid have been accounted for by the modified chemical potentials [114]

$$\tilde{\mu}_j := \mu_j + \Phi_j, \quad j = A, B, S. \quad (\text{A.4})$$

Note that while the modified chemical potentials $\tilde{\mu}_j$ are taken to be constant over the small volume element δV , they vary spatially. This is the case because the interaction potentials Φ_j vary spatially and the chemical potentials μ_j (in the absence of interactions) vary with position due to the fluid mixture being in contact with the source (sink) for the B (A) species at the colloid surface and with the sink (source) for the B (A) species far away from the colloid surface so that the system is out of thermodynamic equilibrium.

The incompressibility condition in Eq. (A.1) implies that only two of the densities n_A , n_B , and n_S are independent. In order to connect straightforwardly to the continuity equations (i.e., mass conservation) in δV for each of the molecular species (see the next paragraphs), it is advantageous to change the variables from number densities to concentrations, i.e., mass fractions, which are defined as

$$\begin{aligned} c_j(\mathbf{r}, t) &:= \frac{\rho_j(\mathbf{r}, t)}{\rho} = \\ &= \frac{m_j n_j(\mathbf{r}, t)}{m_A n_A(\mathbf{r}, t) + m_B n_B(\mathbf{r}, t) + m_S n_S(\mathbf{r}, t)}, \quad j = A, B, S. \end{aligned} \quad (\text{A.5})$$

Here $\rho_j(\mathbf{r}, t) = m_j n_j(\mathbf{r}, t)$ denotes the mass density of species $j = A, B, S$. The concentrations obey the relation $c_A + c_B + c_S = 1$. With $dn_j = (\rho / m_j) dc_j$ and $dc_S = -(dc_A + dc_B)$, Eq. (A.3) takes the form

$$df = -s dT + \bar{\mu}_A dc_A + \bar{\mu}_B dc_B. \quad (\text{A.6})$$

The chemical potentials $\bar{\mu}_j$ conjugated to the concentration variables are given by

$$\bar{\mu}_j := \left(\frac{\tilde{\mu}_j}{m_j} - \frac{\tilde{\mu}_S}{m_S} \right) \rho = \left(\frac{\mu_j}{m_j} - \frac{\mu_S}{m_S} \right) \rho + \frac{W_j}{m_j} \rho, \quad j = A, B. \quad (\text{A.7})$$

Therefore the mixture is described completely by $c_A(\mathbf{r})$ and $c_B(\mathbf{r})$; $c_S(\mathbf{r})$ follows from the incompressibility condition in Eq. (A.1).

The local mass conservation for the species A and B in the region *outside* the impermeable sphere ($r > R$) implies that the concentrations $c_{A,B}(\mathbf{r}, t)$ obey the continuity equations [114] (see Eq. (A.5))

$$\frac{\partial(\rho c_j)}{\partial t} + \nabla \cdot \mathbf{J}_j = 0, \quad j = A, B, \quad (\text{A.8})$$

where, in line with the usual non-equilibrium thermodynamics framework [38, 114], the currents $\mathbf{J}_{A,B}$ are split into a convective part due to the barycentric motion and a "diffusion" part $\mathbf{j}_{A,B}$ due to the motion relative to that of the local center of mass:

$$\mathbf{J}_j := \rho c_j \mathbf{u} + \mathbf{j}_j, \quad j = A, B, \quad (\text{A.9})$$

where \mathbf{u} is the center of mass (barycentric) velocity of the mixture in the volume element δV .

The advantage of the decomposition in Eq. (A.9) is that within the framework of linear non-equilibrium thermodynamics the currents \mathbf{j}_j are the "fluxes" coupled to the thermodynamic forces which, in accordance with the expression for the entropy production (see Ref. [114]), are given by the spatial gradients of the chemical potentials $\bar{\mu}_j$ introduced in Eq. (A.7). Therefore, each of the \mathbf{j}_j can be written as a linear combination of these gradients [114]:

$$\begin{aligned} \mathbf{j}_A &= -\frac{L_{AA}}{T} \nabla \bar{\mu}_A - \frac{L_{AB}}{T} \nabla \bar{\mu}_B, \\ \mathbf{j}_B &= -\frac{L_{BB}}{T} \nabla \bar{\mu}_B - \frac{L_{BA}}{T} \nabla \bar{\mu}_A, \end{aligned} \quad (\text{A.10})$$

where T is the temperature (assumed to be spatially constant) and the couplings $L_{AA} > 0$, $L_{BB} > 0$, and $L_{AB} = L_{BA}$ are the so-called Onsager coefficients.

Furthermore, since we consider low concentrations, so that there are effectively no interactions between the A and B species, we shall disregard the possibility of a direct influence of the dynamics of B on that of A . Therefore we disregard the possibility that currents of A are directly driven by gradients of the concentration and thus of the chemical potential $\bar{\mu}_B$ of the B molecules. Thus we set $L_{AB} = 0$. (In the context of active colloids, the conditions under which this assumption is expected to hold are discussed in more detail in Ref. [93].) Although these cross-terms are sometimes important even for dilute solutions [114], our use of this approximation is motivated by previous reports showing that in many cases the diffusion coefficients (accounting for currents driven by concentration gradients, which are the most relevant terms in our system) in ternary mixtures are such that the cross-terms induced contributions are much smaller than the ones due to self-diffusion [116–121]. (But we note that recently for a ternary mixture cross-term diffusion coefficients have been reported which are of

the same order of magnitude as the self-diffusion ones [122]; however, this was found for comparable concentrations and thus far from the dilute solution limit we are considering here.)

Within this approximation one has

$$\mathbf{j}_A = -\frac{\rho L_{AA}}{T} \nabla \left(\frac{\mu_A}{m_A} - \frac{\mu_S}{m_S} \right) - \frac{\rho L_{AA}}{T} \nabla \left(\frac{W_A}{m_A} \right) \quad (\text{A.11})$$

and the analogous expression for \mathbf{j}_B in which A is replaced by B . This expression shows that the influence of the external interaction potentials has been isolated into a single contribution (the last term on the right hand side of Eq. (A.11)). The mass current is now decomposed into a contribution solely due to the composition of the mixture (i.e., the first term on the right hand side of Eq. (A.11)) and a convective part solely due to the difference W_A (W_B) between the interaction of the A (B) molecules with the colloid and the interaction, weighted by the corresponding mass ratio $m_{A,B}/m_S$, of the S molecules with the colloid.

Under the above assumption, the chemical potentials $\hat{\mu}_A$ and $\hat{\mu}_B$ with

$$\hat{\mu}_{A,B} := \frac{\mu_{A,B}}{m_{A,B}} - \frac{\mu_S}{m_S} \quad (\text{A.12})$$

are functions (see Eq. (A.6)) of the temperature T (assumed to be spatially constant for our system) and of the local concentration c_A of the A molecules ($\hat{\mu}_A$) or of the concentration c_B of the B molecules ($\hat{\mu}_B$), respectively. Explicit expressions for these dependences would require knowledge of the free energy density, i.e., a specific model of the mixture. However, further progress can be made by arguing that, because the concentrations of A and B molecules are assumed to remain very small at all times and the mixture is incompressible, the spatial variations of the chemical potential of the solvent μ_S can be neglected relative to those of the chemical potentials of the solutes. This is so because for an ideal dilute solution the chemical potential of the solute is proportional to the logarithm of the solute concentration, while that of the solvent is proportional to the solute concentration (see Ch. IX in Ref. [115]). This implies that $(\nabla \mu_{A,B})_T \sim \frac{\nabla c_{A,B}}{c_{A,B}}$, while $(\nabla \mu_S)_T \sim \nabla(c_A + c_B)$, and thus the magnitude of the former is greater than that of the latter by a factor $1/c_{A,B}$, which is very large. Therefore, for a dilute solution one can approximate $(\nabla \hat{\mu}_{A,B})_T \simeq \frac{(\nabla \mu_{A,B})_T}{m_{A,B}} = \frac{k_B T}{m_{A,B}} \frac{\nabla c_{A,B}}{c_{A,B}}$ [115], where k_B is the Boltzmann constant. Accordingly the decomposition in Eq. (A.11) implies that the diffusion (relative motion) part of the particle current can be written as the superposition of concentration gradients and convective terms (which are due to the external fields), for which one can directly formulate the usual expression [114]

$$\mathbf{j}_{A,B} = -D_{A,B} [\nabla(\rho c_{A,B}) + \beta \rho c_{A,B} \nabla W_{A,B}] . \quad (\text{A.13})$$

Here ρ is constant, $\beta = 1/(k_B T)$, and $D_{A,B} = (k_B L_{AA,BB})/(m_{A,B} c_{A,B})$ are the heuristically defined diffusion coefficients of the A and B species, respectively. They are expressed in terms of the *unknown* Onsager coefficients L_{AA} and L_{BB} and, in general, the partial derivatives of the chemical potentials $\hat{\mu}_{A,B}$ with respect to the corresponding concentrations at constant temperature. We note that the diffusion coefficients $D_{A,B}$

defined above and entering in Eq. (A.13) are the so-called "collective diffusion" coefficients, which, in general, are different from the single particle ones, introduced in Sec. 2, which are describing the mean-square displacement of the Brownian motion of A (B) molecules. However, in the dilute limit, which is the case considered in this study, the two quantities coincide, thus the use of the same notation.

Using the expression in Eq. (A.13), the total particle current in Eq. (A.9) has the form ($\rho_j = \rho c_j$, Eq. (A.5))

$$\begin{aligned} \mathbf{J}_j &= \rho_j \mathbf{u} - D_j (\nabla \rho_j + \rho_j \nabla (\beta W_j)) \\ &= \frac{D_j \rho}{R} \left(\frac{U_0 R}{D_j} c_j \mathbf{U} - \nabla_\xi c_j - c_j \nabla_\xi (\beta W_j) \right), \quad j = A, B, \end{aligned} \quad (\text{A.14})$$

where U_0 denotes a typical velocity scale for the flow of the mixture, $\xi = r/R$, and $\mathbf{U} = \mathbf{u}/U_0$. In the following we make the additional assumption that for the systems of interest the Peclet number $\text{Pe} = U_0 R / \min(D_A, D_B)$ is much smaller than 1 and thus the effects of the barycentric convection are negligible. As previously reported, this is indeed the case for catalytically active colloids, for which typical Pe numbers are $\text{Pe} \lesssim 10^{-2}$ [9, 43, 94]. With this final approximation, after inserting Eq. (A.14) into the Eq. (A.8), one obtains that the concentrations $c_{A,B}(\mathbf{r}, t)$ obey the following diffusion equations:

$$\begin{aligned} \frac{\partial c_j}{\partial t} &= D_j \nabla \cdot (\nabla c_j + \beta c_j \nabla W_j(r)) \\ &= D_j \nabla \cdot [e^{-\beta W_j(r)} \nabla (e^{\beta W_j(r)} c_j)], \quad j = A, B. \end{aligned} \quad (\text{A.15})$$

Due to $c_j = (m_j/\rho)n_j$ and owing to the assumption of negligible cross-term diffusion (see Eqs. (A.10) and (A.11)), the dynamics of the concentrations of the different species are effectively decoupled. Accordingly, with $c_j = (m_j/\rho)n_j$, Eq. (A.15) can be transcribed in terms of the number density fields, which is a more convenient representation for the system under study (see, c.f., Sec. 4), and yields Eq. (4).

Appendix B. Catalytically induced dissociation

Here we present, using our results in Subsec. 3.3, the derivation of the spatially inhomogeneous, steady state distribution of the product molecules C , which emerge in the catalytically induced dissociation reaction described in Eq. (2).

As in Subsec. 3.3, we suppose that the product molecules C of mass m_C diffuse with the diffusion coefficient D_C and interact with the colloid via a radially symmetric potential $W_C(r)$ (relative to that of the solvent molecules, similar to the definition in Eq. (3) for the A and B molecules). Accordingly, the time evolution of the local density of the reaction product C obeys the differential equation

$$\begin{aligned} 0 &= \frac{D_C}{r^2} \frac{\partial}{\partial r} \left(r^2 \frac{\partial n_C}{\partial r} \right) + \frac{\beta D_C}{r^2} \frac{\partial}{\partial r} \left(r^2 n_C \frac{dW_C}{dr} \right) + \\ &+ \frac{D_C}{r^2 (\sin \theta)} \frac{\partial}{\partial \theta} \left((\sin \theta) \frac{\partial n_C}{\partial \theta} \right), \end{aligned} \quad (\text{B.1})$$

which has the same form as Eqs. (5) and (40). Similarly to Eq. (40), which describes the time evolution of the reaction product B , Eq. (B.1) is to be solved subject to a sink boundary condition at macroscopic distances from the colloid (as in Eq. (41)) and subject to the mixed boundary conditions imposed at the surface of the colloid: the zero current condition at the inert part of the surface and the reactive boundary condition at the catalytically active patch (as in Eq. (42) with B replaced by C).

According to the assumptions of the present model the dynamics of C is decoupled from that of B . (Interactions between B and C and between A and B as well as A and C would change this.) Therefore all results for the B species obtained in the previous subsection can be simply transcribed to the present case with the replacements $B \rightarrow C$ and $j_n \rightarrow h_n$ (see below).

In line with Eq. (43), the steady state distribution of the product C has the form

$$n_C(r, \theta) = n_0 e^{-\beta W_C(r)} \sum_{n=0}^{\infty} \gamma_n h_n(r) P_n(\cos \theta), \quad (\text{B.2})$$

where the functions $h_n(r)$ are those solutions of (compare Eq. (44))

$$h_n''(r) + \left(\frac{2}{r} - \beta W_C'(r) \right) h_n'(r) - \frac{n(n+1)}{r^2} h_n(r) = 0, \quad (\text{B.3})$$

which vanish for $r \rightarrow \infty$ and are normalized such that $h_n(r = R) = 1$. The dimensionless coefficients γ_n are given by (see Eq. (45))

$$\begin{aligned} \gamma_n &= - \frac{Q e^{\beta W_C(R)} \phi_n(\theta_0)}{2 D_C n_0 h_n'(R)} \\ &= - \frac{K_{eff}}{4 \pi D_C R} \frac{e^{\beta W_C(R)} \phi_n(\theta_0)}{R h_n'(R) \phi_0(\theta_0)}, \quad n \geq 0. \end{aligned} \quad (\text{B.4})$$

As in Eq. (46), in the diffusion-controlled limit one has

$$\gamma_n(K^* \rightarrow \infty) = - \frac{D_A}{D_C} \frac{R_D}{R} \frac{e^{\beta W_C(R)} \phi_n(\theta_0)}{R h_n'(R) \phi_0(\theta_0)} f_{dc}(\theta_0), \quad n \geq 0, \quad (\text{B.5})$$

while in the limit of kinetic control the coefficients γ_n are given by (Eq. (47))

$$\gamma_n(D_A \rightarrow \infty) = - \frac{K^*}{4 \pi D_C R} \frac{e^{\beta W_C(R)} \phi_n(\theta_0)}{R h_n'(R) \phi_0(\theta_0)}, \quad n \geq 0, \quad (\text{B.6})$$

and, in this limit, are independent of D_A .

Appendix C. The generalized reciprocal theorem of Teubner

For an easier understanding, here we include a brief derivation of the generalized reciprocal theorem due to Teubner [110], which we use in order to determine the velocity of the self-propelled colloid (Eq. (71)). For a detailed discussion, as well as various applications of this result, the interested reader is referred to the original paper [110] or the textbook by Kim and Karrila [109].

By applying the equivalent of Gauss' theorem for tensor fields [139] and selecting the orientation of the surface elements entering into the surface integral to be the one

given by the inner normals, for arbitrary tensor fields $\hat{\Pi}$ and arbitrary vector fields \mathbf{u}' one obtains

$$\int_{\mathcal{D}} \nabla \cdot (\mathbf{u}' \cdot \hat{\Pi}) d^3 \mathbf{r} = - \int_{\partial \mathcal{D}} \mathbf{u}' \cdot \hat{\Pi} \cdot d\mathbf{s} - \int_{S_\infty} \mathbf{u}' \cdot \hat{\Pi} \cdot d\mathbf{s}_\infty = - \int_{\partial \mathcal{D}} \mathbf{u}' \cdot \hat{\Pi} \cdot d\mathbf{s}. \quad (\text{C.1})$$

\mathcal{D} is that domain in \mathbb{R}^3 which on the inner side is bounded by a closed surface $\partial \mathcal{D}$ (such that \mathcal{D} is the exterior of $\partial \mathcal{D}$) and on the outer side by the surface S_∞ of an enclosing large sphere with radius R_∞ , which extends to infinity. The integral over S_∞ vanishes for $R_\infty \rightarrow \infty$ if \mathbf{u}' and $\hat{\Pi}$ decay sufficiently rapidly upon increasing the distance from \mathcal{D} ; this is the case for the hydrodynamic flows we are interested in, for which $|\mathbf{u}'(r \gg 1)| \sim 1/r$ or faster. A similar relation follows from swapping the primed and unprimed fields. In the following, \mathbf{u} and $\hat{\Pi}$, as well as the corresponding primed quantities, are taken to be the velocity and pressure fields, respectively, entering into the Stokes equations (Eqs. (48) and (49)).

In order to prove the proposition in Eq. (65) we first consider its left hand side which can then be transformed as follows (note that here Einstein's convention of summation over repeated indices is used):

$$\begin{aligned} \mathcal{A} &:= \mu' \left[\int_{\partial \mathcal{D}} \mathbf{u}' \cdot \hat{\Pi} \cdot d\mathbf{s} - \int_{\mathcal{D}} \mathbf{u}' \cdot \mathbf{f} d^3 \mathbf{r} \right] \stackrel{\text{Eq. (C.1)}}{=} \mu' \int_{\mathcal{D}} \left[-\nabla \cdot (\mathbf{u}' \cdot \hat{\Pi}) - \mathbf{u}' \cdot \mathbf{f} \right] d^3 \mathbf{r} \\ &= \mu' \int_{\mathcal{D}} \left[-(\partial_j u'_i) \Pi_{ij} - \mathbf{u}' \cdot (\nabla \cdot \hat{\Pi} + \mathbf{f}) \right] d^3 \mathbf{r} \stackrel{\text{Eq. (48)}}{=} -\mu' \int_{\mathcal{D}} (\partial_j u'_i) \Pi_{ij} d^3 \mathbf{r} \\ &\stackrel{i \leftrightarrow j}{=} -\frac{1}{2} \mu' \int_{\mathcal{D}} [(\partial_j u'_i) \Pi_{ij} + (\partial_i u'_j) \Pi_{ji}] d^3 \mathbf{r} \stackrel{\Pi_{ij} = \Pi_{ji}}{=} -\frac{1}{2} \int_{\mathcal{D}} [\mu' (\partial_j u'_i + \partial_i u'_j)] \Pi_{ij} d^3 \mathbf{r} \\ &\stackrel{\text{Eq. (49)}}{=} -\frac{1}{2} \int_{\mathcal{D}} \Pi'_{ij} \Pi_{ij} d^3 \mathbf{r} - \frac{1}{2} \int_{\mathcal{D}} P' \delta_{ij} [\mu (\partial_i u_j + \partial_j u_i) - P \delta_{ij}] d^3 \mathbf{r} \\ &= -\frac{1}{2} \int_{\mathcal{D}} \hat{\Pi}' : \hat{\Pi} d^3 \mathbf{r} - \int_{\mathcal{D}} \mu P' \nabla \cdot \mathbf{u} d^3 \mathbf{r} + \frac{3}{2} \int_{\mathcal{D}} P' P d^3 \mathbf{r} \\ &\stackrel{\text{Eq. (48)}}{=} \frac{1}{2} \int_{\mathcal{D}} [-\hat{\Pi}' : \hat{\Pi} + 3P' P] d^3 \mathbf{r}. \quad (\text{C.2}) \end{aligned}$$

As stated above, Eq. (C.1) also holds after swapping the primed and unprimed fields (because they are defined in the same domain and are assumed to decay sufficiently rapidly at infinity). Therefore a similar sequence of transformations as in Eq. (C.2) can be applied to the rhs of Eq. (65). Since the last line in Eq. (C.2) is invariant with respect to interchanging the primed and unprimed quantities, one concludes that the lhs and the rhs are equal, so that Eq. (65) holds.

Appendix D. Triangular-well interaction potentials

In this appendix we summarize the derivations of the results presented in Sec. 5 for the particular choice of triangular-well interaction potentials, which are defined by Eqs. (81) and (84) and depicted in Fig. 2. By focusing on the interaction between the colloid and the molecules of species A we determine the corresponding Debye radius R_D (Eq. (17)), the radial functions $g_0(r)$ and $g_1(r)$ (Eq. (15)), as well as their derivatives at the wall (i.e., at the colloid surface $r = R$). From these quantities we obtain the force integral I_A (Eq. (55)) and the velocity integral J_A (Eq. (73)). The corresponding quantities associated with the interactions between the colloid and the species B and C are obtained by simply replacing the labels: $A \rightarrow B$ or $A \rightarrow C$. Finally, in the leading order in $\lambda_A/R \ll 1$, we determine the expression for the first derivative at the wall of the radial functions $g_n(r)$ for arbitrary $n > 1$. This allows us to infer the asymptotic behavior of the steric factor $f_{dc}(\theta_0)$ (Eq. (31)) for $\lambda_A/R \ll 1$.

D1: Debye radius

For triangular-well interaction potentials Eq. (17) yields

$$R_D^{-1} = \exp\left(\varepsilon_w^A + \Delta\varepsilon_A \frac{R}{\lambda_A}\right) \int_R^{R+\lambda_A} \frac{dr}{r^2} \exp\left(-\Delta\varepsilon_A \frac{r}{\lambda_A}\right) + \exp\left(\frac{(R+\Lambda_A)}{(\Lambda_A-\lambda_A)}\varepsilon_m^A\right) \int_{R+\lambda_A}^{R+\Lambda_A} \frac{dr}{r^2} \exp\left(-\frac{\varepsilon_m^A}{(\Lambda_A-\lambda_A)}r\right) + \int_{R+\Lambda_A}^{\infty} \frac{dr}{r^2}. \quad (\text{D.1})$$

The integrals in Eq. (D.1) can be calculated analytically and lead to a rather cumbersome combination of exponential integrals. Focusing on the physically relevant limit $\lambda_A \ll R$ (i.e., $q_A = \lambda_A/R \ll 1$) and $\Lambda_A \ll R$ (i.e., $Q_A = \Lambda_A/R \ll 1$) while the ratio $z_A = \Lambda_A/\lambda_A > 1$ is fixed (see Fig. 2), from Eq. (D.1) one finds that in leading and first sub-leading order in q_A the Debye radius is given by

$$\frac{R_D}{R} = 1 - \frac{\left[\Delta\varepsilon_A - \varepsilon_w^A e^{\varepsilon_m^A} + \varepsilon_m^A e^{\varepsilon_w^A} - \Delta\varepsilon_A z_A \left(1 + \varepsilon_m^A - e^{\varepsilon_m^A}\right)\right]}{\varepsilon_m^A \Delta\varepsilon_A} q_A. \quad (\text{D.2})$$

In Eq. (D.2) the first sub-leading term can be positive or negative, depending on whether the attractive or the repulsive part of the interaction potential dominates. In particular, for small values of ε_m^A and ε_w^A , the expansion of the exponentials in Eq. (D.2) in terms of power series up to second order in these parameters renders

$$\frac{R_D}{R} = 1 - \frac{\varepsilon_w^A + z_A \varepsilon_m^A}{2} q_A. \quad (\text{D.3})$$

This implies that, for small values of ε_w^A and ε_m^A , one has $R_D < R$ if $\varepsilon_w^A > z_A |\varepsilon_m^A|$, i.e., the repulsive part of the interaction potential dominates, while one has $R_D > R$ for $\varepsilon_w^A < z_A |\varepsilon_m^A|$, i.e., if the attractive part of the interaction potential prevails.

D2: The solution of Eq. (15) for $n = 0$ and its derivative at the surface

Since the potential $W_A(r)$ is a piece-wise continuous function of r , which has different functional forms in the inner ($r \in (R, R + \lambda_A)$), intermediate ($r \in (R + \lambda_A, R + \Lambda_A)$), and outer ($r \in (R + \Lambda_A, \infty)$) regions, respectively, we solve Eq. (15) for each region and connect the pieces by requiring the continuity of the solution and of its first derivative at the two connecting points between the three intervals. In the following we denote the solutions of Eq. (15) (for general n) in the corresponding intervals as $g_n^<(r)$, $g_n^I(r)$, and $g_n^>(r)$ for the inner, intermediate, and outer interval, respectively.

For $n = 0$ and with $W_A(r)$ given by Eqs. (81), (84), and (86) Eq. (15) leads to

$$g_0^<(r) = C_0^{(1)} F_{1,0}(r) + C_0^{(2)}, \quad g_0^I(r) = C_0^{(3)} f_{1,0}(r) + C_0^{(4)}, \quad g_0^>(r) = C_0^{(5)} \frac{R}{r}, \quad (\text{D.4})$$

where we have introduced

$$\begin{aligned} f_{1,0}(r) &= -\frac{\varepsilon_m^A}{(\Lambda_A - \lambda_A)} \text{Ei} \left(-\frac{\varepsilon_m^A}{(\Lambda_A - \lambda_A)} r \right) - \frac{1}{r} \exp \left(-\frac{\varepsilon_m^A}{(\Lambda_A - \lambda_A)} r \right), \\ F_{1,0}(r) &= \frac{\Delta \varepsilon_A}{\lambda_A} \text{Ei} \left(-\frac{\Delta \varepsilon_A}{\lambda_A} r \right) + \frac{1}{r} \exp \left(-\frac{\Delta \varepsilon_A}{\lambda_A} r \right), \end{aligned} \quad (\text{D.5})$$

with $\text{Ei}(\cdot)$ denoting the exponential integral [142].

The constants $C_0^{(k)}$, $k = 1, 2, \dots, 5$, are determined from the boundary and the continuity conditions: $g_0(R) = 1$ with $g_0(r)$ and $g_0'(r)$ continuous at $r = R + \lambda_A$ and $r = R + \Lambda_A$. These conditions lead to

$$\begin{aligned} C_0^{(1)} &= \frac{f'_{1,0}(r)|_{r=R+\lambda_A}}{L_0(\lambda_A, \Lambda_A)}, \quad C_0^{(2)} = 1 - \frac{F_{1,0}(R) f'_{1,0}(r)|_{r=R+\lambda_A}}{L_0(\lambda_A, \Lambda_A)}, \quad C_0^{(3)} = \frac{F'_{1,0}(r)|_{r=R+\lambda_A}}{L_0(\lambda_A, \Lambda_A)}, \\ C_0^{(4)} &= -\frac{f_{1,0}(R + \Lambda_A) F'_{1,0}(r)|_{r=R+\lambda_A}}{L_0(\lambda_A, \Lambda_A)} - \frac{R(1 + Q_A) f'_{1,0}(r)|_{r=R+\Lambda_A} F'_{1,0}(r)|_{r=R+\lambda_A}}{L_0(\lambda_A, \Lambda_A)}, \\ C_0^{(5)} &= -\frac{R(1 + Q_A)^2 f'_{1,0}(r)|_{r=R+\Lambda_A} F'_{1,0}(r)|_{r=R+\lambda_A}}{L_0(\lambda_A, \Lambda_A)}, \end{aligned} \quad (\text{D.6})$$

where $Q_A = \Lambda_A/R$ and

$$\begin{aligned} L_0(\lambda_A, \Lambda_A) &= (F_{1,0}(R) - F_{1,0}(R + \lambda_A)) f'_{1,0}(r)|_{r=R+\lambda_A} \\ &+ \left(f_{1,0}(R + \lambda_A) - f_{1,0}(R + \Lambda_A) - R(1 + Q_A) f'_{1,0}(r)|_{r=R+\Lambda_A} \right) F'_{1,0}(r)|_{r=R+\lambda_A}. \end{aligned} \quad (\text{D.7})$$

The derivative of $g_0(r)$ at the wall (i.e., $r = R$) is thus given by

$$g_0'(R) = \left(\frac{d}{dr} g_0^<(r) \right) \Big|_{r=R} = \frac{f'_{1,0}|_{r=R+\lambda_A} F'_{1,0}(r)|_{r=R}}{L_0(\lambda_A, \Lambda_A)} = -\frac{\Delta \varepsilon_A \varepsilon_m^A e^{\Delta \varepsilon_A}}{R \mathcal{L}_0} \quad (\text{D.8})$$

where $q_A = \lambda_A/R$, $z_A = Q_A/q_A$, $Q_A = \Lambda_A/R$, and

$$\begin{aligned} \mathcal{L}_0 &= \frac{((e^{\Delta \varepsilon_A} (1 + q_A)^2 - 1) \varepsilon_m^A + (z_A - 1) \Delta \varepsilon_A) q_A}{(1 + q_A)^2} \\ &+ e^{-\varepsilon_m^A} \frac{(q_A + \varepsilon_m^A + (\varepsilon_m^A - 1) z_A q_A) \Delta \varepsilon_A}{(1 + z_A q_A)^2}. \end{aligned} \quad (\text{D.9})$$

For $q_A \ll 1$, in leading and first sub-leading order Eq. (D.8) renders

$$g'_0(R) = -\frac{e^{\varepsilon_w^A}}{R} + \left[\varepsilon_m^A e^{\varepsilon_m^A} (e^{\Delta\varepsilon_A} - 1) + \Delta\varepsilon_A (1 - e^{\varepsilon_m^A}) - z_A \Delta\varepsilon_A (1 - e^{\varepsilon_m^A} + \varepsilon_m^A) \right] \frac{e^{\varepsilon_w^A}}{\Delta\varepsilon_A \varepsilon_m^A R} q_A. \quad (\text{D.10})$$

The second term in Eq. (D.10) vanishes for $\Delta\varepsilon_A = 0$ as well as for $\varepsilon_m^A = 0$.

D3: The solution of Eq. (15) for $n \geq 1$

For $n \geq 1$, the solutions $g_n^<(r)$, $g_n^I(r)$, and $g_n^>(r)$ of Eq. (15) corresponding to the inner, intermediate, and outer region, respectively, are given by

$$\begin{aligned} g_n^<(r) &= C_n^{(1)} F_{1,n}(r) + C_n^{(2)} F_{2,n}(r), & g_n^I(r) &= C_n^{(3)} f_{1,n}(r) + C_n^{(4)} f_{2,n}(r), \\ g_n^>(r) &= C_n^{(5)} \left(\frac{R}{r} \right)^{n+1}, \end{aligned} \quad (\text{D.11})$$

where

$$\begin{aligned} F_{1,n}(r) &= r^n \exp\left(-\frac{\Delta\varepsilon_A}{\lambda_A} r\right) U\left(n+2, 2n+2; \frac{\Delta\varepsilon_A}{\lambda_A} r\right), \\ F_{2,n}(r) &= r^n \exp\left(-\frac{\Delta\varepsilon_A}{\lambda_A} r\right) M\left(n+2, 2n+2; \frac{\Delta\varepsilon_A}{\lambda_A} r\right), \\ f_{1,n}(r) &= r^n U\left(n, 2n+2; -\frac{\varepsilon_m^A}{(\Lambda_A - \lambda_A)} r\right), \\ f_{2,n}(r) &= r^n M\left(n, 2n+2; -\frac{\varepsilon_m^A}{(\Lambda_A - \lambda_A)} r\right), \end{aligned} \quad (\text{D.12})$$

with $M(\cdot)$ and $U(\cdot)$ as Kummer's and Tricomi's hypergeometric function, respectively [142].

The coefficients $C_n^{(k)}$ are spatially constant and determined by the boundary and the continuity conditions (similar to the case $n = 0$). We find that the constants $C_n^{(k)}$ ($n \geq 1$) are given by the following explicit (albeit rather lengthy) expressions:

$$\begin{aligned} C_n^{(1)} &= \frac{f_{1,n}(R + \lambda_A) l_\Lambda^{(2)} \left(L_\lambda^{(2)} - l_\lambda^{(1)} \right)}{F_{1,n}(R + \lambda_A) f_{1,n}(R + \Lambda_A) L_n(\lambda_A, \Lambda_A)} - \frac{f_{2,n}(R + \lambda_A) l_\Lambda^{(1)} \left(L_\lambda^{(2)} - l_\lambda^{(2)} \right)}{F_{1,n}(R + \lambda_A) f_{2,n}(R + \Lambda_A) L_n(\lambda_A, \Lambda_A)}, \\ C_n^{(2)} &= \frac{f_{2,n}(R + \lambda_A) l_\Lambda^{(1)} \left(L_\lambda^{(1)} - l_\lambda^{(2)} \right)}{F_{2,n}(R + \lambda_A) f_{2,n}(R + \Lambda_A) L_n(\lambda_A, \Lambda_A)} - \frac{f_{1,n}(R + \lambda_A) l_\Lambda^{(2)} \left(L_\lambda^{(1)} - l_\lambda^{(1)} \right)}{F_{2,n}(R + \lambda_A) f_{1,n}(R + \Lambda_A) L_n(\lambda_A, \Lambda_A)}, \\ C_n^{(3)} &= \frac{l_\Lambda^{(2)} \left(L_\lambda^{(2)} - L_\lambda^{(1)} \right)}{f_{1,n}(R + \Lambda_A) L_n(\lambda_A, \Lambda_A)}, & C_n^{(4)} &= -\frac{l_\Lambda^{(1)} \left(L_\lambda^{(2)} - L_\lambda^{(1)} \right)}{f_{2,n}(R + \Lambda_A) L_n(\lambda_A, \Lambda_A)}, \\ C_n^{(5)} &= \frac{(1 + Q_A)^{n+1} \left(L_\lambda^{(2)} - L_\lambda^{(1)} \right) \left(l_\Lambda^{(2)} - l_\Lambda^{(1)} \right)}{L_n(\lambda_A, \Lambda_A)}, \end{aligned} \quad (\text{D.13})$$

where

$$\begin{aligned}
L_n(\lambda_A, \Lambda_A) = & \frac{F_1(R)}{F_1(R + \lambda_A)} \left(\frac{f_1(R + \lambda_A) l_\Lambda^{(2)} (L_\lambda^{(2)} - l_\lambda^{(1)})}{f_1(R + \Lambda_A)} - \right. \\
& \left. - \frac{f_2(R + \lambda_A) l_\Lambda^{(1)} (L_\lambda^{(2)} - l_\lambda^{(2)})}{f_2(R + \Lambda_A)} \right) \\
& - \frac{F_2(R)}{F_2(R + \lambda_A)} \left(\frac{f_1(R + \lambda_A) l_\Lambda^{(2)} (L_\lambda^{(1)} - l_\lambda^{(1)})}{f_1(R + \Lambda_A)} - \right. \\
& \left. - \frac{f_2(R + \lambda_A) l_\Lambda^{(1)} (L_\lambda^{(1)} - l_\lambda^{(2)})}{f_2(R + \Lambda_A)} \right), \tag{D.14}
\end{aligned}$$

while $l_\lambda^{(i)}$, $l_\Lambda^{(i)}$, and $L_\lambda^{(i)}$ ($i = 1, 2$) are given as the logarithmic derivatives of the expressions in Eq. (D.12) :

$$\begin{aligned}
l_\Lambda^{(i)} &= \frac{n+1}{R(1+Q_A)} + \frac{d}{dr} \ln(f_{i,n}(r)) \Big|_{r=R+\Lambda_A}, \quad l_\lambda^{(i)} = \frac{n+1}{R(1+Q_A)} + \frac{d}{dr} \ln(f_{i,n}(r)) \Big|_{r=R+\lambda_A}, \\
L_\lambda^{(i)} &= \frac{n+1}{R(1+Q_A)} + \frac{d}{dr} \ln(F_{i,n}(r)) \Big|_{r=R+\lambda_A}. \tag{D.15}
\end{aligned}$$

D4: The radial function $g_1(r)$ and its derivative at the surface

We discuss in more detail the radial function $g_1(r)$ because it enters into the force and the velocity integrals (see Sec. 4) while its derivative $g_1'(R)$ at the surface determines the expansion coefficient a_1 (Eq. (27)). For $n = 1$ Eq. (D.12) yields

$$\begin{aligned}
F_{1,1}(r) &= \frac{(\lambda_A)^3}{(\Delta\varepsilon_A)^3 r^2} \exp\left(-\Delta\varepsilon_A \frac{r}{\lambda_A}\right), \quad f_{1,1}(r) = r U\left(1, 4; -\frac{\varepsilon_m^A}{(z_A - 1)\lambda_A} r\right), \\
F_{2,1}(r) &= \frac{(\lambda_A)^3}{(\Delta\varepsilon_A)^3 r^2} \left(6 \left(1 - \exp\left(-\Delta\varepsilon_A \frac{r}{\lambda_A}\right) \right) + \frac{3\Delta\varepsilon_A r}{\lambda_A} \left(\frac{\Delta\varepsilon_A r}{\lambda_A} - 2 \right) \right), \\
f_{2,1}(r) &= \frac{(z_A - 2)^3 (\lambda_A)^3}{(\varepsilon_m^A)^3 r^2} \left(6 \left(1 - \exp\left(-\frac{\varepsilon_m^A}{(z_A - 2)\lambda_A} r\right) \right) - \right. \\
&\quad \left. - \frac{3\varepsilon_m^A r}{(z_A - 2)\lambda_A} \left(2 - \frac{\varepsilon_m^A r}{(z_A - 2)\lambda_A} \right) \right). \tag{D.16}
\end{aligned}$$

We consider the actually interesting limits $q_A = \lambda_A/R \ll 1$ and $Q_A = \Lambda_A/R \ll 1$ (while $z_A = Q_A/q_A > 1$ is fixed). The coefficients $C_{n=1}^{(k)}$, which are spatially constant, contain a non-analytic part, diverging – in the limit $q_A \rightarrow 0$ – either exponentially or as a power-law, and a part which is an analytic function of q_A . We keep the non-analytic contribution, but expand the analytic part into a Taylor series in powers of q_A and retain from it only the leading term (independent of q_A) and the first sub-leading term (linear in q_A). This leads to the following approximate expressions for $C_{n=1}^{(k)}$:

$$C_1^{(1)} = \frac{2(\Delta\varepsilon_A)^2}{Rq_A^2} \exp\left(\varepsilon_w^A + \frac{\Delta\varepsilon_A}{q_A}\right) \left(1 - \left[e^{-\varepsilon_m^A} (z_A \Delta\varepsilon_A - \varepsilon_w^A) - 3(z_A - 1)\Delta\varepsilon_A + 2\varepsilon_m^A \right] \right)$$

$$\begin{aligned}
& + 2e^{\varepsilon_m^A} \left(e^{\Delta\varepsilon_A} \varepsilon_m^A + z_A \Delta\varepsilon_A - \varepsilon_w^A \right) - (z_A - 2) \varepsilon_m^A \Delta\varepsilon_A \left] \frac{q_A}{\varepsilon_m^A \Delta\varepsilon_A} \right), \\
C_1^{(2)} &= \frac{\Delta\varepsilon_A}{3Rq_A} \left(1 - \frac{2 \left(e^{\varepsilon_w^A} - 1 \right)}{\Delta\varepsilon_A} q_A \right), \quad C_1^{(3)} = -\frac{\varepsilon_m^A}{Rq_A(z_A - 1)} \left(1 - \right. \\
& \left. - \frac{2 \left[e^{\varepsilon_m^A} \left(e^{\Delta\varepsilon_A} \varepsilon_m^A + z_A \Delta\varepsilon_A - \varepsilon_w^A \right) - (z_A - 1) \Delta\varepsilon_A \right]}{\varepsilon_m^A \Delta\varepsilon_A} q_A \right), \quad (\text{D.17}) \\
C_1^{(4)} &= -\frac{(\varepsilon_m^A)^2}{3Rq_A^2(1 - z_A)^2} \exp \left(\frac{(1 + q_A z_A) \varepsilon_m^A}{(z_A - 1) q_A} \right) \\
& \times \left(1 + \frac{(z_A \varepsilon_m^A + z_A - 1) \Delta\varepsilon_A - 2e^{\varepsilon_m^A} \left(e^{\Delta\varepsilon_A} \varepsilon_m^A + z_A \Delta\varepsilon_A - \varepsilon_w^A \right)}{\varepsilon_m^A \Delta\varepsilon_A} q_A \right), \\
C_1^{(5)} &= 1 + \frac{2 \left((z_A \varepsilon_m^A + z_A - 1) \Delta\varepsilon_A - e^{\varepsilon_m^A} \left(e^{\Delta\varepsilon_A} \varepsilon_m^A + z_A \Delta\varepsilon_A - \varepsilon_w^A \right) \right)}{\varepsilon_m^A \Delta\varepsilon_A} q_A.
\end{aligned}$$

Since $g_1'(r = R)$ is given by

$$g_1'(R) = \left(\frac{d}{dr} g_1^<(r) \right) \Big|_{r=R} = C_1^{(1)} F'_{1,1}(r) \Big|_{r=R} + C_1^{(2)} F'_{2,1}(r) \Big|_{r=R}, \quad (\text{D.18})$$

by using Eqs. (D.16) and (D.17) we obtain the following approximation in the limit $q_A \ll 1$

$$\begin{aligned}
g_1'(R) &= -\frac{2e^{\varepsilon_w^A}}{R} + \left[\left(e^{-\varepsilon_m^A} + 2e^{\varepsilon_m^A} \right) \left(\varepsilon_m^A e^{\Delta\varepsilon_A} + z_A \Delta\varepsilon_A - \varepsilon_w^A \right) - \right. \\
& \left. - \left((z_A - 2) \varepsilon_m^A + 3(z_A - 1) \right) \Delta\varepsilon_A \right] \frac{2e^{\varepsilon_w^A}}{\varepsilon_m^A \Delta\varepsilon_A R} q_A. \quad (\text{D.19})
\end{aligned}$$

The leading term in this expansion has been used in Eq. (88) in Sec. 5. For $\varepsilon_m^A = \varepsilon_w^A = 0$ the sub-leading term vanishes.

D5: Force and velocity integrals

First we consider the integral I_A in Eq. (55). To this end we write $I_A = I_A^< + I_A^I$, where the first term and the second term result from integrations over the inner (repulsive) and the intermediate (attractive) regions of the pair potential, respectively. (The contribution due to the integration over the outer region vanishes because there $W_A^>(r) \equiv 0$.)

By using the above results, we find that in leading and sub-leading order in q_A the integral $I_A^<$ is given by

$$\begin{aligned}
I_A^< &= \int_R^{R+\lambda_A} dr r^2 \frac{W_A^<(r)}{dr} g_1^<(r) \exp(-\beta W_A^<(r)) \\
&= -\frac{e^{-\varepsilon_w^A} (e^{\Delta\varepsilon_A} - 1) R^2}{\beta} \left(1 - \frac{2}{\Delta\varepsilon_A} \left[1 + e^{\varepsilon_w^A} - \frac{\Delta\varepsilon_A e^{\Delta\varepsilon_A} (e^{\varepsilon_m^A} + 1)}{e^{\Delta\varepsilon_A} - 1} \right] q_A \right). \quad (\text{D.20})
\end{aligned}$$

The leading order term in Eq. (D.20) is negative for $\Delta\varepsilon_A > 0$ and vanishes if $\Delta\varepsilon_A = 0$ (i.e., if there is no interaction), and it is proportional to R^2 . Similarly, in leading and sub-leading order in q_A the integral I_A^I is given by

$$\begin{aligned} I_A^I &= \int_{R+\lambda_A}^{R+\Lambda_A} dr r^2 \frac{W_A^I(r)}{dr} g_1^I(r) \exp(-\beta W_A^I(r)) \\ &= \frac{(e^{-\varepsilon_m^A} - 1) R^2}{\beta} \left(1 - \frac{2}{\varepsilon_m^A \Delta\varepsilon_A (e^{-\varepsilon_m^A} - 1)} \left[\varepsilon_m^A e^{\varepsilon_w^A} (e^{-\varepsilon_m^A} - 1) - (\varepsilon_w^A + z_A \Delta\varepsilon_A) e^{\varepsilon_m^A} \right. \right. \\ &\quad \left. \left. + \Delta\varepsilon_A (z_A - 1 - \varepsilon_m^A) e^{-\varepsilon_m^A} + ((2z_A -) \Delta\varepsilon_A - 1) \varepsilon_m^A \right] q_A \right). \end{aligned} \quad (\text{D.21})$$

The leading term in this expression is positive for all $\varepsilon_m^A \leq 0$, and, as $I_A^<$, it is proportional to R^2 .

It follows that the integral I_A is, in leading and sub-leading order in q_A , given by

$$\begin{aligned} I_A &= - \frac{(1 - e^{-\varepsilon_w^A}) R^2}{\beta} - \left[(\varepsilon_w^A - z_A \Delta\varepsilon_A) \sinh(\varepsilon_m^A) - \right. \\ &\quad \left. - \varepsilon_m^A (\sinh(\varepsilon_w^A) - z_A \Delta\varepsilon_A) \right] \frac{4\lambda_A R}{\beta \varepsilon_m^A \Delta\varepsilon_A}. \end{aligned} \quad (\text{D.22})$$

The leading order term in Eq. (D.22) is used in Eq. (87) in Sec. 5. It depends only on ε_w^A , it is negative for $\varepsilon_w^A > 0$, and it is proportional to R^2 . If $\varepsilon_w^A = 0$, the first term in Eq. (D.22) vanishes; in this case, in leading order in q_A the force integral I_A takes the form

$$I_A = z_A \left(\frac{\sinh(\varepsilon_m^A)}{\varepsilon_m^A} - 1 \right) \frac{4\lambda_A R}{\beta}, \quad (\text{D.23})$$

which implies that it is positive and depends only linearly on R .

Next we consider the integral J_A (Eq. (73)), which enters into the definition of the velocity V (Eqs. (72) and (75)) and of the stall force F_{ext} (Eqs. (79) and (80)). As for the integral I_A , we write $J_A = J_A^< + J_A^I$ (the contribution from the outer region vanishes in this case, too), where

$$\begin{aligned} J_A^< &= \int_R^{R+\lambda_A} dr r^2 \frac{W_A^<(r)}{dr} g_1^<(r) \left(1 + \frac{1}{2} \left(\frac{R}{r} \right)^3 - \frac{3R}{2r} \right) \exp(-\beta W_A^<(r)) \\ &= - \frac{3e^{-\varepsilon_w^A}}{2(\Delta\varepsilon_A)^2} (e^{\Delta\varepsilon_A} (1 + (\Delta\varepsilon_A - 1)^2) - 2) \frac{(\lambda_A)^2}{\beta} + \\ &\quad + \left[6e^{-\varepsilon_w^A} + 2(3e^{\Delta\varepsilon_A} (1 + (\Delta\varepsilon_A - 1)^2) - \Delta\varepsilon_A^3 - 6) + \right. \\ &\quad \left. + e^{-\varepsilon_m^A} (\Delta\varepsilon_A (6 - \Delta\varepsilon_A (3 - \Delta\varepsilon_A)) - 6) \right] \frac{(\lambda_A)^2}{2\beta(\Delta\varepsilon_A)^3} q_A, \end{aligned} \quad (\text{D.24})$$

and

$$J_A^I = \int_{R+\lambda_A}^{R+\Lambda_A} dr r^2 \frac{W_A^I(r)}{dr} g_1^I(r) \left(1 + \frac{1}{2} \left(\frac{R}{r} \right)^3 - \frac{3R}{2r} \right) \exp(-\beta W_A^I(r))$$

$$\begin{aligned}
&= \frac{3}{2(\varepsilon_m^A)^2} \left((z_A - 1)^2 (e^{-\varepsilon_m^A} - 1) + (\varepsilon_m^A - z_A + 1)^2 e^{-\varepsilon_m^A} - (1 + z_A \varepsilon_m^A - z_A)^2 \right) \frac{(\lambda_A)^2}{\beta} \\
&- \frac{1}{(\varepsilon_m^A)^3 \Delta \varepsilon_A} \left[6\varepsilon_m^A \left((\varepsilon_m^A)^2 - 2(z_A - 1)\varepsilon_m^A + 2(z_A - 1)^2 \right) e^{\Delta \varepsilon_A} - \right. \\
&- \Delta \varepsilon_A \left(-(\varepsilon_m^A)^3 + 3(z_A - 1)(\varepsilon_m^A)^2 - 6(z_A - 1)^2 \varepsilon_m^A + 6(z_A - 1)^3 \right) e^{-\varepsilon_m^A} - \\
&- 6\varepsilon_m^A (2 + 2z_A(\varepsilon_m^A - 2) + (z_A)^2 (2 + \varepsilon_m^A(\varepsilon_m^A - 2))) e^{\varepsilon_m^A} + \\
&+ 6(\varepsilon_m^A - (z_A - 1)\Delta \varepsilon_A) (2 + 2z_A(\varepsilon_m^A - 2) + (z_A)^2 (2 + \varepsilon_m^A(\varepsilon_m^A - 2))) e^{\varepsilon_m^A} - \\
&- \left((6 + 2\Delta \varepsilon_A - (z_A)^3 \varepsilon_A) (\varepsilon_m^A)^3 - 3(z_A - 1) (4 + \Delta \varepsilon_A (2 + (z_A)^2)) (\varepsilon_m^A)^2 + \right. \\
&\left. + 6(z_A - 1)^2 (2 + \Delta \varepsilon_A (2 + z_A)) \varepsilon_m^A - 18\Delta \varepsilon_A (z_A - 1)^3 \right) \left. \right] \frac{(\lambda_A)^2}{2\beta} q_A. \tag{D.25}
\end{aligned}$$

One finds that for any $\Delta \varepsilon_A > 0$ the leading order term in $J_A^<$ is negative (similarly to the behavior exhibited by $I_A^<$ (Eq. (D.20))), and is independent of R . Equations (D.24) and (D.25) lead to

$$J_A = \mathcal{J}_A \frac{(\lambda_A)^2}{\beta} + S_A \frac{(\lambda_A)^2}{2\beta} q_A. \tag{D.26}$$

The contribution from the leading term $\mathcal{J}_A (\lambda_A)^2 / \beta$ (see Eq. (102)) is used in Eq. (101) in Sec. 5. The sub-leading contribution S_A in Eq. (D.26) collects all terms in square brackets in Eqs. (D.24) and (D.25).

D6: Asymptotic behavior of $f_{dc}(\theta_0)$ in the limit $q_A \rightarrow 0$

Finally we consider the asymptotic behavior of the steric factor $f_{dc}(\theta_0)$ in the limit $q_A \rightarrow 0$. According to Eq. (31) this amounts to the analysis of the behavior of the ratio $g'_0(R)/g'_n(R)$.

This behavior contains the following subtle issue. Due to Eqs. (D.11) and (D.12), the radial functions $g_n(r)$ are defined explicitly via Kummer's and Tricomi's hypergeometric functions $M(\cdot)$ and $U(\cdot)$. In the limit $q_A \rightarrow 0$ the arguments of both functions become large, which facilitates the derivation of the asymptotic behavior. On the other hand, the sub-dominant terms in the expansions of these hypergeometric functions for large arguments also depend on whether the parameters of the hypergeometric function are fixed and finite, or are allowed to vary and become large. Accordingly, the calculation of the correction terms to the leading order behavior poses a mathematically very involved problem. We therefore focus only on the leading order behavior of $g'_n(r=R)$ (with $g_n(r)$ defined by Eqs. (D.11) and (D.12)):

$$g'_n(R) = C_n^{(1)} F'_{1,n}(r) \Big|_{r=R} + C_n^{(2)} F'_{2,n}(r) \Big|_{r=R}. \tag{D.27}$$

In the limit $q_A \ll 1$, the leading order behavior of the terms in Eq. (D.27) is

$$\begin{aligned}
C_n^{(1)} &\sim \frac{(n+1)\Delta \varepsilon_A}{q_A} \left(\frac{\Delta \varepsilon_A}{q_A R} \right)^n \exp \left(\varepsilon_w^A + \frac{\Delta \varepsilon_A}{q_A} \right), \\
F'_{1,n}(R) &\sim -\frac{q_A}{R\Delta \varepsilon_A} \left(\frac{Rq_A}{\Delta \varepsilon_A} \right)^n \exp \left(-\frac{\Delta \varepsilon_A}{q_A} \right), \tag{D.28}
\end{aligned}$$

and

$$C_n^{(2)} \sim \frac{\Gamma(n+1)\Delta\varepsilon_A}{\Gamma(2n+2)} \left(\frac{\Delta\varepsilon_A}{q_A R}\right)^n,$$

$$F'_{2,n}(R) \sim (-1)^{n+1} \frac{\Gamma(2n+2)q_A}{\Gamma(n)\Delta\varepsilon_A} \left(\frac{q_A R}{\Delta\varepsilon_A}\right)^n \exp\left(-\frac{\Delta\varepsilon_A}{q_A}\right). \quad (\text{D.29})$$

These expressions imply that the first term in Eq. (D.27) provides the dominant contribution, which is independent of q_A , while the second term is proportional to q_A . Therefore one finds for the leading behavior

$$g'_n(R) \sim -\frac{(n+1)}{R} e^{\varepsilon_w^A}, \quad (\text{D.30})$$

which is consistent with Eqs. (D.10) and (D.19) and implies $g'_n(R)/g'_0(R) \sim (n+1)$, so that $f_{dc}(\theta_0) \sim f_{dc}^{sls}(\theta_0)$ (see Eq. (33)).

Appendix E. Notations and definitions

A, B, C (near Fig. 1): reactant and product molecular species;

D_j (near Fig. 1), $j = A, B, C$: diffusion constant of the molecules of species j ;

$\mathbf{F}_{chem}, \mathbf{F}_{hyd}$ (after Eq. (71); Eq. (72)): contributions to the force on the colloid due to the direct interactions with the molecules of various species and due to the flow of the solution, respectively;

\mathbf{F}_{ext} (Eqs. (71), (95)-(98)): external force acting on the colloid; stall force, if it corresponds to $\mathbf{V} = 0$;

$F_{ext}^j, V_j, j = A, B, C$ (Eqs. (122), (123)): that part of the stall force and of the velocity, respectively, which is due to the species j ;

$I_j, j = A, B, C$ (Eq. (73)): force integrals in the definition of F_{chem} ;

$J_j, j = A, B, C$ (Eqs. (91) - (94)): velocity integrals in the definition of V ;

$\mathcal{J}_j, j = A, B, C$ (Eq. (119)): dimensionless factor in the velocity integral J_j for species j ;

\mathbf{J}_j and $\mathbf{j}_j, j = A, B, C$ (Eqs. (10)-(12)): particle current in the laboratory frame and relative to the (local) center of mass motion, respectively;

$K = W_0 V_a$ (near Eq. (23)): total number of reaction events per unit time (rate of reaction W_a) in a volume V_a ;

K_{eff} (Eq. (37)): effective reaction rate;

$K_{eff}^{(0)}$ (Eq. (43)): effective reaction rate in the absence of interactions between molecules and the colloid;

K_S (after Eq. (38)): Schmoluchowski constant;

K^* (Eq. (41)): effective reaction rate for an elementary reaction act;

K_{SD} (Eq. (40)): Schmoluchowski-Debye constant;

$L_{ij}, i, j = A, B, C$ (Eq. (12)): Onsager coefficients;

P (Eqs. (67)): hydrostatic pressure (the isotropic part of the stress tensor);

Pe, Re (near Eqs. (16) and (66)): Péclet and Reynolds numbers, respectively;

- Q (Eqs. (8) and (11)): constant negative particle current over the catalytic patch;
 R (Fig. 1): radius of the colloid;
 R_D (Eq. (31)): Debye radius;
 S : solvent molecular species;
 T : absolute temperature;
 \mathbf{V} , $V = |\mathbf{V}|$: velocity of the colloid and its magnitude, respectively;
 \mathcal{V} : volume of the system
 $W_j = \Phi_j(r) - \frac{m_j}{m_S} \Phi_S(r)$, $j = A, B, C$ (Eq. (2)): effective (relative to the solvent) interaction potential of molecules of type j with the colloid;
- a (near Eq. (1)): minimal distance between a molecule of species A and the colloid surface;
 a_n , b_n , γ_n (Eqs. (28), (33), (54), (56), (62), (63)): coefficients in the series expansion of the radial functions of integer index $n \geq 0$ describing the dependence on r of the number densities n_A , n_B , and n_C , respectively;
 c_j , $j = A, B, C$: concentration (mass fraction) of molecular species j ;
 f_g (Eq. (23)): geometric steric factor;
 f_{dc} (Eqs. (39), (42)): effective (diffusion-controlled) steric factor;
 $f_{dc}^{(sl_s)}$ (Eq. (44)): effective steric factor in the absence of interactions between molecules and the colloid;
 \tilde{f} , f (Eq. (68)): force density on the fluid with (tilde) or without the contribution due to the gradient of the interactions between the solvent molecules and the colloid, respectively;
 g_n , j_n , h_n (Eqs. (29), (55), (62)): radial functions of integer index $n \geq 0$ describing the dependence on r of the number densities n_A , n_B , and n_C , respectively;
 k_B : Boltzmann constant ;
 m_j , $j = A, B, C, S$ (near Fig. 1): molecular mass of species j ;
 n_j (near Eq. (1)), $j = A, B, C$: number density of molecular species j ;
 n_0 (near Eq. (1)): bulk value of the number density of species A ;
 $n_0^{(S)}$ (near Eq. (1)): mean number density of solvent molecules;
 p (Eq. (1)): probability of the conversion $A \rightarrow B$;
 q_j , Q_j , z_j (after Eq. (104)): dimensionless parameters of the triangular-well potential for species j ;
 \mathbf{r} , $r = |\mathbf{r}|$ (Fig. 1): position vector and radial coordinate measured from the center of the colloid, respectively;
 $\tilde{r} = r - R$ (Fig. 1): distance from the surface of the colloid;
 $\mathbf{u}(\mathbf{r})$ (near Eq. (4)): hydrodynamic flow of the solution;
- $\hat{\mathbf{\Pi}}$ (Eqs. (66), (67)): Newtonian fluid stress tensor;
 $\tilde{\Phi}_j(\tilde{r})$ and $\Phi_j(r) = \tilde{\Phi}_j(r - R)$, $j = A, B, C, S$ (near Eq. (2)): interaction potential between a molecule of species j and the colloid;
 $\Omega^{(AB)}$ (Eq. (75)), $\Omega^{(ABC)}$ (Eq. (81)): contribution to parts in the force integrals which

are independent of θ_0 ;

$\beta = 1/(k_B T)$ (Eq. (15));

$\delta\mathcal{V}$ (near Eq. (4)): small volume element in the solution;

θ_0 (Fig. 1): opening polar angle (in spherical coordinates) of the catalytic patch;

θ (Fig. 1): polar angle in spherical coordinates;

κ (Eqs. (22), (23)): effective velocity defining the particle currents due to reactions at the catalytic patch;

μ (near Eq. (1)): viscosity of solution;

μ_j and $\tilde{\mu}_j = \mu_j + \Phi_j$, $j = A, B, C, S$ (Eqs. (5), (6)): chemical potential of molecular species j ;

$\hat{\mu}_j = (\mu_j/m_j) - (\mu_S/m_S)$, $j = A, B, C$ (Eq. (14)): chemical potential relative to that of the solvent;

$\bar{\mu}_j = [(\tilde{\mu}_j/m_j) - (\tilde{\mu}_S/m_S)]\rho$, $j = A, B, C$ (Eq. (9)): chemical potential of the molecular species j relative to that of solvent molecules, including the contribution from the interactions with the colloid;

$\xi_{1,2}^j$, λ_j , Λ_j , $\Delta\epsilon_j$, ϵ_w^j , and ϵ_m^j , $j = A, B, C$ (Eqs. (99)-(103)): parameters of the triangular-well potential for species j ;

ρ (Eq. (3)): mass density of the solution;

σ_j , ϵ_j , $j = A, B, C, S$ (after Eq. (2)): parameters of the Lennard-Jones pair potential between molecules of species j and molecules composing the colloid;